TAU SEEDING IN HEALTH AND DISEASE

APPROVED BY SUPERVISORY COMMITTEE

Marc Diamond, M.D.

Joachim Herz, M.D.

Lukasz Joachimiak, Ph.D.

Yunsun Nam, Ph.D.

Luke Rice, Ph.D.

TAU SEEDING IN HEALTH AND DISEASE

by

MICHAEL SHANE LACROIX

DISSERTATION / THESIS

Presented to the Faculty of the Graduate School of Biomedical Sciences

The University of Texas Southwestern Medical Center at Dallas

In Partial Fulfillment of the Requirements

For the Degree of

DOCTOR OF PHILOSOPHY

The University of Texas Southwestern Medical Center at Dallas

Dallas, Texas

AUGUST, 2022

Acknowledgments

First and foremost, I would like to acknowledge the unwavering support of my family. Although many miles apart, they have sacrificed their time to visit me, encourage me, and enjoy life with me. Without them this dissertation would not exist. Every vacation with my brothers and visit from my parents helped me to put one more foot forward. I thank the friends I've made here in Dallas who taught me how to have fun again after I got lost in science, with special thanks to Jacob Mercier and Matthew Bradley for always being stoked to climb rocks and to Brittany Witt for her unending belief in me.

I owe many thanks to my thesis mentor, Marc Diamond, whose scientific spirit is contagious. His guidance, encouragement, and patience were paramount to me seeing this journey through. I would like to thank my dissertation committee consisting of Yunsun Nam, committee chair, Joachim Herz, Lukasz Joachimiak, and Luke Rice.

My work would not be possible without crucial scientific tools developed by those before me, especially Jaime Vaquer-Alicea, Victor Manon, Brian Hitt, and Brandon Holmes, to whom I give many thanks.

I thank all the Diamond Lab members for creating an enriching work environment with special thanks to Dana Dodd, Ting Yang, Valerie Perez, Vaibhav Bommareddy, and Sandi Jo Estill-Terpack.

Finally, my work would be impossible without the generous donations of human specimens. For that I whole-heartedly thank every donating individual, and their families for assisting my work, and the work of the scientific community. For the collection of specimens, I thank Hilda Mirbaha, Charles White, Bret Evers, Olaf Stuve, Bradley Lega, Kelly Gleason, and Carol Tamminga.

This work was supported by grants from the Chan Zuckerberg Initiative (Neurodegeneration Challenge Network) and NIH/NIA 1R01AG059689.

ABSTRACT OF THE DISSERTATION

Tau Seeding in Health and Disease

by

Michael Shane LaCroix, Ph.D.

The University of Texas Southwestern Medical Center at Dallas, 2022

Supervising Professor: Marc Diamond, M.D.

An abundance of evidence supports that the protein tau adopts a wide variety of conformations with the ability to self-assemble and propagate in living systems, and that this prion behavior may drive neurodegeneration in tauopathies. However, the inciting events that lead to tau seed formation and aggregation are unknown. It remains possible that tau can act as a prion outside the context of disease, as part of its normal function, and the accumulation of tau prions in neurodegenerative diseases reflects a loss of control of this normal function. During my dissertation research, I completed a series of investigations on tau's ability to form seeds outside the context of classical tauopathies. I discovered that tau seeds are present in the cerebral cortex of healthy individuals. Tau seeds form in a region and species specific manner, being absent in the cerebellum of healthy individuals and undetectable in murine models. Seeding in healthy individuals was independent of age, implying it is not a result of emerging tauopathy but rather, that prion formation is a normal aspect of tau biology. This may be related to its interactions with RNA. I also surveyed for tau seeding in several inflammatory diseases with neurodegenerative components that have been reported to exhibit tau accumulation based on immunohistochemistry. I found seeds at levels beyond that of

healthy individuals in temporal lobe epilepsy as well as multiple sclerosis. Thus, tau may be a target of many convergent pathways that lead to neurodegeneration. The work here highlights the significant role that tau plays in human health and disease. Further understanding of how normal biological processes, as well as inflammation, affect tau's prion state will be essential for the development of therapeutic strategies for the prevention and treatment of tauopathies.

Table of Contents

List of Figures

Chapter 1

Chapter 2

Chapter 3

Chapter 4

Chapter 5

List of Tables

List of Appendices

Chapter 1

Introduction and Perspective

TAU PROTEIN

The protein tau was initially discovered as a key factor critical for the stabilization of microtubules *in vitro* (Weingarten et al., 1975). Since its discovery, tau has remained the focus of intense research. The human tau protein is encoded by the microtubule-associated protein tau (MAPT) gene, located on chromosome 17q21 (Neve et al., 1986), and is highly expressed in neurons, with dominant axonal localization (Binder et al., 1985). Tau protein is primarily expressed as six unique isoforms derived from alternative splicing (Figure 1.1) (Goedert et al., 1989), although a larger "big tau" isoform is expressed in the peripheral nervous system (Couchie et al., 1992). The isoforms differ based on the inclusion or exclusion of two N-terminally located inserts and one of the four repeats found within tau's repeat domain. Tau's functional domains consist of four unique regions based on its interaction with microtubules: an N-terminal projection domain that projects away from the microtubule's surface when tau is bound, a proline-rich domain, a repeat domain or microtubule-binding domain consisting of 3 or 4 non-identical repeats which mediate tau's binding to microtubules, and a C-terminal domain (Mandelkow and Mandelkow, 2012). Tau is comprised of primarily hydrophilic residues, limiting its ability to fold into a definite conformation. Indeed, its unique amino acid composition renders tau "natively unfolded" or "intrinsically disordered" (Mukrasch et al., 2009; Schweers et al., 1994). Despite being "natively unfolded" regions of the tau protein may exhibit local structure that contribute to tau's ability to self-assemble (Chen et al., 2019; Mirbaha et al., 2018).

As tau was originally discovered in association with microtubules, its function is most extensively described as being a microtubule stabilizer. The majority of tau in cells is in fact bound to microtubules, and, *in vitro,* tau accelerates the polymerization of tubulin (Weingarten *et al.*, 1975). However, tau primarily localizes with *dynamic* microtubules that are most susceptible to drug induced depolymerization in cultured cells (Kempf et al., 1996). Additionally, siRNA knockdown of tau in primary neurons has no effect on the number or polymerization state of microtubules (King et al., 2006). Indeed, tau knockout mouse models show few if any deficits (Dawson et al., 2001), and tau knockout and knockdown ameliorates some aspects of pathology in Alzheimer's disease (AD) and seizure mouse models (DeVos et al., 2013; Roberson et al., 2007). Thus, microtubule stabilization seems not to be a critical function of tau in animals. While microtubule stabilization may not an essential function of tau in living systems, it is of particular interest that the same microtubule binding domain that allows for tau to interact with microtubules also comprises the core of virtually all tauopathy fibril structures (Shi et al., 2021).

Tauopathies

Essentially all common adult-onset neurodegenerative diseases feature the deposition in the nervous system of misfolded proteins into beta-sheet rich insoluble aggregates. Accumulation of intracellular amyloid assemblies of the tau protein as neurofibrillary tangles (NFTs) underlies the multitude of neurodegenerative diseases termed tauopathies (Lee and Trojanowski, 1999). The clinical syndrome of a tauopathy generally includes dementia, behavioral abnormalities, and motor impairments (Williams, 2006). The minority of

tauopthies are caused by inherited mutations in the *MAPT* gene. Tau was first linked as causal to neurodegeneration when dominant mutations in *MAPT* were found to cause familial Frontotemporal dementia with Parkinsonism linked to chromosome 17 (FTDP-17) (Hutton et al., 1998; Poorkaj et al., 1998; Spillantini et al., 1998). The preponderance of disease-causing mutations in tau lie within its repeat domain (Figure 1.2, adapted from Vaquer-Alicea et al., 2021), with most mutations increasing tau's aggregation propensity (Vaquer-Alicea et al., 2021). The majority of tauopathies are sporadic, without a known definite cause. Alzheimer's disease (AD) is the most common tauopathy, afflicting ~50 million people worldwide and is predicted to harm ~150 million by 2050 (Guerchet et al., 2020). Despite a lack of clear cause in most cases of tauopathy, mutations in tau that result in aggregation are sufficient to drive neurodegeneration suggesting that tau deposition alone is sufficient to cause disease. In tauopathies, tau deposits in a consistent and hierarchical pattern in the brain, and NFTs track with disease severity (Arriagada et al., 1992). 32 unique *MAPT* mutations have been described in association with FTDP-17, and many of these mutations cause pathology by promoting tau aggregation (Goedert and Jakes, 2005). Why tau begins to aggregate in sporadic cases, which represent the majority of tauopathies, remains unclear.

Tau Aggregation and Prion Behavior

Considerable experimental evidence has accumulated in the past decade that clearly demonstrates tau's ability to undergo templated conformation change, which is called seeding, and that prion mechanisms underpin the spread of tau aggregates along functionally connected networks, driving neurodegeneration in tauopathies. Initial work from our group

and others suggested that tau can stably propagate unique fibrillar structures *in vitro* (Frost et al., 2009b). The same was found for cells. Exogenously introduced tau amyloids are taken up by cultured cells, which can serve as templates for intracellular aggregation (Frost et al., 2009a). Similarly, tau inoculated into transgenic mouse brain induced intracellular pathology (Clavaguera et al., 2009). These results demonstrate tau's ability to stably propagate an aggregated state in living systems. Further work solidified tau's prion-like behavior. Diverse neuropathologies formed upon the inoculation of a tauopathy mouse model brain with tau fibrils prepared from human tauopathies (Clavaguera et al., 2013). Similar to the prion protein, we have observed that tau forms a variety of unique structures, or strains with the ability to propagate indefinitely (Figure 1.3). Tau strains transmit readily in cultured cells, retain their identity after propagation in mouse brain, and produce unique and transmissible neuropathologies (Sanders et al., 2014). In a larger survey of 18 tau strains propagated in cells, each gave rise to a unique pattern of neuropathology following inoculation into a mouse model (Kaufman et al., 2016).

The advances of cryo-electron microscopy (cryo-EM) in the past decade have confirmed initial work on tau prion strains that suggested that tau fibrils from unique tauopathies form unique structures that can be used to define a given tauopathy. Tau fibril structures from different tauopathies determined via cryo-EM have revealed unique fibril core structural features that correlate with different neuropathological diagnosis, while also confirming that for each tauopathy fibril, the repeat domain forms the core of the fibril structure (Figure 1.4) (Falcon et al., 2018; Falcon et al., 2019; Fitzpatrick et al., 2017; Shi et al., 2021; Zhang et al.,

2020a). Even within a given neuropathological diagnosis there can exist fibril structure diversity (Shi et al., 2021), which is consistent with the isolation of distinct tau strains from individual brains (Sanders et al., 2014). Considerable evidence supports that distinct tau fibril structures drive the development of unique tauopathies. Despite our vastly expanded understanding of tau's prion behavior and the multitude of structures it can adopt, we still lack an understanding for what initiates sporadic tauopathies.

Inflammation and Tau

Increasingly, the role of inflammation in the neurodegenerative process is gaining appreciation. Once thought to be a protected organ, it is evident that inflammation occurs in the brain and complex and diverse molecular pathways with a variety of cellular mediators govern inflammation in the CNS. For example, multiple sclerosis (MS) is a prototypic neuroinflammatory disorder with focal infiltration of the brain and spinal cord by peripheral immune cells causing demyelination and subsequent neurodegeneration (Milo et al., 2020). In AD, inflammatory features include activated microglia and the production of inflammatory mediators including nitric oxide, reactive oxygen species, and proinflammatory cytokines and chemokines, which in turn promote cell death (Akiyama et al., 2000; Kitazawa et al., 2004). For any given neurodegenerative disease, a specific inducing inflammatory signature exists that characterizes the inflammatory signal of that particular disease, with specific mediators playing a greater or lesser role in the pathophysiology depending on the disease (Glass et al., 2010). Additionally, there are shared features of inflammation amongst

neurodegenerative diseases, with common molecular mediators (IL-1B, IL-6, IL-12, TNF-a) playing key roles in a variety of diseases (Guzman-Martinez et al., 2019).

How inflammatory signaling pathways may influence tau and tau's conversion to seed competent species remains unclear. NFTs are composed of tau that has been excessively phosphorylated on a myriad of its 85 putative phosphorylation sites, termed "hyperphosphorylated" tau (Morris et al., 2015). For AD, tau phosphorylation events can be seen as hierarchical in terms of disease progression, with some residues being phosphorylated earlier in the disease process, and others later (Laurent et al., 2018). Recent work found direct positive spatial correlation of tau pathology and neuroinflammatory microglia in early AD (Terada et al., 2019), suggesting that inflammatory changes coincide with the present of NFT's. Whether inflammation is inducing NFT formation, specific tau species are neurotoxic and recruit inflammatory cells, or some combination of both, remains to be delineated. It seems plausible that events that activate proinflammatory kinases have the potential to phosphorylate tau and promote its self-assembly (Ballatore et al., 2007). In turn, toxic tau species may further promote inflammation in a toxic, neurodegenerative cascade (Glass *et al.*, 2010).

Expanding the Role of Tau in Disease

The presence of tau accumulation in several lesser known disorders suggests that tau has a much broader impact on human health and disease than its well-studied role in classical tauopathies, and promotes the idea that insults to the CNS may insight inflammatory

conditions that led to tau strain formation and eventual deposition. NFTs have been described in the brain of those with subacute sclerosing panencephalitis (SSPE), which is a progressive neurological condition that occurs after infection with the measles virus (McQuaid et al., 1994). NFT's have also been found in several regions of the brains of patients with postencephalitic parkinsonism (PEP), which occurred in individuals exposed to the influenza pandemic of 1915-1930 (Hof et al., 1992). Nodding Syndrome, a neurodegenerative epileptic disorder endemic to Uganda that seems to occur after infection with *Onchocerca volvulus*, was recently shown to have NFTs throughout the cerebral cortex (Pollanen et al., 2018), and a predominant neuroinflammatory signature (Hotterbeekx et al., 2019). NFT's are even found in and around focal inflammatory lesions in the prototypical neuroinflammatory disease MS, (Anderson et al., 2009; 2010). Clearly, a relationship between neuroinflammation and tau accumulation exists. Despite reports of tau accumulation in these and other disorders, they role that tau plays in the degenerative aspects of these diseases remains unclear and understudied, even downplayed as to not seem important (Hotterbeekx *et al.*, 2019). In addition, whether tau in these conditions is seed-competent, *i.e.* has the ability to self-assemble and transfer that assembly structure from one cell to another, remains to be tested. I hypothesize that events that incite inflammation in the CNS (e.g. trauma, infection) initiate molecular pathways with tau being one target, whether that be through direct phosphorylation of tau via the activation of kinases and subsequence aggregation, or the accumulation of tau via reduced clearance pathways. If this hypothesis is correct, tau seeds should be detectable in the brains of patients with these disorders and would indicate that tau

may be playing a critical role in these conditions that extends past what we know about classical tauopathies.

Summary

Tauopathies are a diverse group of neurodegenerative diseases that feature the assembly and dispersion of tau strains throughout the brain along functionally connected neuronal networks. This spreading process appears to drive the progression of disease. Advancements in cryo-EM have allowed for the structural determination of fibrils derived from different tauopathies and confirmed experimental evidence that suggested unique conformations exist that define a given tauopathy. Despite this, the cause of tau aggregation remains elusive. Inflammation in the brain closely tracks with tau deposition in tauopathies. Degenerative inflammatory diseases of the CNS also exhibit tau accumulation. Although in the literature much less attention is given to the role of tau in these disorders, they further solidify a relationship between CNS inflammation and tau accumulation. The work described here focuses on expanding our understanding of tau seeding in neuroinflammatory conditions as well as in normal brain biology.

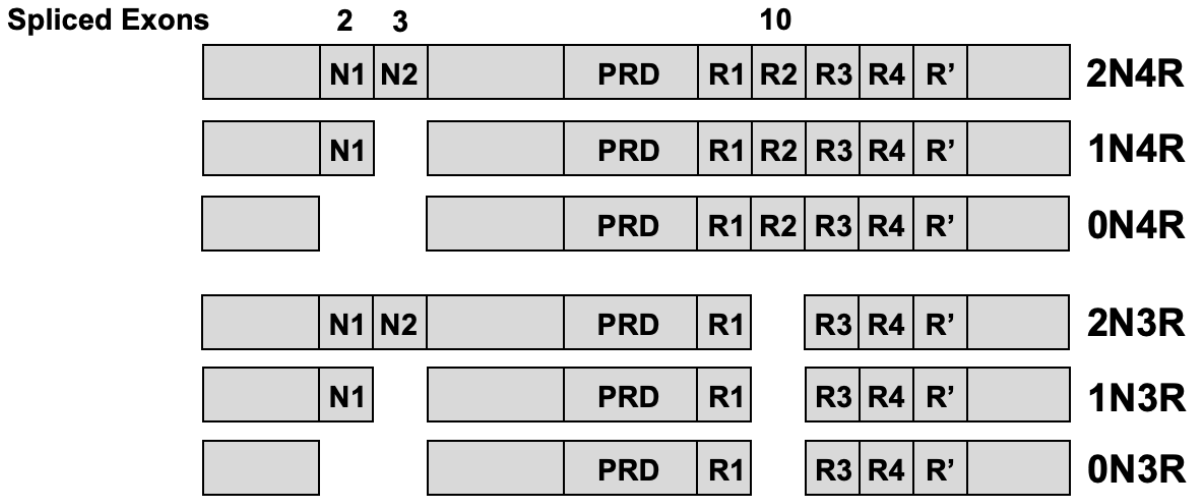

Figure 1.1. Schematic of tau splicing isoforms. Tau is expressed in the mature nervous system as a mix of isoforms containing 3 (3R) or 4 repeats (4R) based on the splicing of exon 10, corresponding to repeat 2. Alternative splicing of exon 3, or exon 2 and 3 yield three unique n-terminal variants (0N, 1N, 2N). Together, alternative splicing of tau generates three unique 4R isoforms and three unique 3R isoforms.

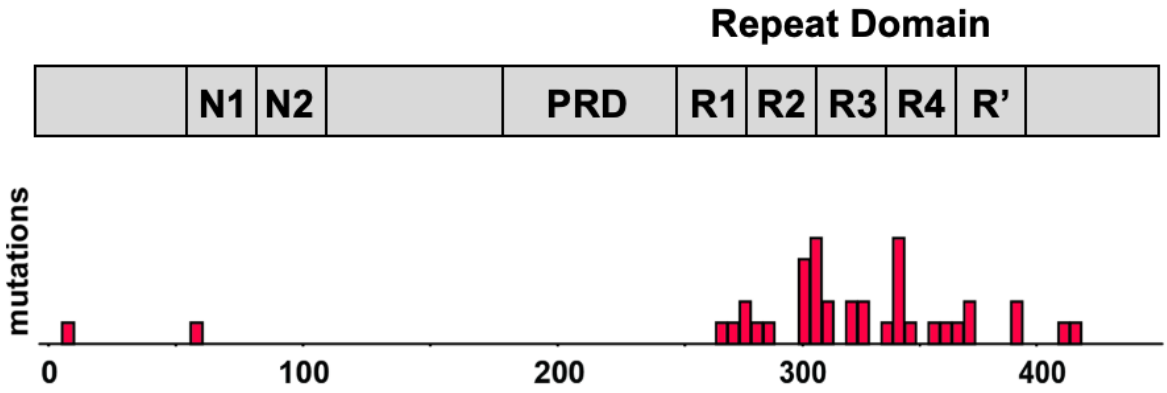

Figure 1.2. Disease causing mutations in tau primarily fall within or near the repeat domain, also known as the microtubule binding domain. Most mutations decrease tau's ability to bind microtubules while increasing its aggregation propensity (adapted from Vaquer-Alicea et al., 2021).

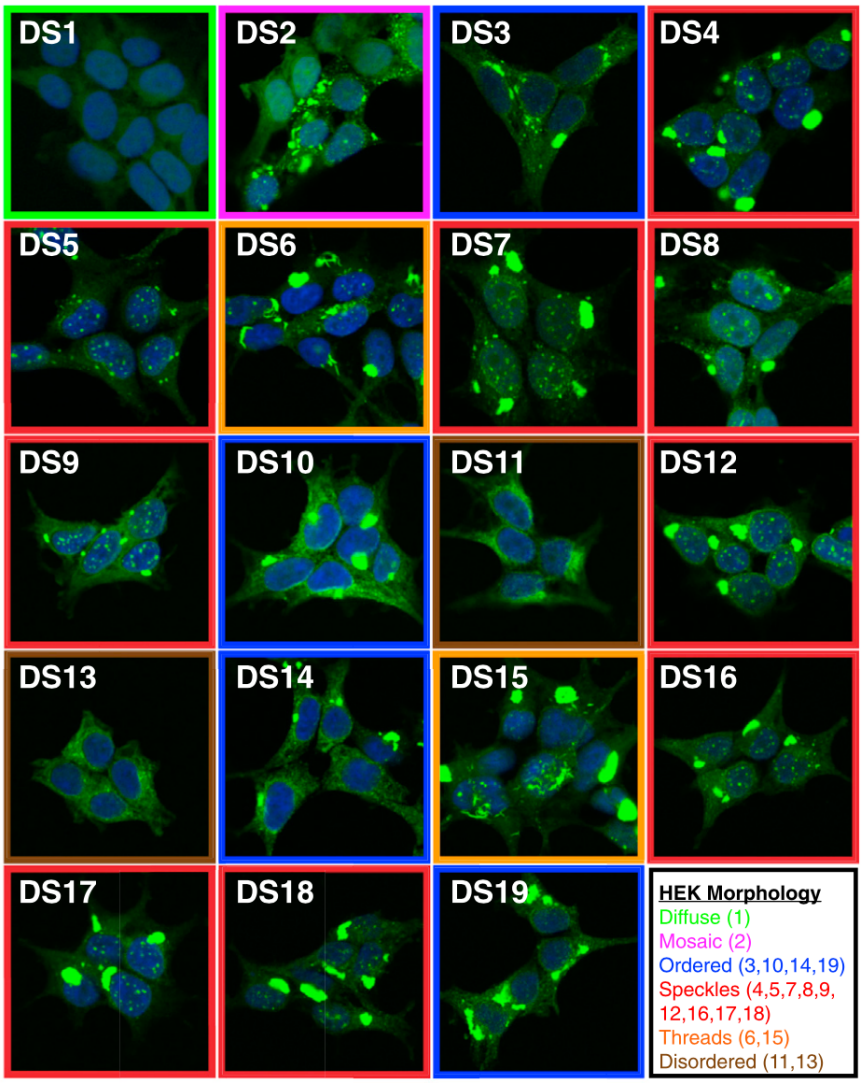

Figure 1.3. HEK cells expressing tau repeat domain with two familial tauopathy mutations (P301L/V337M) fused to yellow fluorescent protein display a variety of unique tau aggregate morphologies representing the isolation of putatively distinct tau strains. Aggregate-free DS1 cells were inoculated with recombinant fibrils or brain homogenate and monoclonal lines were isolated for inclusion morphology analysis (adapted from Kaufman et al., 2016).

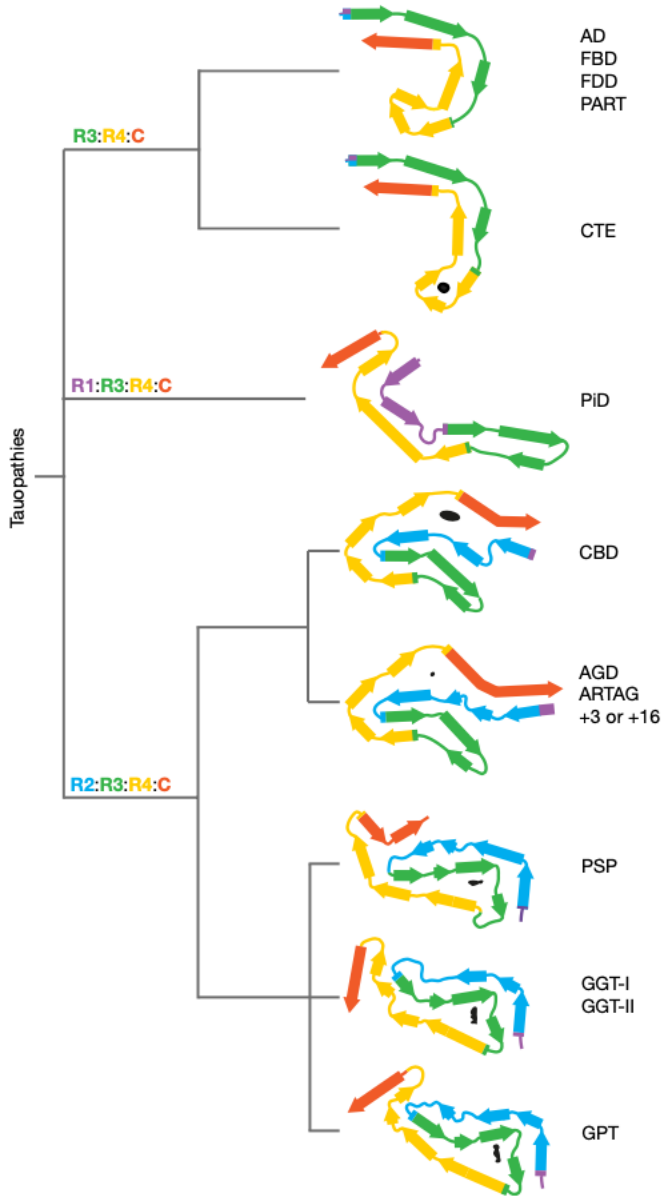

Figure 1.4. Tauopathies classified by cryo-EM structure. Tau fibrils can be organized based on a combination β-strand folding and the inclusion or exclusion of 3R/4R isoforms within the fibrils. The precise folding and alignment of beta strands differs amongst tauopathies, however, all tauopathy cores contain β-strands from R3 and R4 (adapted from Shi et al., 2021).

Chapter 2

A Search for Tau Seeds in Inflammatory CNS Disorders

Preface

This chapter contains unpublished data. All experiments were designed and performed by M.S.L. All text was written by M.S.L.

Specific critical reagents were provided as follows. Muscle Biopsies were provided by the Neuromuscular division of Neurology at the University of Texas Southwestern Medical Center. Nodding Syndrome sections were provided by Robert Colebunders of the University of Antwerp. Temporal Lobe Epilepsy biopsies were obtained and provided by Dr. Bradley Lega of the University of Texas Southwestern Medical Center,

ABSTRACT

Tauopathies are a class of over twenty diseases, typically neurological, defined by the aggregation of misfolded soluble tau and accumulation of deposited insoluble tau. Tau isolated from these diseases typically behaves as a prion to corrupt inert forms of the protein into seed competency. Many other diseases of the central nervous system, and even muscle, have been reported to contain tau aggregates when examined histologically. The ability of the tau aggregates to act as prions in these diseases has not been previously tested. Here we test if tau from three unique diseases, not considered to be tauopathies but reported to contain tau aggregates, has the capacity to act as a prion and self-assemble via templated conformational change. We find evidence that tau in biopsies of patients with temporal lobe epilepsy can act as a prion, while tau derived from fixed tissues of nodding syndrome and sporadic inclusion body myositis cannot. Further studies with larger samples sizes studying fresh frozen tissue will help to clarify these ongoing questions.

INTRODUCTION

In various diseases not yet defined as tauopathies, phosphorylated tau accumulation occurs in the brain or other tissues. Whether that is due to a lack of awareness, the diseases having other more prominent features that overshadow the tau accumulation, or some combination of these and or other factors is unknown. Included in this group are sporadic inclusion body myositis (sIBM), nodding syndrome (NS), temporal lobe epilepsy (TLE), and even the pediatric neurological disorder caused by measles virus, subacute sclerosing panencephalitis (SSPE) (Askanas et al., 2015; McQuaid *et al.*, 1994; Pollanen *et al.*, 2018; Tai et al., 2016). It remains unclear if the tau deposition seen in these potential tauopathies is a reflection of tau adopting conformations that act as prions. If so, it would argue strongly that tau has a critical role in the degenerative aspects of these diseases, and would suggest they be defined as secondary tauopathies.

Tau and Sporadic Inclusion Body Myositis

Sporadic inclusion body myositis (sIBM) is a late onset inflammatory myopathy, the most common acquired myopathy for those over the age of 50 (de Camargo et al., 2018). sIBM is characterized biochemically by inflammatory infiltration of the muscle tissue and the subsequent abnormal deposition of protein aggregates. In addition to protein deposition, a marked degenerative phenotype is typical for cases of sIBM. Interestingly, amyloid-beta and phosphorylated tau in paired helical filaments is found within muscle fibers (Askanas *et al.*, 2015), rendering the biochemical phenotype quite similar to that of protein deposition seen in AD.

Of clinical significance, Tau positron emission tomography imaging can be used to diagnose sIBM (Zhang et al., 2020b). Early reports of tau in sIBM showed accumulation within rimmed vacuoles and immunoreactivity on western blotting demonstrated reactivity for larger isoforms than what is seen in CNS tauopathies (Maurage et al., 2004). One study on a mouse model of sIBM indicated that inflammation activates the GSK3-beta kinase pathways, which in turn phosphorylate tau, similar to what is seen in AD (Kitazawa et al., 2008). Despite this body of work, the exact mechanistic pathways tying inflammation to neurodegeneration in human sIBM are still not well understood. In addition, it is completely unknown whether the tau aggregates present in sIBM are seed competent, and how that may be contributing to the degenerative aspect of sIBM.

Tau and Nodding Syndrome

Nodding Syndrome (NS) is a rare pediatric, epileptic disease endemic to Uganda. NS is characterized by atonic seizures, cognitive impairment, and brain atrophy and degeneration. The leading theory behind the cause of NS is that it is an autoimmune disorder caused by molecular mimicry initiated after infection with the parasitic worm *Onchocerca Volvulus* (Johnson et al., 2017). Recently, NS was reported to be a tauopathy (Pollanen *et al.*, 2018). Pollanen et al. found neurofibrillary tangles throughout the cerebral cortex with routine tau histochemical staining. When they examined their cohort for phosphorylated tau, they described tangles and pretangles with immunoreactivity in neuropil and neuropil threads. Tau accumulation was distributed throughout the brain, with most severe changes occurring in the

prefrontal cortex, temporal, and parietal cortices. Despite these robust findings, the field has not accepted NS as a tauopathy, with some groups arguing that NS is defined more by its neuroinflammatory signature and less by the accumulation of phosphorylated tau (Hotterbeekx et al., 2018). Despite the discordance of viewpoints, it remains possible that there is interplay between tau and neuroinflammation that leads to tau deposition, which in turn contributes to the degeneration of the NS brain (Pollanen et al., 2022).

Tau and Temporal Lobe Epilepsy

Temporal lobe epilepsy (TLE) is a common disorder that features seizures and other comorbidities such as cognitive impairment (Hermann and Seidenberg, 2007). Progressive cognitive decline has been shown in people with TLE (Jokeit and Ebner, 1999; Oyegbile et al., 2006). The factors leading to progressive degeneration of cognitive function in TLE are unknown. In one cohort of TLE patients, roughly two thirds of TLE cases examined showed tau pathology at Braak stages 2-4, with a significant increase of cases in middle Braak stages with middle cage compared to non-epileptic age matched controls (Thom et al., 2011). Additionally, tau levels in CSF have been found to increase after seizure (Palmio et al., 2009). In one comprehensive analysis of temporal lobe resections from patients who had surgical resection for the treatment of TLE, 31 of 33 (94%) of cases demonstrated tau pathology (Tai *et al.*, 2016). Tai et al. also found that the extent of tau pathology in a given case, the greater cognitive decline that subject experienced over the following year. Taken together, their results suggest the presence of epilepsy-related tauopathy, which may explain the cognitive decline in TLE. Interestingly, other diseases have prominent seizure phenotype

and have been shown to harbor hyperphosphorylated tau, including focal cortical dysplasia, Christanson Syndrome, hemimegalencephaly, SYNJ1 mutations, and nodding syndrome (Dyment et al., 2015; Garbern et al., 2010; Pollanen *et al.*, 2018; Sarnat et al., 2012; Sen et al., 2007).

Studies of animal models of seizures have also yielded a relationship between seizure and tau. Tau reduction, genetically or through anti-sense oligonucleotides has been shown to ameliorate seizure phenotypes in AD mouse models as well as in chemically induced seizure models (DeVos *et al.*, 2013; Roberson *et al.*, 2007), suggesting that tau plays a critical role in regulating neuronal hyperexcitability. Even in mouse models of autism with seizure phenotypes, tau reduction prevents seizures (Tai et al., 2020). And when tau is altered to make it more prone to aggregate via mutations that cause human FTD and overexpressed in mouse brain, spontaneous epileptic activity ensues (Garcia-Cabrero et al., 2013). Ultimately, the key mechanistic links between tau deposition, neuronal excitability, and epilepsy remain to be determined. However, the frank accumulation of tau in a majority of TLE cases that is associated with accelerated cognitive decline suggests that it is plausible that conformation change of tau into seed competent species may be underpinning these findings.

With abundant evidence that tau deposition is a feature of these three diseases, we sought out to test if tau adopts seed competent conformations in the muscle tissue of sIBM, and the brains of those with NS and TLE, using well characterized and highly sensitive tau seed biosensors.

MATERIALS AND METHODS

Biosensor Cell Line v2H

Highly sensitive second-generation tau biosensor cells termed v2H (Hitt et al., 2021) were used for seeding assays. These cells are based on expression of tau repeat domain fragment (246-378) containing the disease-associated P301S mutation (tau-RD) fused to mCerulean3 or mClover3 (Figure 2.1). The v2H line was selected for high expression with low background signal and high sensitivity. Seeding experiments used previously established protocols (Holmes et al., 2014).

Cell Culture

v2H biosensors were grown in Dulbecco's Modified Eagle's medium (Gibco) supplemented with 10% fetal bovine serum (HyClone), and 1% glutamax (Gibco). For terminal experiments, 1% penicillin/streptomycin (Gibco) was included. Cells were tested free of mycoplasma (VenorGem, Sigma) and cultured at 37°C with 5% CO_2 in a humidified incubator. To avoid false-positive signal from v2H biosensors, cells were passaged prior to ~80% confluency.

Human Brain Samples

AD and control brain tissues were obtained through the Neuropathology Core with Institutional Review Board (IRB) approval at University of Texas Southwestern Medical Center. Epilepsy biopsies were obtained through Dr. Bradley Lega in collaboration with Dr. Gena Konopka with Institutional Review Board (IRB) approval at University of Texas

Southwestern Medical Center. All nodding syndrome brain samples were obtained from the University of Antwerp in collaboration with Dr. Robert Colebunders. Informed written consent for donation of tissue was obtained from next of kin prior to collection. Brains were fixed, fixed and then frozen in liquid nitrogen for long-term storage at -80°C, or sectioned and flash frozen in liquid nitrogen for long-term storage at -80°C. Pulverized fresh frozen tissue from the cortex was used to prepare total soluble protein lysates and fixed tissue was was used to prepare brain lysates where indicated or used for immunohistochemical analysis.

Human Sample Preparation

Fresh frozen pulverized tissue or fixed tissue was suspended in tris-buffered saline (TBS) containing cOmplete mini protease inhibitor tablet (Roche) at a concentration of 10% w/vol. Parrafin-embedded formalin-fixed (PEFF) tissues were washed in 70°C ethanol 5 times followed by drying and weighing. Dried PEFF tissues were then suspended in tris-buffered saline (TBS) containing cOmplete mini protease inhibitor tablet (Roche) at a concentration of 10% w/vol. Samples were then dounce homogenized, followed by pulsing probe sonication at 75 watts for 10 min (Q700, QSonica) on ice in a hood. The sonication probe was washed with a sequence of ethanol, bleach, and distilled water to prevent cross-contamination. Lysates were then centrifuged at 23,000 x g for 30 min and the supernatant was retained as the total soluble protein lysate. Protein concentration was measured with the BCA assay (Pierce). Fractions were aliquoted and stored at -80°C prior to immunoprecipitation and seeding experiments.

Immunoprecipitation from protein lysate or tau monomer

Immunoprecipitations were performed using 50 µL of magnetic Protein A Dynabead slurry (Thermofisher), washed twice with immunoprecipitation (IP) wash buffer (0.05% Triton-X100 in PBS), followed by a 1 hour room temperature incubation with 20 µg of anti-tau antibody. Beads were washed three times in IP wash buffer, 1000 µg of total protein lysate or 500 ng of recombinant tau monomer was added to the Protein A/anti-tau antibody complexes on the beads and rotated overnight at 4 °C. After overnight incubation, supernatant was removed as the tau-depleted fraction and the beads were washed three times in IP wash buffer and then moved to clean tubes for elution. IP wash buffer was removed and beads were then incubated in 65 µL of IgG Elution Buffer (Pierce) for 7 min to elute tau. The elution buffer was collected in a separate microcentrifuge tube and a second elution step in 35 µL of IP elution buffer was performed for 5 min and pooled with the initial elution. The elution was then neutralized with 10 µL of Tris-HCl pH 8.4 to finalize the tau-enriched IP pellet.

Transduction of biosensor cell lines, flow cytometry and seeding analyses

The seeding assay was conducted as previously described (Holmes *et al.*, 2014) with the following changes: v2H cells were plated 20 hours before seed transduction at a density of 16,000 cells/well in a 96-well plate in a media volume of 180 µL per well. Mouse and human total protein lysates were thawed on ice, while tau-depleted IP supernatants and tau-enriched IP pellets were isolated just before seeding. For total protein lysates and tau-depleted supernatants 1-10 µg of protein was used per well as indicated. For tau-enriched pellets, 1-10

μL of elution was used per well as indicated. Samples were incubated for 30 min with 0.5 μL Lipofectamine 2000 (Invitrogen) and OptiMEM such that the total treatment volume was 20 μL. For each experiment, cells treated with OptiMEM alone and Lipofectamine 2000 in OptiMEM were used as negative controls. The v2H line, which expresses high levels of tau RD, can show false-positive FRET signal when treated with Lipofectamine 2000, which is mitigated by passaging prior to ~80% confluency. Recombinant tau fibrils at 1 pM and 100 fM (monomer equivalent) were used for positive controls. Cells were incubated for an additional 48 hours after treatment prior to harvesting. Cells were harvested with 0.25% trypsin and fixed in 4% PFA for 10 min, then resuspended in flow cytometry buffer (HBSS plus 1% FBS and 1 mM EDTA). The LSRFortessa SORB (BD Biosciences) was used to perform FRET flow cytometry. Single cells double-positive for mCerulean and mClover were identified and the % FRET positive cells within this population was quantified following a gating strategy previously described (Holmes *et al.*, 2014). For each experiment 10,000 cells were analyzed in triplicate. Flow data analysis was performed using FlowJo v10 software (Treestar).

Immunofluorescence

30 μm parrafin-embedded fixed sections were cut and stained with biotinylated monoclonal AT8 primary antibody (Invitrogen) diluted 1:1000 in normal goat serum followed by secondary incubation with AlexaFluor-594 conjugated streptavidin diluted 1:500. Images were obtained using the LSM 780 Inverted confocal microscope (Zeiss) and analyzed via Imaris 9 software (Oxford Instruments).

Statistical analyses

Coded samples were obtained by M.S.L. from the lab of C.A.T. M.S.L. remained blinded prior to all seeding analyses. Flow cytometry gating and analysis of seeding activity was completed prior to decoding and interpreting the results. All statistical analysis was performed using GraphPad Prism v9.2.0 for Mac OS and Excel v16.52 (Microsoft).

RESULTS

To test if the inflammation in IBM induces tau seeding activity within muscle tissue, we obtained 11 frozen biopsies from individuals with IBM. We prepared clarified lysate from the frozen biopsies and transduced 10 μL of muscle tissue lysate into v2L and v2H biosensors. We found no evidence of seeding activity when using either biosensor cell line (Figure 2.1). We concluded that tau seeds are not present at detectable levels within IBM muscle tissues.

Evidence suggests that phosphorylated tau accumulates heavily in some cases of Nodding Syndrome. To test if that accumulation coincides with the presence of tau seeds, we analyzed PEFF tissues from various regions of two Nodding Syndrome brains. Clarified lysates were prepared from PEFF tissues sections from the and increasing volumes of lysate were introduced into v2H biosensors. PEFF sections from control and AD brains were used as negative and positive controls, respectively. We found little evidence of tau seeding in fixed sections from the initial brain regions of Nodding Syndrome that we tested (Figure 2.2 B,C), with only the frontal cortex of Nodding Syndrome Case 1 showing statistically significant seeding. The AD positive control did show seeding activity, suggesting that tau seeds can be detected in fixed tissues (Figure 2.2 D). To extend our analysis, we prepared clarified lysates from the remaining tissue regions. We found no evidence of tau seeding activity in the clarified lysates derived from Nodding Syndrome PEFF tissues (Figure 2.3), while positive seeding was detected in AD fixed tissues. Interestingly, on repeat analysis the frontal cortex of Case 1 did not show any seeding activity. Finally, a third case of Nodding Syndrome that

was not paraffin embedded, merely fixed, was used to prepare clarified lysates. There was no significant seeding activity in any region analyzed (Figure 2.4 A,B). We concluded that tau seeding activity is undetectable in clarified lysates prepared from fixed Nodding Syndrome tissues.

As reports indicate phosphorylated tau accumulation in the brains of patients with TLE, we sought to test if temporal lobe biopsies taken for treatment refractory TLE contain tau seeds. We prepared clarified lysates from frozen biopsies of a pilot cohort of five subjects with TLE. We were able to detect statistically significant seeding in the lysate from one of biopsies tested (Figure 2.5 A). To improve our detection sensitivity, we performed tau immunopurification using the conformation specific antibody MD3.1 and tested the immunoprecipitation pellets for tau seeding activity. We detected statistically significant tau seeding in one additional biopsy, as well as detecting tau seeding activity in the originally positive case (Figure 2.5 B). Fixed sections were obtained from the same biopsies and stained with the anti-phospho tau antibody AT8, the standard antibody used for neuropathological examination of tau pathology. Moderately positive somatic staining and minor staining of neurotic processes was observed in three of the five cases, while AD brain showed markedly positive neurons and processes (Figure 2.6).

DISCUSSION

In summary, we were unable to detect tau seeds in fixed muscle tissue or fixed brain tissue from sIBM or NS, respectively. We did, however, detect significant seeding in the temporal lobe biopsies of two of five TLE cases, as well as identified AT8-positive neurons in three of five TLE cases.

Tau Seeding in IBM and Nodding Syndrome

While we ultimately did not detect tau seeding in sIBM tissues or NS tissues, this does preclude the possibility that tau seed are present in these diseases. First most, the tissues we analyzed came from fixed specimens. As evidenced by the generally low seeding activity of AD fixed tissue derived lysates compared to fresh frozen derived lysates, fixation appears to drastically reduce the availability of tau seeds to be detected in our biosensor systems. It is plausible that the mere fixation of the sIBM and NS tissues abolished what tau seeding activity may have been present. In addition, it is known that the conformation of particular tau strains renders them more or less detectable to Tau(P301S)-expressing biosensors. A biosensor with different mutations in the expressed RD of tau may better detect seeds that may be present in sIBM or NS, if any are. Finally, immunopurification of tau from clarified lysates generally improves our detection sensitivity. This was not performed. Future studies on fresh frozen tissue that include immunopurification with a panel of different tau antibodies would be more definitive in ruling in or out the presence of tau seeds in sIBM and NS.

Tau Seeding in TLE

In our small cohort of TLE cases, we detected statistically significant seeding in two of five cases after immunoprecipitation. We also identified clear neuronal AT8 staining in three of five, indicating that tau is pathologically phosphorylated in those cases. Without a larger sample size, it is difficult to make definitive conclusions regarding the presence of tau seeds in TLE as a whole. In addition, the seeding level we detected in the two cases of TLE was on the higher range, but potentially within normal limits, compared to seeding activity detected in healthy brain (chapter 4), which confounds our interpretation of the seeding found in TLE. It does remains possible that tau accumulation in TLE and even tau seeding may play a role in mediating the degenerative aspect of some cases of TLE. However, future studies with larger cohorts are required to further elucidate the role of tau seeds in mediating features of TLE.

In summary, the full scope of what diseases should be considered secondary tauopathies remains to be fully uncovered. Future studies should focus on using large cohorts and study fresh frozen tissues for more definitive analysis.

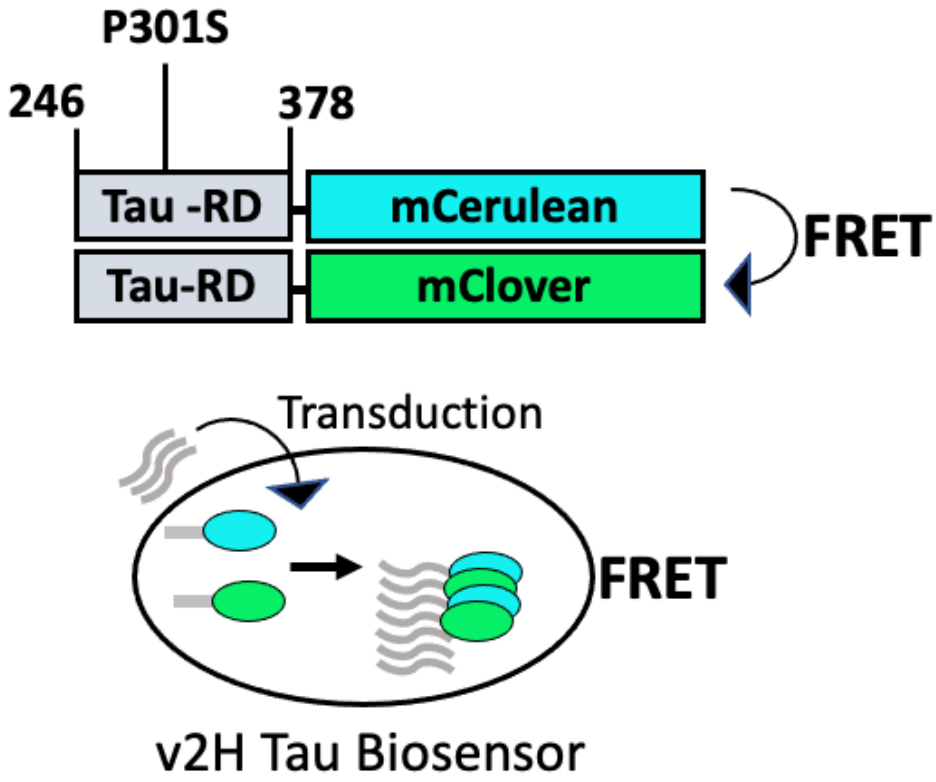

Figure 2.1. A schematic of the v2H Tau-RD(P301S) biosensors used for the detection of tau seeds. Tau-RD (amino acids 246-378 of the 2N4R isoform) are expressed with mCerulean and mClover fluorescent proteins, which can participate in FRET when in close proximity. Tau seeds are transduced into the biosensor cells via Lipofectamine, where they interact with and initate the aggregation of the tau-RD constructs. mCerulean and mClover within aggregates can participate in FRET which is detected via flow cytometry.

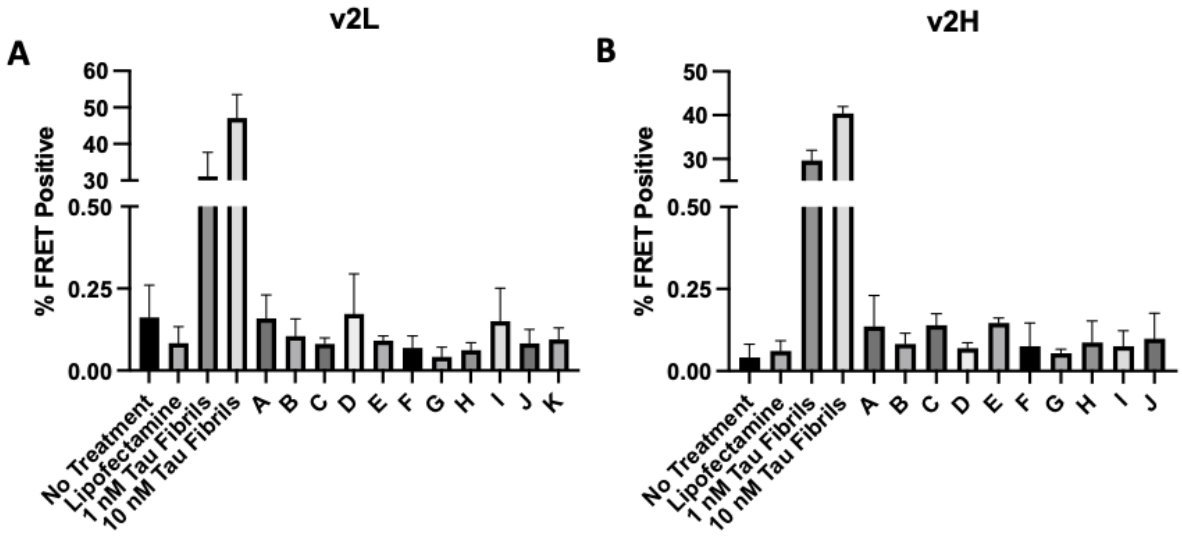

Figure 2.2. No tau seeding activity was detected above control cells in a pilot cohort of muscle biopsies taken from patients with Inclusion Body Myositis. 48 hours after treatment cells were fixed and analyzed via FRET flow cytometry. (**A**) v2L biosensors were treated with 10ug of IBM muscle biopsy lysate, tau fibrils as a positive control, and Lipofectamine as a negative control. Cells were incubated for 48 hours prior to quantification of FRET-positive cells. (**B**) v2H biosensors were treated with 10ug of IBM muscle biopsy lysate, tau fibrils as a positive control, and Lipofectamine as a negative control, and incubated for 48 hours prior to quantification of FRET-positive cells.

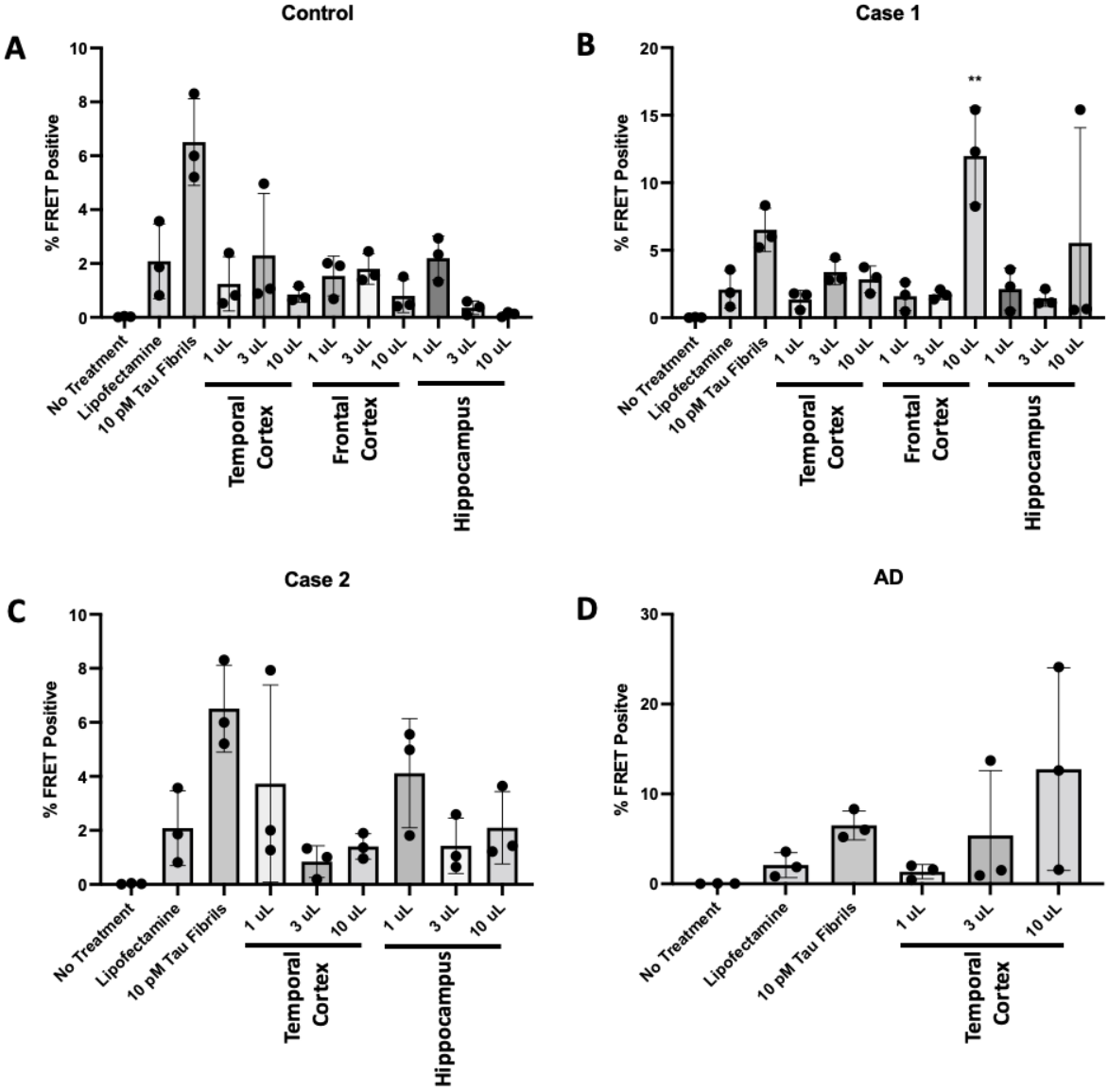

Figure 2.3. Initial screening of various brain regions from two cases of Nodding Syndrome revealed no significant tau seeding activity from paraffin-embedded formalin-fixed tissue sections. Cells were fixed and analyzed via FRET flow cytometry 48 hours after treatment. (**A**) No tau seeding activity was detected in age-matched control brain clarified protein homogenate prepared from paraffin-embedded formalin-fixed tissue. Increasing volumes of homogenate was transduced into v2H biosensors. (**B**) No seeding activity detected in PEFF

tissue from Nodding Syndrome Case 1 using v2H biosensors. (**C**) No seeding activity detected in PEFF tissue from nodding syndrome Case 2 using v2H biosensors. (**D**) Seeding activity was detected in PEFF tissue from the temporal cortex of an AD case used as a positive control with v2H biosensors. Statistical significance was determined by performing one-way ANOVA followed by Dunnett's multiple comparisons testing of all samples compared against Lipofectamine treated negative controls, *$p < 0.05$, **$p < 0.01$, ***$p < 0.001$, ****$p < 0.0001$. Errors bars = S.D.

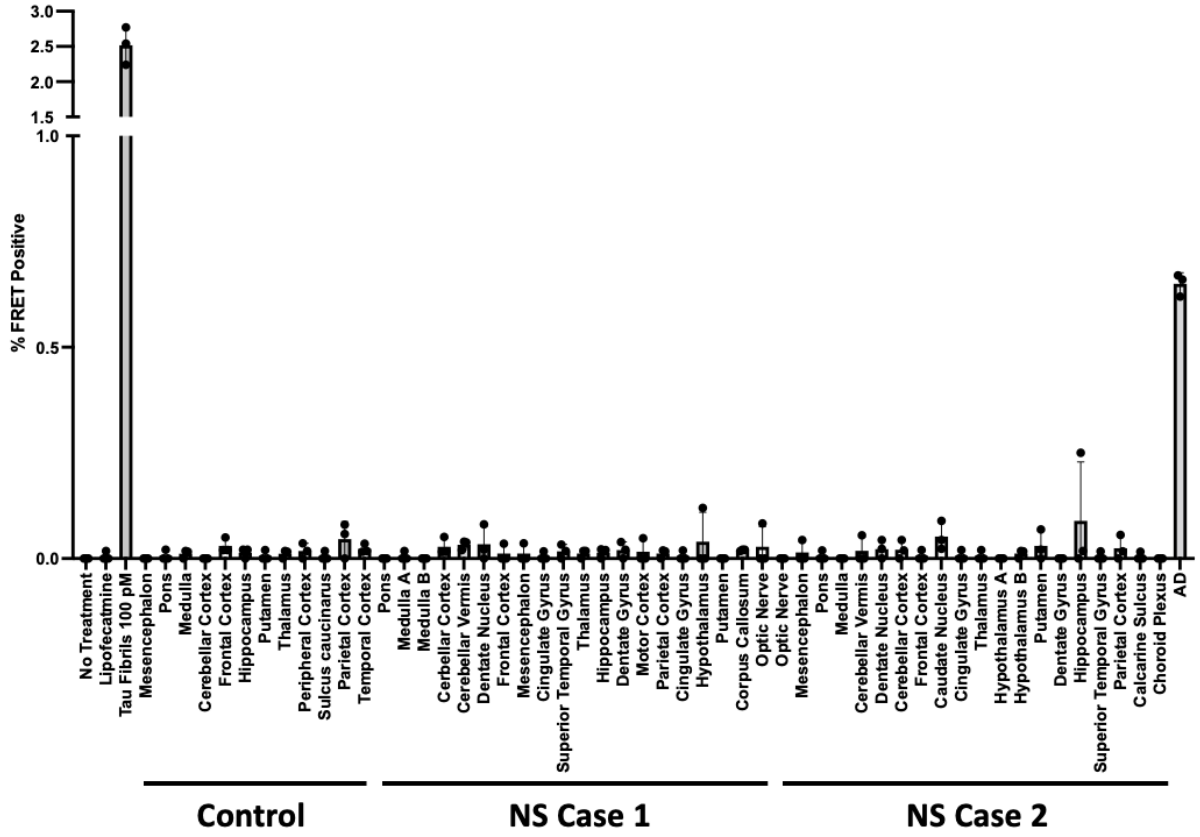

Figure 2.4. Further regional analysis of two Nodding Syndrome cases did not reveal tau seeding activity in brain region. Tissue homogenates derived from PEFF sections from nodding syndrome, negative control, and an AD positive control case were used to treat v2H biosensor cells. 10 µL of lysate was transduced into v2H biosensors. Cells were fixed and analyzed via FRET flow cytometry 48 hours after treatment.

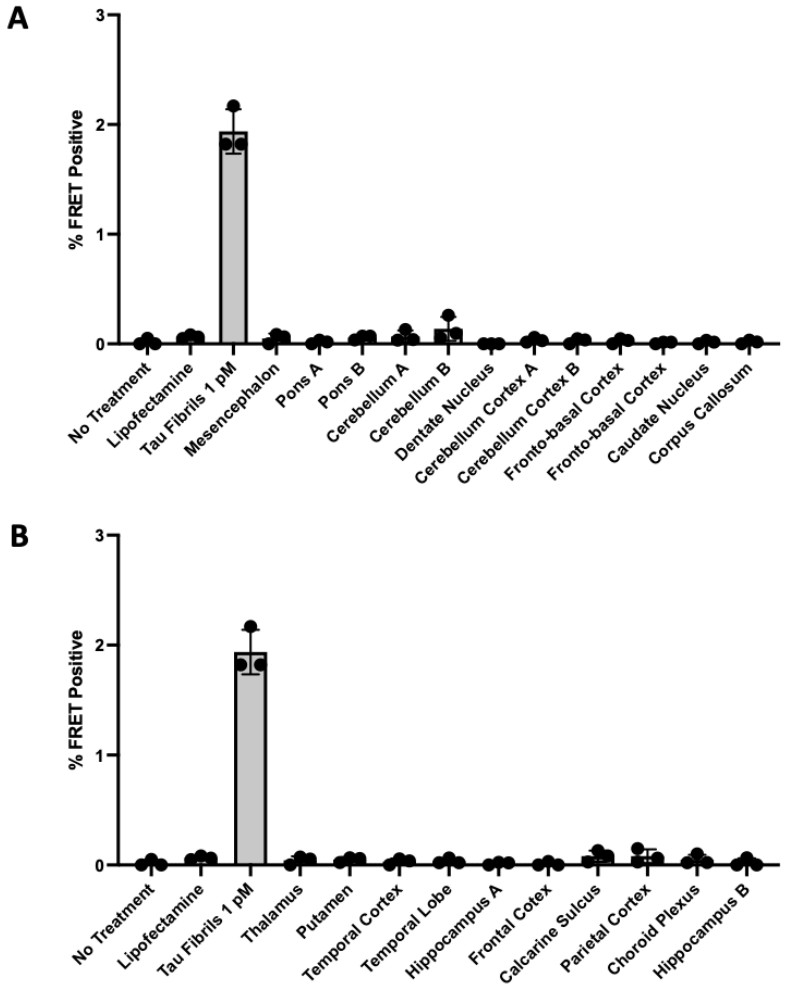

Figure 2.5. Analysis of a third case of Nodding Syndrome revealed no seeding activity. Fixed tissue was used to create total (T) clarified lysate [10% (wt/vol). 10 µL of lysate was transduced into v2H biosensors. Cells were fixed and harvested after 48 hours for FRET flow cytometry analysis. (**A**) No tau seeding was detected in any of the first twelve regions from nodding syndrome Case 3. (**B**) No tau seeding activity was detected in any of the ten additional regions from nodding syndrome Case 3.

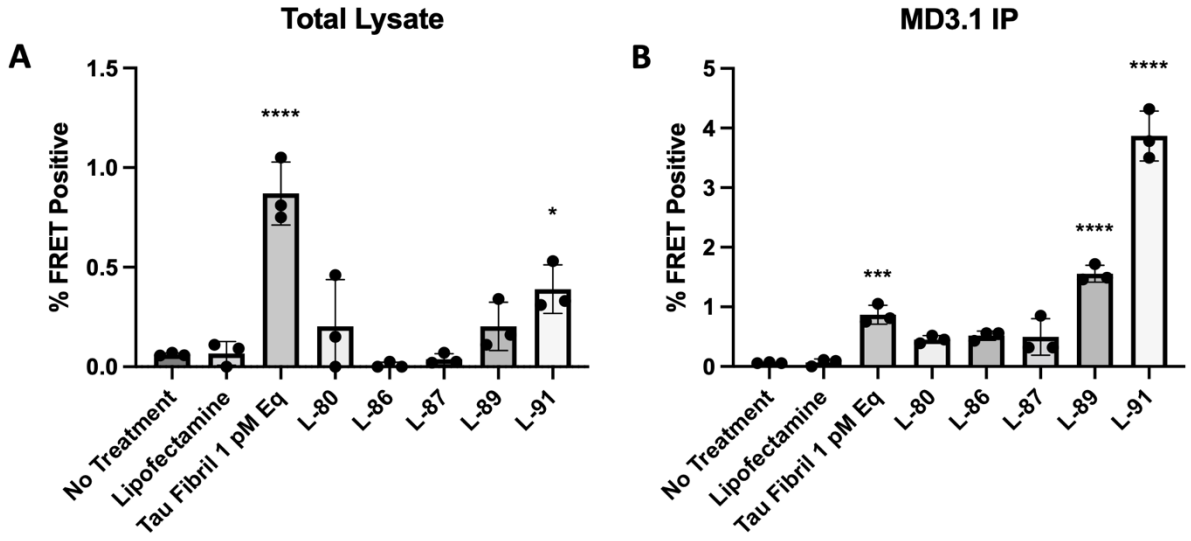

Figure 2.6. Tau seeding is detected in temporal lobe biopsies from two cases of temporal lobe epilepsy. Temporal Lobe biopsy fresh frozen samples from 5 individuals with intractable temporal lope epilepsy were used to create total (T) clarified lysate [10% (wt/vol)] followed by immunoprecipitation (IP) with the MD3.1 antibody to generate a tau enriched pellet (P). Tau seeding was reliably detected in two of five IP pellets. (**A**) Seeding from total lysate of five cases of temporal lobe epilepsy. (**B**) Seeding from tau-enriched IP pellets shows statistically significant seeding in two cases of temporal lobe epilepsy. Columns represent the mean FRET positivity from three technical replicates (dots). Statistical significance was determined by performing one-way ANOVA followed by Dunnett's multiple comparisons testing of all samples compared against Lipofectamine treated negative controls, *$p < 0.05$, **$p < 0.01$, ***$p < 0.001$, ****$p < 0.0001$. Errors bars = S.D.

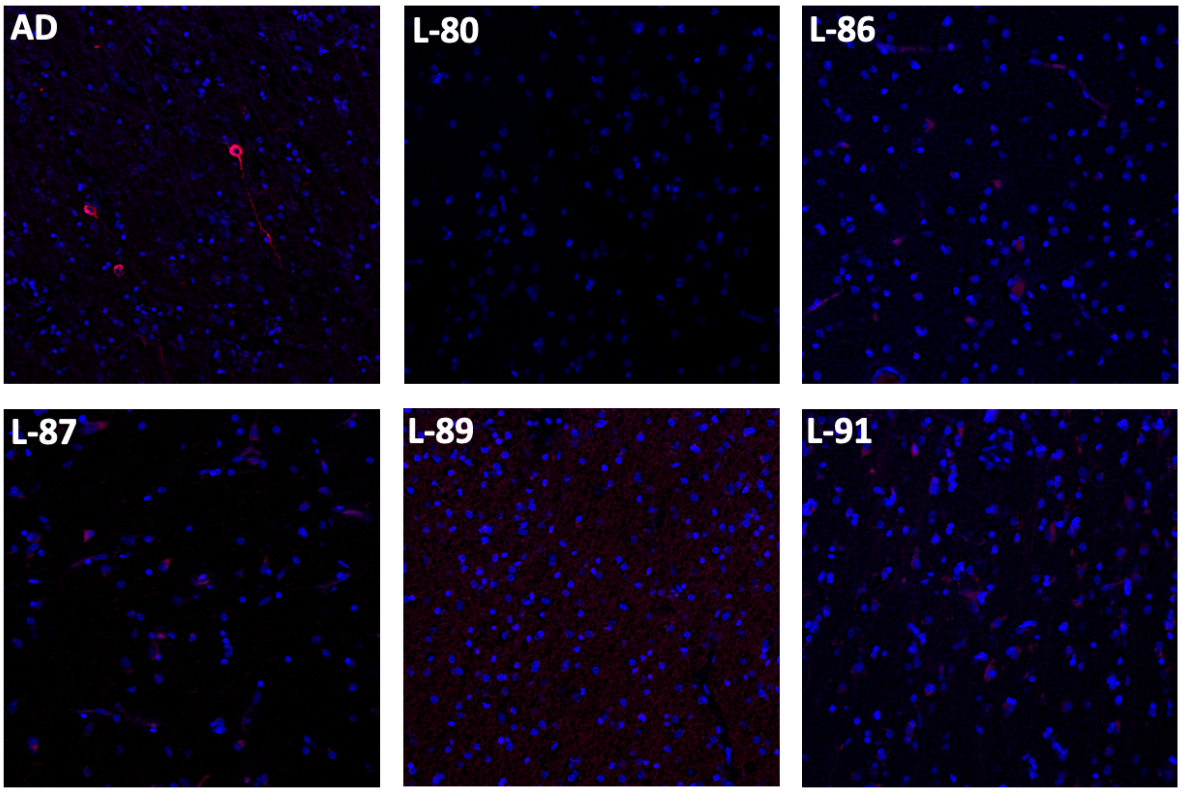

Figure 2.7. AT8 (red) and DAPI (blue) staining in five cases of temporal lope epilepsy reveals weak to moderate positivity in three cases of TLE. (**Top Left**) An AD case used as positive control demonstrates dystrophic neurite staining, a classic finding in AD. (**Top Middle**) Little to no staining is found in TLE case L-80. (**Top Right**) Minor staining of somas and axons is present in TLE case L-86. (**Bottom Left**) Moderate staining of several somas and neuronal processes is present in TLE case L-87. (**Bottom Middle**) TLE case L-89 demonstrates high background signal staining without specific neuronal staining. (**Bottom Right**) Moderate staining of several somas and neuronal processes are present in TLE case L-91.

Chapter 3

Tau Seeding in Multiple Sclerosis

PREFACE

This chapter contains a manuscript in preparation:

LaCroix, M.S., Mirbaha, H., Shang, P., White, C.L., Stuve, O., Diamond, M.I. Tau Seeding in a Case of Multiple Sclerosis. Manuscript in preparation.

Author contributions for the citation above:

Author Contributions: M.S.L. and M.I.D. designed research; M.S.L and P.S. performed research; H.M. contributed new reagents; M.S.L., C.L.W., O.S. and M.I.D. analyzed data; M.S.L. and M.I.D. wrote the text.

ABSTRACT

Multiple Sclerosis is a chronic inflammatory disorder of the central nervous system characterized by lymphocytic infiltration leading to demyelination and the destruction of axons. Most cases of MS begin with a relapsing phyenotype and transition to a progressive phenotype with a strong neurodegenerative component. It is currently unclear what mediates the neurodegenerative aspect of MS. Evidence of tau accumulation in and around multiple sclerosis lesions suggests that tau may be a key mediator of neurodegeneration in MS. We hypothesized that tau seed propagation may contribute to the neurodegeneration seen in MS. To test this, we used tau biosensors in combination with immunopurification. We detected tau seeding activity in a cohort of MS patients and across the brain of a single case. Based on the ability of a panel of tau antibodies to isolate tau seeds from MS brain lysate, the conformation of tau assemblies from MS brain appear to differ from AD and control brain. This is the first report of tau seeds in MS brain and positions tau as a critical mediator of neurodegeneration in MS, as well as other inflammatory conditions that show tau accumulation.

INTRODUCTION

Multiple sclerosis (MS) is a heterogeneously presenting chronic inflammatory disorder of the central nervous system characterized by lymphocytic infiltration leading to demyelination and destruction of axons (Compston and Coles, 2008). The disease course of MS varies. The most common presentation is relapsing-remitting, in which lesions affect separate CNS sites at different times and generally respond to immunotherapy. A substantial fraction transition to a secondary-progressive neurodegenerative phase that is refractory to therapy. A minority of cases present with an initial progressive course (Bar-Or and Li, 2021; Lassmann et al., 2012). Despite these differences, epidemiological evidence supports a primary neurodegenerative process shared in all cases of MS (Milo et al., 2020; Trapp and Nave, 2008). The cause of MS is unknown, but prior reports have suggested that pathological tau aggregation of the microtubule associated protein tau might underlie this neurodegenerative process.

The formation of tau assemblies, typically detected by immunohistochemistry, is known to underlie myriad disorders collectively known as “tauopathies” (Lee and Trojanowski, 1999). In many tauopathies it has been possible to detect detergent-insoluble filaments, which are now known to be comprised of distinct, disease-associated structures (Sanders *et al.*, 2014; Shi *et al.*, 2021). Considerable experimental evidence suggests that prion mechanisms may underlie the progression of neurodegenerative tauopathies, whereby pathological assemblies that form in one or several neurons, exit those cells, gain entry to connected neurons, and thereby propagate disease through specific brain networks, dependent on their conformation

(Vaquer-Alicea *et al.*, 2021). The detection of tau "seeds," which are conformers that have the ability to serve as templates for their own replication, has been facilitated through the development of specialized "biosensor" cell systems based on expression of the core tau repeat domain fused to fluorescent proteins. Biosensor cells are highly sensitive and specific for tau pathology (Hitt *et al.*, 2021; Holmes *et al.*, 2014), and have been used by our group and others to quantify levels of pathological tau in a variety of disease states.

Several studies have indicated that tau accumulates in progressive MS, as measured both by the presence of phospho-tau epitopes in brain (Anderson et al., 2008; Anderson *et al.*, 2009; 2010). Insoluble tau has been reported in in progressive MS, but not in relapsing MS, which may reflect the cause of neurodegeneration (Anderson *et al.*, 2009; 2010). No prior studies have evaluated MS brain for the presence of tau seeds. Here, we test several sources of MS brain tissue for tau seeding activity before and after tau immunopurification enrichment.

MATERIALS AND METHODS

Biosensor Cell Line v2H

Highly sensitive second-generation tau biosensor cells termed v2H (Hitt *et al.*, 2021) were used for seeding assays. These cells are based on expression of tau repeat domain fragment (246-378) containing the disease-associated P301S mutation (tau-RD) fused to mCerulean3 or mClover3. The v2H line was selected for high expression with low background signal and high sensitivity. Seeding experiments used previously established protocols (Holmes *et al.*, 2014).

Cell Culture

v2H biosensors were grown in Dulbecco's Modified Eagle's medium (Gibco) supplemented with 10% fetal bovine serum (HyClone), and 1% glutamax (Gibco). For terminal experiments, 1% penicillin/streptomycin (Gibco) was included. Cells were tested free of mycoplasma (VenorGem, Sigma) and cultured at 37°C with 5% CO_2 in a humidified incubator. To avoid false-positive signal from v2H biosensors, cells were passaged prior to ~80% confluency.

Human Brain Samples

AD and control brain tissues were obtained through the Neuropathology Core with Institutional Review Board (IRB) approval at University of Texas Southwestern Medical Center. Multiple Sclerosis tissues were obtained through Dr Olaf Stuve in collaboration with

Montreal Neurological Institute at McGill University or the Neuropathology Core with Institutional Review Board (IRB) approval at University of Texas Southwestern Medical Center with Institutional Review Board (IRB) approval at University of Texas Southwestern Medical Center. Informed written consent for donation of tissue was obtained from next of kin prior to collection. Brains were fixed, fixed and then frozen in liquid nitrogen for long-term storage at -80°C, or sectioned and flash frozen in liquid nitrogen for long-term storage at -80°C. Pulverized fresh frozen tissue from the cortex was used to prepare total soluble protein lysates and fixed tissue was was used to prepare brain lysates where indicated or used for immunohistochemical analysis.

Human Sample Preparation

Fresh frozen pulverized tissue or fixed tissue was suspended in tris-buffered saline (TBS) containing cOmplete mini protease inhibitor tablet (Roche) at a concentration of 10% w/vol. Parrafin-embedded formalin-fixed (PEFF) tissues were washed in 70°C ethanol 5 times followed by drying and weighing. Dried PEFF tissues were then suspended in tris-buffered saline (TBS) containing cOmplete mini protease inhibitor tablet (Roche) at a concentration of 10% w/vol. Samples were then dounce homogenized, followed by pulsing probe sonication at 75 watts for 10 min (Q700, QSonica) on ice in a hood. The sonication probe was washed with a sequence of ethanol, bleach, and distilled water to prevent cross-contamination. Lysates were then centrifuged at 23,000 x g for 30 min and the supernatant was retained as the total soluble protein lysate. Protein concentration was measured with the BCA assay

(Pierce). Fractions were aliquoted and stored at -80°C prior to immunoprecipitation and seeding experiments.

Mouse lines

We used mice on BL6 background with the human MAPT gene knocked in at the mouse tau locus that express all six isoforms of human tau as a source of murine-expressed human tau (gift from Pfizer), and verified by genomic sequencing in the Diamond lab. All mice involved in this study were housed under a 12 hour light/dark cycle, and were provided food and water *ad libitum*. All experiments involving animals were approved by the University of Texas Southwestern Medical Center Institutional Animal Care and Use Committee (IACUC).

Experimental Autoimmune Encephalomyelitis

EAE was induced as described by (Steffen et al., 1996) with some modifications. Briefly, hTau mice were immunized with myelin peptide MOG35-55 (200 µg; Sigma Aldrich, M4939) in 200 µL of emulsified complete Freund's adjuvant (Sigma-Aldrich, F5506) containing *Mycobacterium tuberculosis* (2 mg/ml; Thermo Fisher Scientific, DF3114-33-8). 400 ng of pertussis toxin (Thermo Fisher Scientific, NC9282261) was administered intraperitoneally on days 0 and 2. Mice were allowed to survive as long as possible up to 70 days prior to sample collection and preparation.

Mouse sample collection and preparation

Mice were anesthetized with isoflurane and perfused with chilled phosphate buffered saline (PBS) + 0.03% heparin. The forebrain and cerebellum were separated and weighed prior to flash freezing in liquid nitrogen and storage at -80°C. As described previously for human tissues, fresh frozen forebrain was suspended in TBS containing cOmplete mini protease inhibitor tablet (Roche) at a concentration of 10% w/vol. Samples were then dounce homogenized, followed by pulsing probe sonication at 75 watts for 10 min on ice in a hood (Q700, QSonica). The sonication probe was washed with a sequence of ethanol, bleach, and distilled water to prevent cross-contamination of seeding activity. Lysates were then centrifuged at 23,000 x g for 30 min and the supernatant was retained as the total soluble protein lysate. Protein concentration was measured with the BCA assay (Pierce). Fractions were aliquoted and stored at -80°C prior to immunoprecipitation and seeding experiments.

Immunoprecipitation from protein lysate or tau monomer

Immunoprecipitations were performed using 50 µL of magnetic Protein A Dynabead slurry (Thermofisher), washed twice with immunoprecipitation (IP) wash buffer (0.05% Triton-X100 in PBS), followed by a 1 hour room temperature incubation with 20 µg of anti-tau antibody. Beads were washed three times in IP wash buffer, 1000 µg of total protein lysate or 500 ng of recombinant tau monomer was added to the Protein A/anti-tau antibody complexes on the beads and rotated overnight at 4 °C. After overnight incubation, supernatant was removed as the tau-depleted fraction and the beads were washed three times in IP wash buffer and then moved to clean tubes for elution. IP wash buffer was removed and beads were then incubated in 65 µL of IgG Elution Buffer (Pierce) for 7 min to elute tau. The

elution buffer was collected in a separate microcentrifuge tube and a second elution step in 35 µL of IP elution buffer was performed for 5 min and pooled with the initial elution. The elution was then neutralized with 10 µL of Tris-HCl pH 8.4 to finalize the tau-enriched IP pellet.

Transduction of biosensor cell lines, flow cytometry and seeding analyses

The seeding assay was conducted as previously described (Holmes *et al.*, 2014) with the following changes: v2H cells were plated 20 hours before seed transduction at a density of 16,000 cells/well in a 96-well plate in a media volume of 180 µL per well. Mouse and human total protein lysates were thawed on ice, while tau-depleted IP supernatants and tau-enriched IP pellets were isolated just before seeding. For total protein lysates and tau-depleted supernatants 1-10 µg of protein was used per well as indicated. For tau-enriched pellets, 1-10 µL of elution was used per well as indicated. Samples were incubated for 30 min with 0.5 µL Lipofectamine 2000 (Invitrogen) and OptiMEM such that the total treatment volume was 20 µL. For each experiment, cells treated with OptiMEM alone and Lipofectamine 2000 in OptiMEM were used as negative controls. The v2H line, which expresses high levels of tau RD, can show false-positive FRET signal when treated with Lipofectamine 2000, which is mitigated by passaging prior to ~80% confluency. Recombinant tau fibrils at 1 pM and 100 fM (monomer equivalent) were used for positive controls. Cells were incubated for an additional 48 hours after treatment prior to harvesting. Cells were harvested with 0.25% trypsin and fixed in 4% PFA for 10 min, then resuspended in flow cytometry buffer (HBSS plus 1% FBS and 1 mM EDTA). The LSRFortessa SORB (BD Biosciences) was used to

perform FRET flow cytometry. Single cells double-positive for mCerulean and mClover were identified and the % FRET positive cells within this population was quantified following a gating strategy previously described (Holmes *et al.*, 2014). For each experiment 10,000 cells were analyzed in triplicate. Flow data analysis was performed using FlowJo v10 software (Treestar).

Immunofluorescence

30 µm parrafin-embedded fixed sections were cut and stained with biotinylated monoclonal AT8 primary antibody (Invitrogen) diluted 1:1000 in normal goat serum followed by secondary incubation with AlexaFluor-594 conjugated streptavidin diluted 1:500. Images were obtained using the LSM 780 Inverted confocal microscope (Zeiss) and analyzed via Imaris 9 software (Oxford Instruments).

Statistical analyses

Coded samples were obtained by M.S.L. from the lab of C.A.T. M.S.L. remained blinded prior to all seeding analyses. Flow cytometry gating and analysis of seeding activity was completed prior to decoding and interpreting the results. All statistical analysis was performed using GraphPad Prism v9.2.0 for Mac OS and Excel v16.52 (Microsoft).

RESULTS

Multiple Sclerosis Brain Tissue Harbors Tau Seeds

To address the MS brain harboring tau seeds, we prepared soluble protein lysates from cohort of eight MS patients from Montreal Neurological Institute at McGill University (Table 3.1). In an intital pilot screening of these eight patients, we observed statistically significant seeding activity in one of eight clarified lysates by transducing 10 μg of total clarified lysate into v2H biosensors. Control and AD brain lysates were used as negative and postivie controls, respectively (Figure 3.1). While only one lysate had significant seeding, we found this to be a promising result and wondered if enriching tau via immunopurification would allow us to identify significant seeding an additional MS brains. We then immunopurified tau using three different tau antibodies from two MS brain lysates, and transduced the immunopurification pellet into the v2H biosensors. We found statistically significant seeding in both brain lysates tested and observe that the TauB antibody enriched tau seeds to the greatest degree relative to the other tau antibodies tested (Figure 3.2). We did not observe seeding in the control amyloid-beta antibody HJ3.4 IP pellet, demonstrating the specificity of our assay for tau seeds (Figure 3.2). To further ensure that seeding in our IP pellets from MS brain lysate is from tau, and not other amyloids, we subjected our v2H biosensors to a battery of various fibrilized recombinant amyloid proteins. Statistically significant seeding was found when v2H biosensors were treated with tau amyloids, but not with alpha synuclein, TDP-43, or amyloid beta peptides 40 or 42 (Figure 3.3).

Tau Seeding Activity is abolished in MS Tissues after Fixation

Paraffin-embedded formalin fixed tissues can readily be used to detect seeding and for immunohistochemical analyses, allowing for correlation of immunohistochemical pathologies with tau seeding levels (Kaufman *et al.*, 2016). Through collaboration with Dr. Claudia Lucchinetti, we were able to obtain tissue sections from six PEFF MS cases. Clarified lysates were prepared from 25 μm tissues followed by transduction of PEFF derived lysates into v2H biosensors. We were unable to detect any seeding activity in PEFF MS tissues (Figure 3.4).

Immunopurification Improves the Detection Sensitivity of Tau Seeds in MS

Our initial results seemed promising that MS brain tissue does indeed contain tau seeds. To increase our sensitivity, we performed immunopurification with double the amount of clarified lysate starting material compared to initial IP tests (Figure 3.2), 1000 μg total clarified lysate, and used the seed specific antibody MD3.1 which isolates tau seeds more efficiently than the TauB antibody (data not shown). We found statistically significant seeding in six of the eight cases from the original cohort from the Montreal Neurological Institute (Figure 3.5). We concluded that MS brain tissue does carry tau seeds at significant levels and that the MD3.1 antibody can efficiently isolate them when using a large amount of starting protein.

Tau Seeds are Prevalent Across Many Regions of the MS Brain

To further test if MS brain contains tau seeds, and to test if seeding exists within MS plaques, we obtained fresh frozen tissue from plaque-bearing regions as well as adjacent brain regions

from a deceased 52 y.o. female subject with a 19-year history of relapsing-remitting MS that was well controlled until a rapid decline over the final year of life. We detected no seeding activity in soluble protein lysates derived from plaque-bearing tissue. By contrast we detected significant seeding activity in neighboring regions, including the temporal cortex, hippocampus, substantia nigra and the olfactory bulb (Figure 3.6A).

To increase detection sensitivity, we used the conformation-specific antibody MD3.1, which was designed to recognize a local structure in tau associated with a seed-competent conformation (Mirbaha *et al.*, 2018). We performed immunoprecipitation from brain homogenates, and tested the pellet for seeding activity. We detected seeding in regions we had previously observed, and we detected signal also in the frontal and parietal cortices (Figure 3.6B).

Next, we used standard immunohistochemical analyses to assess brain regions for phospho-tau accumulation. We observed characteristic findings of active phase demyelinated plaque formation in plaque-bearing regions (Figure 3.7A). We also observed evidence of pathological tau accumulation based on immunoreactivity with anti-tau monoclonal antibodies AT8 and MD3.1 (Figures 3.7B-I).

MS Tau Seeds vary in Conformation Relative to AD or Control

Distinct tau seed conformations are associated with different tauopathies (Sanders *et al.*, 2014; Shi *et al.*, 2021), and create unique patterns of transmissible pathology upon

inoculation into experimental mouse models (Kaufman *et al.*, 2016). Anti-tau antibodies directed against distinct epitopes, especially within the repeat domain, differentially bind different seed conformers. We used a panel of antibodies, measuring their ability to immunoprecipitate tau seeds from MS brain lysate (Figure 3.8A). The overall pattern of tau immunoprecipitation efficiency from MS was relatively similar to AD, but one monoclonal antibody (MD6.1) failed to bind seeds of the MS brain, while it worked well for AD (Figure 3.8 B,C,D). We concluded that tau assemblies present in MS brain have different epitopes accessible compared to control or AD tau.

EAE Animal Model does not Induce Tau Seeding to a Detectable Level

Finally, to test if tau seeding could be induced in an animal model of CNS inflammation, we immunized hTau mice with myelin peptide MOG35-55 in emulsified complete Freund's adjuvant containing *Mycobacterium tuberculosis* to induce a CNS-directed inflammatory response. We allowed the animals to recover from EAE for 70 days and performed seeding analysis on cortical lysates from the hTau EAE animals. We observed no significant seeding activity in this experimental paradigm and concluded that we did not induce tau seeding to a detectable level in the cortex of hTau mice when testing clarified lysates.

DISCUSSION

In summary, we observed tau seeding in six of eight fresh frozen MS tissues. We increased the tau seeding detected through immunopurification, and found that the seeding was specific to tau amyloids. Despite detecting tau seeds in fresh frozen MS brain tissue, we were unable to detect tau seeding activity in PEFF MS brain slices or in an EAE animal model of CNS inflammation. Finally, we found seeding activity in a variety of brain regions of a single MS case that rose above control seeding level and demonstrated that the seeds isolated likely are of a different conformation based on the differential ability of a panel of tau antibodies to isolate seeds from the MS brain vs. AD or control.

Tau Seeding in Fixed MS Tissues

The lack of seeding activity in the PEFF is likely due to loss of seeding activity from tissue fixation. AD brain lysate can generally convert ~30-60% of v2H cells in a given treated population to FRET positive depending on the amount of material transduced into the biosensors. It's clear that PEFF AD tissues do not exhibit such robust seeding, only converting around 8% of the cell population. It's likely that the fixation of MS brain abolishes the seeding activity that is present, or reduces it to such an extent as to make it undetectable. It remains to be tested if lysates from fixed MS tissues could be enriched by IP.

Tau Seeds are Present in Fresh Frozen MS Tissue

Despite the lack of seeding in PEFF tissues, it appears that fresh frozen MS brain tissue does in fact contain tau seeds. We were able to detect statistically significant seeding in seven of

nine MS cases for which we had fresh frozen tissue. In addition, we found seeding activity in a variety of regions in MS Case I, further demonstrating that ubiquity of tau seeds in the MS brain.

In our studies, we were unable to detect tau seeding activity in plaque bearing tissue despite occasional positive tau staining by immunohistochemistry. Likely this is due to altered cellular and molecular composition of plaque-bearing tissues. Of note, we detected tau seeding in the soluble lysate without purification, which is unexpected if the seeding level was at a basal level, as control's generally have statistically significant seeding activity above lipofectamine treated cells only with tau immunopurification (LaCroix et al., in prep). MD3.1 appeared to efficiently isolate tau seeds from plaque-adjacent regions as well as detect tau aggregates via immunohistochemistry, which supports previous work showing tau aggregation in MS brain (Anderson *et al.*, 2008; Anderson *et al.*, 2009; 2010).

This study is the first to describe the presence of tau seeds in MS. In agreement with previous work, tau aggregates were found via immunohistochemistry across several regions of the MS brain (Anderson *et al.*, 2008; Anderson *et al.*, 2009; 2010). These findings imply an accumulation of tau aggregates in MS that is beyond the scope of healthy tau biology and highlight a potential role for tau as a key mediator of neurodegeneration in MS. More so, tau deposits have been described in other inflammatory CNS diseases such as Nodding syndrome, Chronic Traumatic Encephalopathy, and Subacute Sclerosing Panencephalitis (McKee et al., 2015; McQuaid *et al.*, 1994; Pollanen *et al.*, 2018). This positions tau as a

critical mediator key mediator connecting CNS inflammation and neurodegeneration. Future studies will be required to elucidate the interplay between neuroinflammation and tau seed accumulation in MS and other inflammatory diseases.

Case	Sex	Age	Diagnoses	Source
A	M	26	RRMS	Montreal
B	F	51	RRMS	Montreal
C	M	48	SPMS	Montreal
D	F	55	SPMS	Montreal
E	F	50	SPMS	Montreal
F	F	60	SPMS	Montreal
G	M	61	SPMS	Montreal
H	M	65	SPMS	Montreal
I	F	52	RRMS	UTSW

Table 3.1. Demographic data from the multiple sclerosis cases studied. Abbreviations: **F/M** – female/male; **age** – age in years; **RRMS** – relapsing-remitting multiple sclerosis, **SPMS** – secondary-progressive multiple sclerosis.

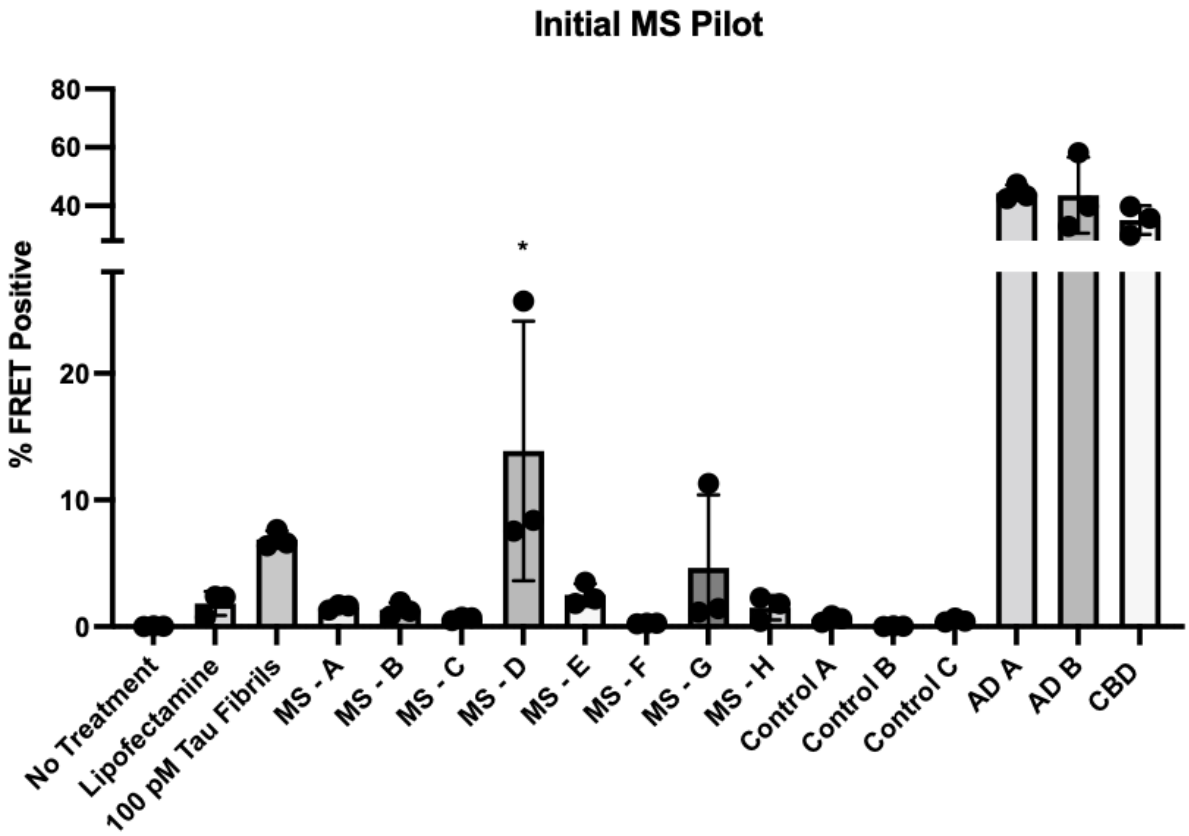

Figure 3.1. An initial screening of a pilot cohort of eight multiple sclerosis brain samples shows statistically significant tau seeding in the protein lysate from one case of secondary-progressive MS. Fresh frozen cortical tissue samples was used to create clarified lysate [10% (wt/vol)]. Control brain, and Lipofectamine alone was used as negative control. Tau fibrils, AD brain, and CD brain samples were used as positive controls. 10 μL of clarified lysate from each sample was transduced into v2H biosensors. Cells were fixed and analyzed via FRET flow cytometry 48 hours after treatment. Statistical significance was determined by performing one-way ANOVA followed by Dunnett's multiple comparisons testing of all samples compared against Lipofectamine treated negative controls, *$p < 0.05$, **$p < 0.01$, ***$p < 0.001$, ****$p < 0.0001$. Errors bars = S.D.

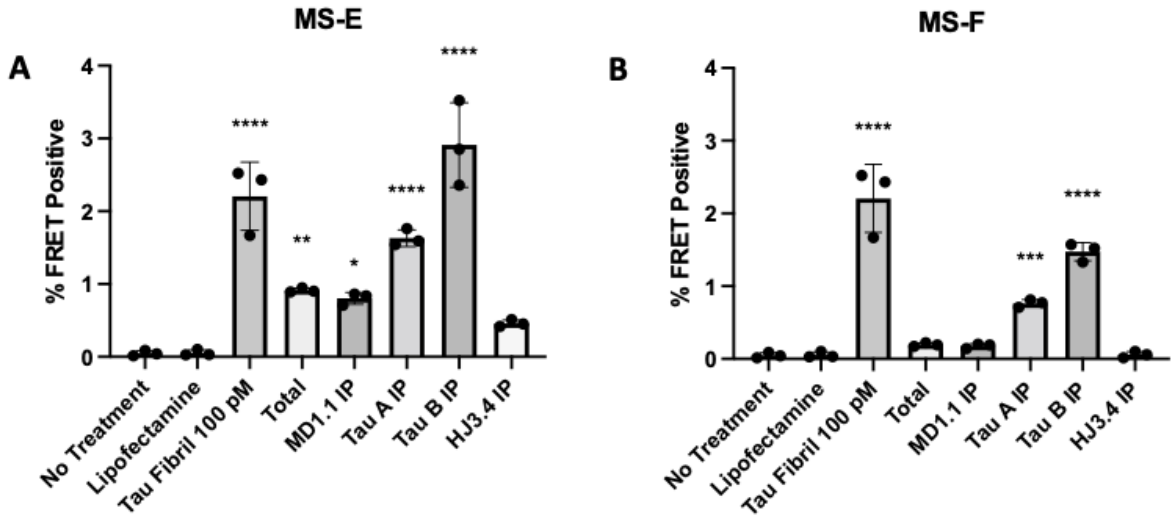

Figure 3.2 . Immunoprecipitation with tau specific antibodies reveals specific tau seeding activity in two cases of multiple sclerosis. Immunoprecipitation with MD1.1, Tau A, and Tau B antibodies was performed on clarified lysate from cases MS-E and MS-F to generate tau-enriched IP pellets. 10 µg of clarified lysate protein (Total) and 10 µL of IP pellets were transduced into v2H biosensor cells. Cells were fixed and harvested for FRET flow cytometry 48 hours after treatment. Tau fibrils were used as positive control. Lipofectamine treated and untreated cells were used as negative controls. (**A**) MS-E has significant seeding activity in Total and tau-enriched IP pellets. (**B**) MS-F has significant seeding activity in TauA and TauB tau-enriched IP pellets. Statistical significance was determined by performing one-way ANOVA followed by Dunnett's multiple comparisons testing of all samples compared against Lipofectamine treated negative controls, *$p < 0.05$, **$p < 0.01$, ***$p < 0.001$, ****$p < 0.0001$. Errors bars = S.D.

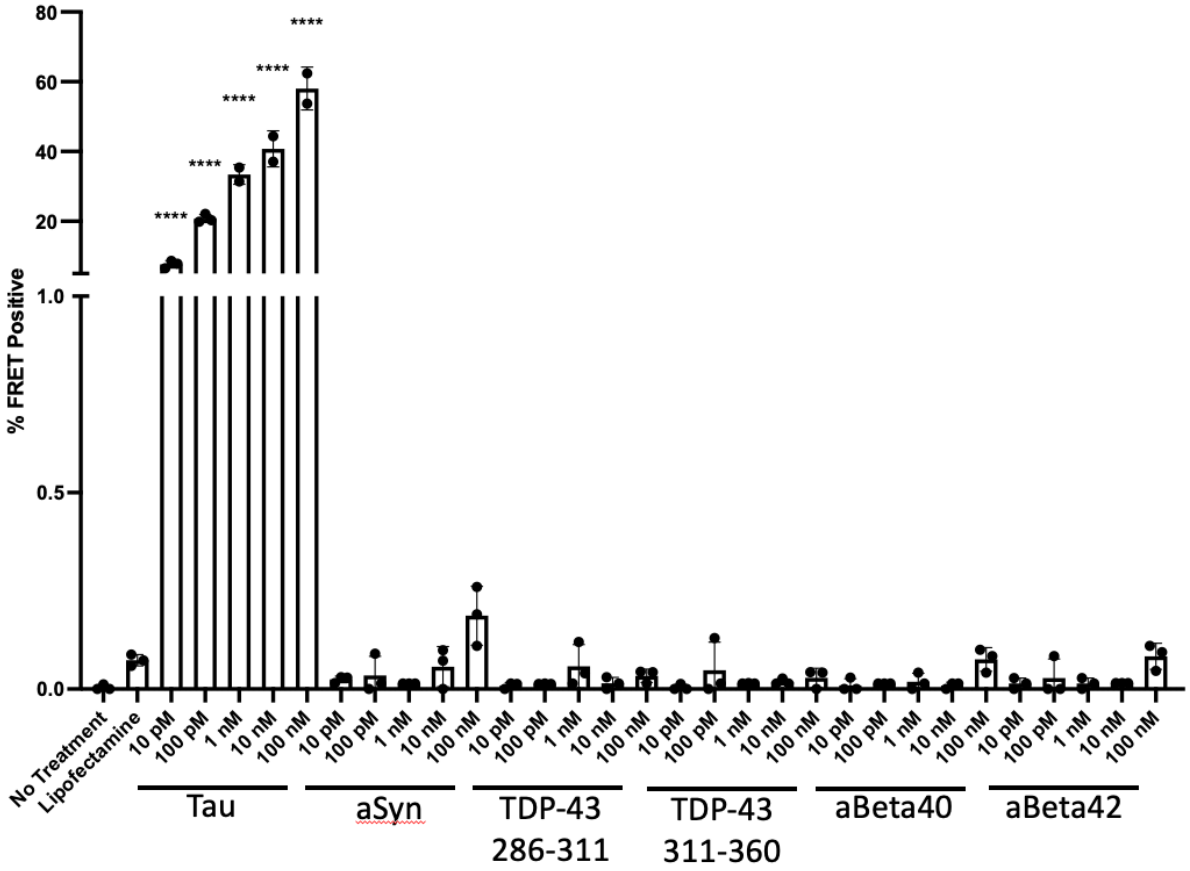

Figure 3.3. v2H tau biosensors respond specifically to tau fibrils and not to amyloids made of other proteins or peptides. Increasing concentrations of tau, and other amyloids, were transduced onto v2H biosensors. Statistically significant seeding is seen in biosensors treated with tau fibrils only, not in biosensors treated with other amyloids. Statistical significance was determined by performing one-way ANOVA followed by Dunnett's multiple comparisons testing of all samples compared against Lipofectamine treated negative controls, *$p < 0.05$, **$p < 0.01$, ***$p < 0.001$, ****$p < 0.0001$. Errors bars = S.D.

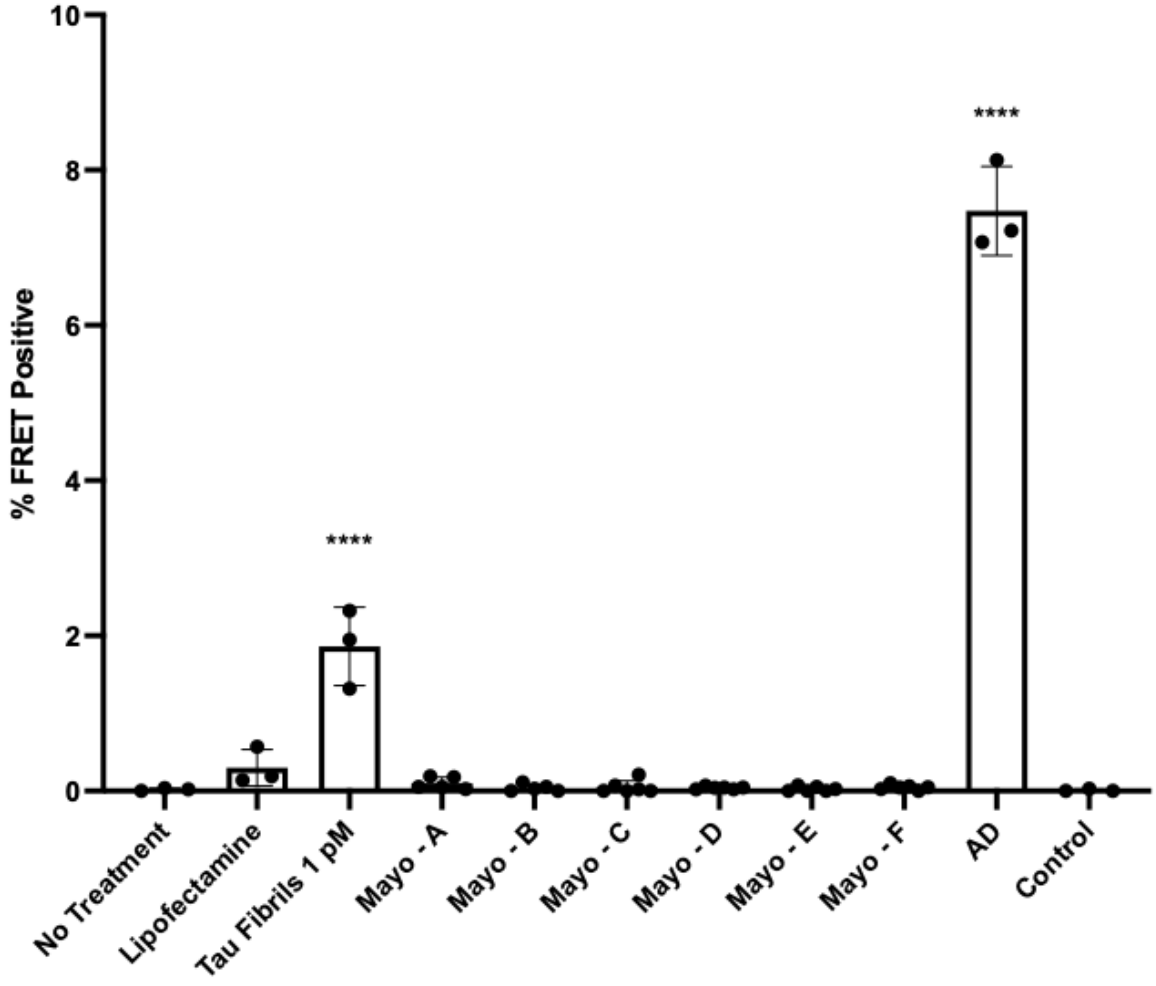

Figure 3.4. No tau seeding activity was detected in a cohort of MS patients from Mayo Clinic. Clarified homogenate was prepared from two paraffin-embedded formalin-fixed tissue sections per case. 10 µL of clarified lysate from PEFF tissues was transduced into v2H biosensor cells. Cells were fixed and analyzed via FRET flow cytometry 48 hours after treatment. Columns represent the mean FRET positivity from two biological replicates with three technical replicates each for MS samples. Columns represent the mean FRET positivity from three technical replicates (dots) for all other treatment conditions. Statistical significance was determined by performing one-way ANOVA followed by Dunnett's

multiple comparisons testing of all samples compared against Lipofectamine treated negative controls, *p < 0.05, **p < 0.01, ***p < 0.001, ****p < 0.0001. Errors bars = S.D.

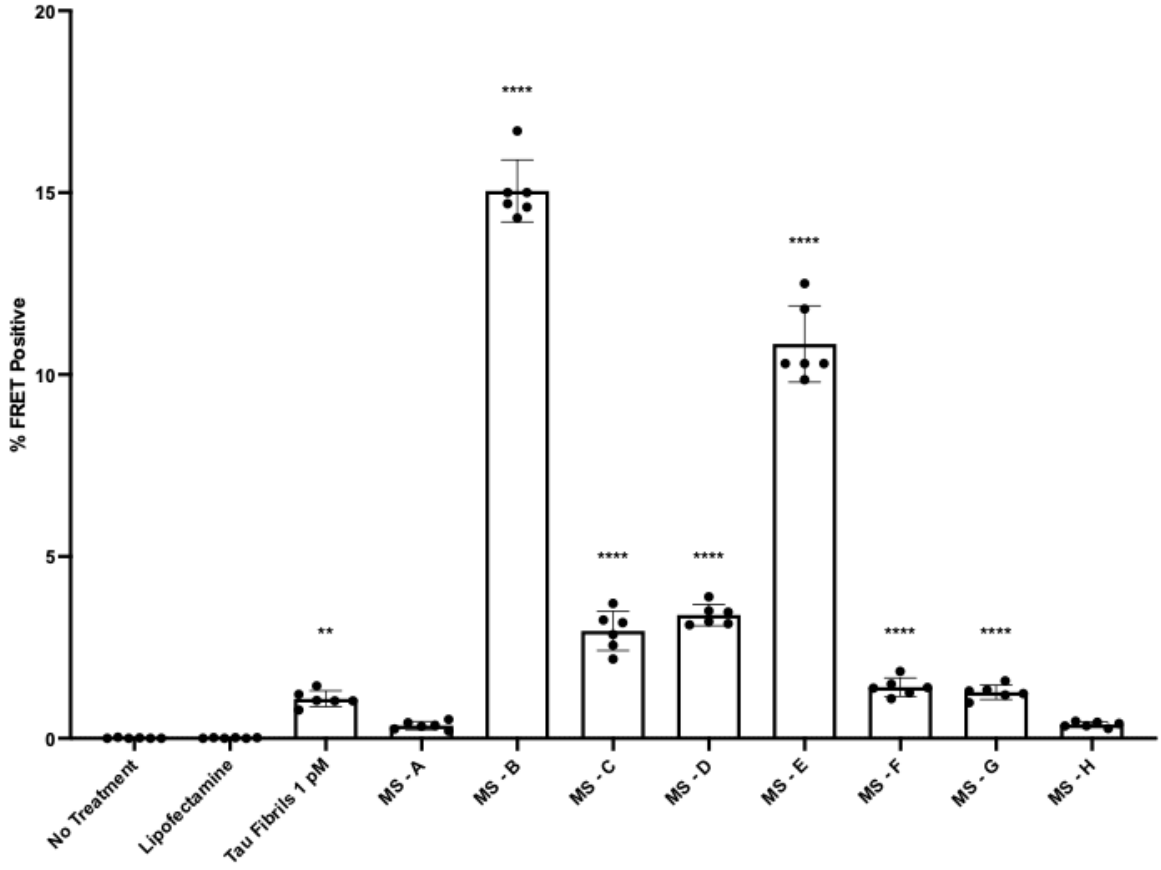

Figure 3.5. Repeat MD3.1 immunoprecipitation and seeding analysis of freshly prepared from MS cases A-H reveal statistically significant seeding in 6 of 8 samples. Newly prepared clarified homogenates were used for immmunopurification with the antibody MD3.1. v2H biosensor cell were transfected with 10 µL of IP pellet. Cells were fixed and analyzed via FRET flow cytometry 48 hours after treatment. Columns represent the mean FRET positivity from three technical replicates (dots). Statistical significance was determined by performing one-way ANOVA followed by Dunnett's multiple comparisons testing of all samples compared against Lipofectamine treated negative controls, *$p < 0.05$, **$p < 0.01$, ***$p < 0.001$, ****$p < 0.0001$. Errors bars = S.D.

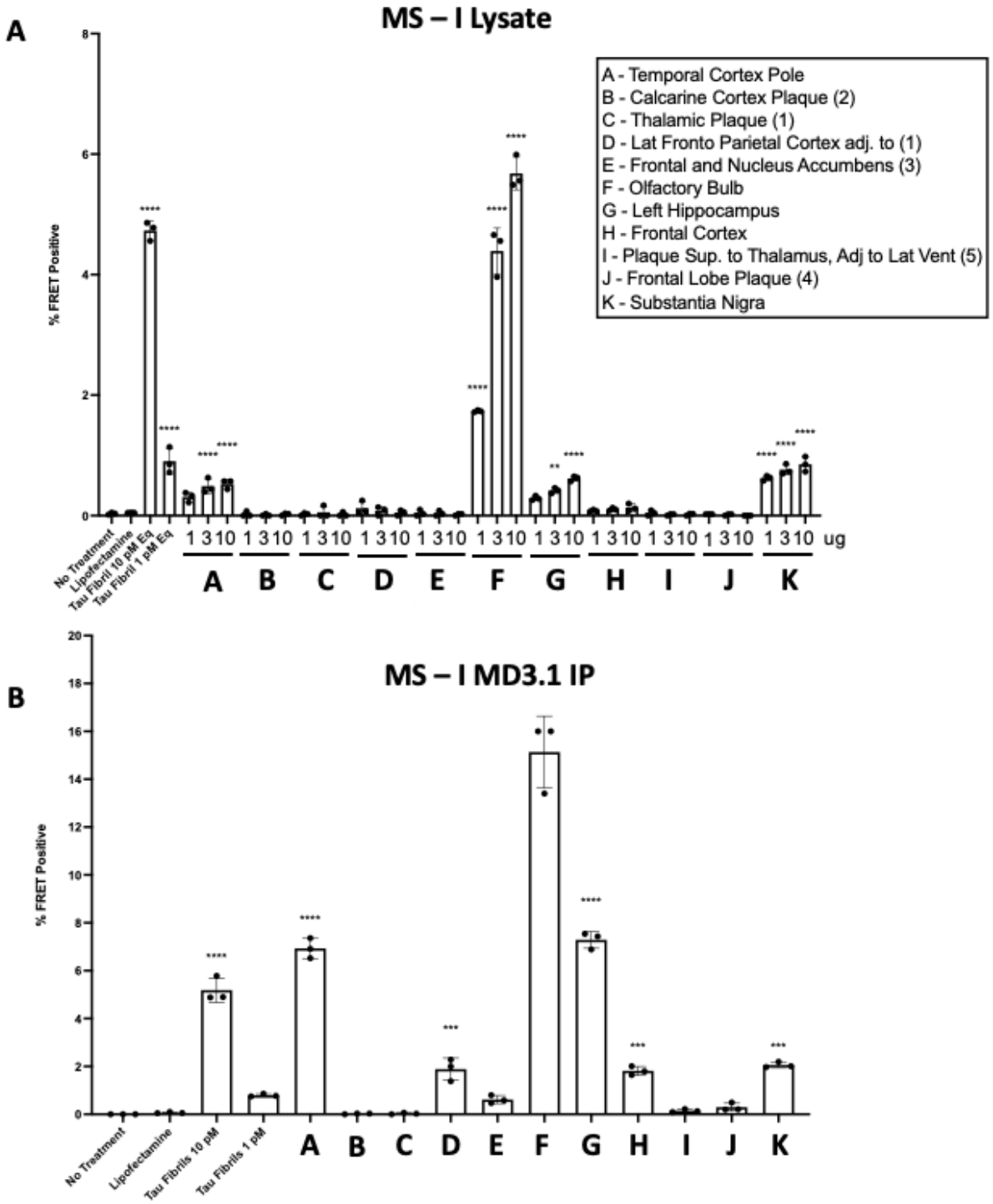

Figure 3.6. Tau seeding activity is revealed across several regions of MS Case I in both clarified lysate and MD3.1 IP. Five brain regions baring MS lesions and six neighboring

brain regions were used to prepare clarified protein lysate [10% (wt/vol)]. Clarified lysates were used for seeding directly, or for tau immunopurification with the MD3.1 antibody followed by seeding with tau-enriched IP pellets. v2H biosensor cell were transfected with clarified protein lysate or tau-enriched IP pellet. Cells were fixed and analyzed via FRET flow cytometry 48 hours after treatment. (**A**) Tau seeding activity was detected in 10 μg of clarified lysate from the temporal cortex, olfactory bulb, and hippocampus, and substantia nigra. (**B**) Tau enrichment via immunopurification with MD3.1 antibody revealed statistically significant seeding in 10 μL of tau-enriched IP pellets from temporal cortex, latero-frontal parietal cortex, olfactory bulb, hippocampus, frontal cortex, and the substantia nigra. Columns represent the mean FRET positivity from three technical replicates (dots). Statistical significance was determined by performing one-way ANOVA followed by Dunnett's multiple comparisons testing of all samples compared against Lipofectamine treated negative controls, *$p < 0.05$, **$p < 0.01$, ***$p < 0.001$, ****$p < 0.0001$. Errors bars = S.D.

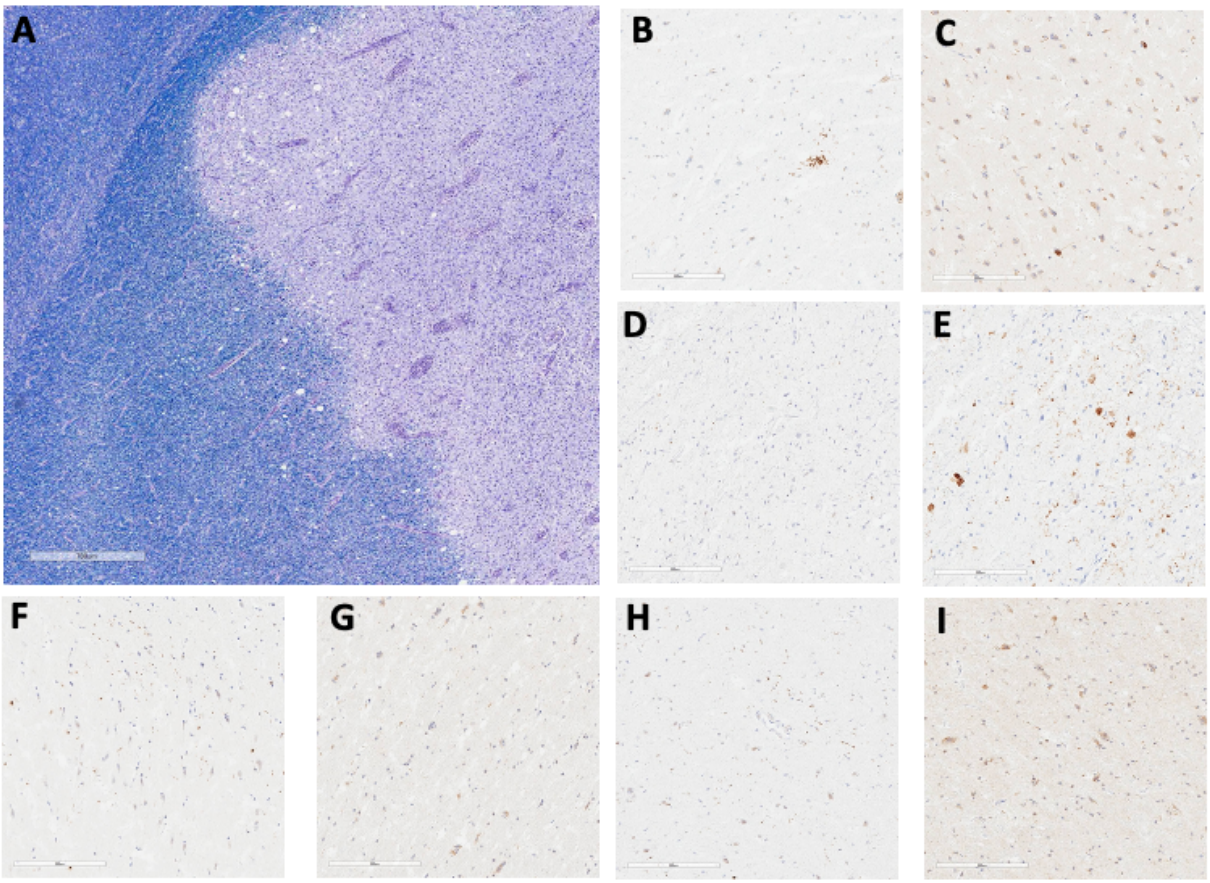

Figure 3.7 Histological accumulation of tau in a case of MS. (A) Periphery of an MS plaque stained with Luxol fast blue-PAS-hematoxylin, showing preserved myelin in adjacent brain (left) and loss of myelin within the plaque (right); plaque also contains abundant macrophages, and the interface between plaque and adjacent brain contains many swollen axons. (B-I) Tau immunohistochemistry (AT8 and MD3.1) in plaque-adjacent brain regions: (B,C) temporal lobe, showing a collection of AT8-immunoreactive neuropil threads and MD3.1-immunoreactive tangle-like structures in 2 neurons; (D,E) parietal lobe, showing MD3.1-immunoreactive structures at the periphery of a plaque (consistent with swollen axons), but no AT8 immunoreactivity; (F,G) hippocampus, showing AT8-immunoreactive neuropil threads in entorhinal cortex, which are MD3.1-negative; and (H,I) substantia nigra, showing sparse AT8-immunoreactive neuropil threads, but no MD3.1 immunoreactivity.

Antibody	Epitope
MD1.1	22-34
MD4.1	145-160
AT8	p202/p205
TauA	244-266
MD2.1	263-281 (R1R2)
MD2.2	263-281 (R1R2)
MD3.1	263-311 Δ275-305 (R1R3)
MD3.2	263-311 Δ275-305 (R1R3)
MD5.1	326-343 (R3R4)
MD6.1	358-375 (R4R')
MD6.2	358-375 (R4R')

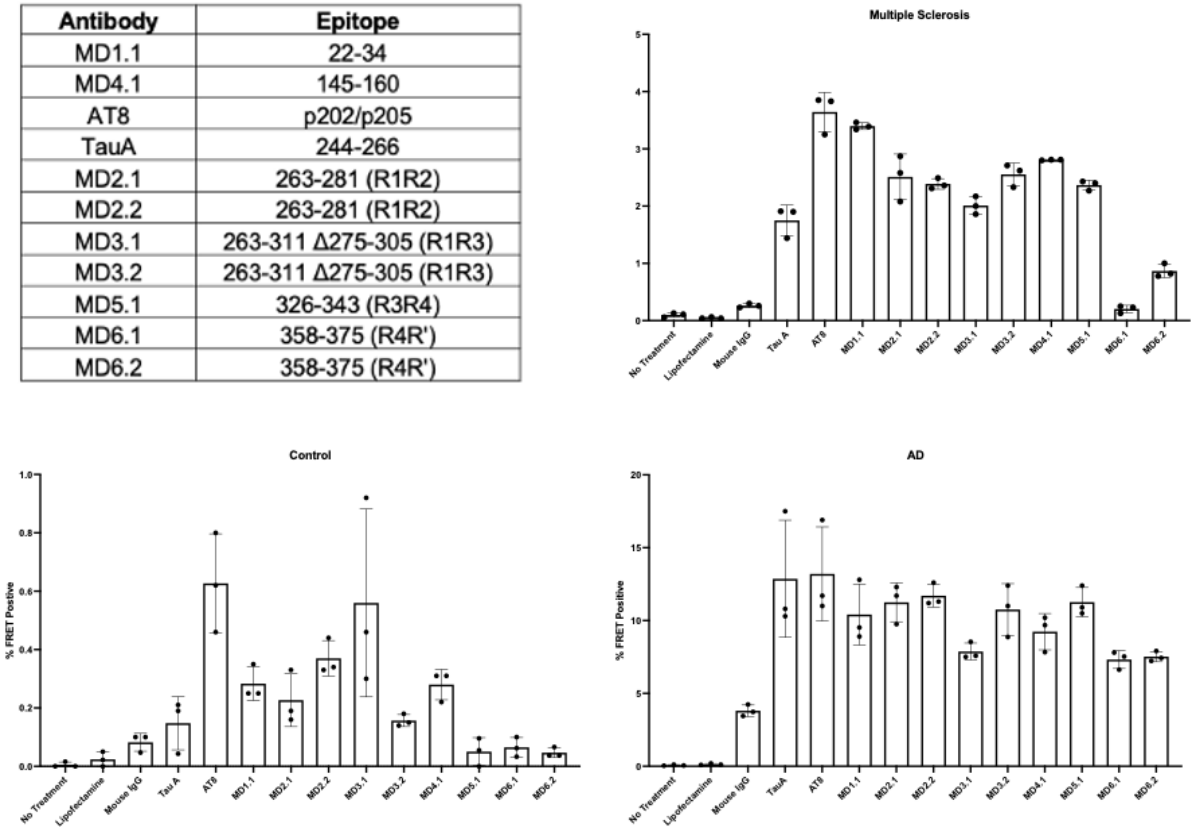

Figure 3.8. Differential seed capture efficiency from MS Case - I compared to control and AD brain. A custom antibody panel reveals unique epitope exposure of tau seeds in a MS brain versus control and AD. (**A**) Epitopes of antibodies used. (**B**) Differential antibody IP from hippocampus of an MS brain. (**C**) Differential antibody IP efficiencies from parietal cortex of control brain. (**D**) Differential antibody IP efficiencies from temporal cortex of AD brain.

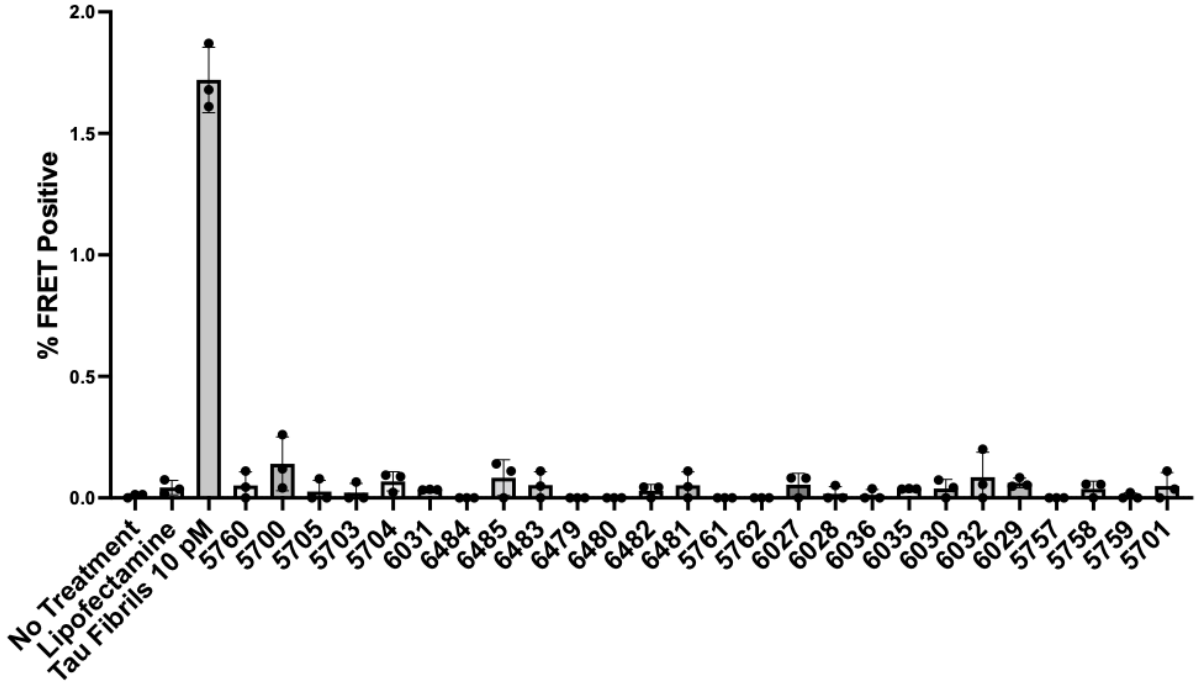

Figure 3.9. Tau seeding activity was not detected in the brains of human tau expressing mice used in the experimental autoimmune encephalomyelitis model of central nervous system inflammation. Mice were induced and harvested at 70 days post induction unless the severity of induction necessitated sacrificing the animal. The cortex was dissected and used to prepare clarified protein lysate [10% (wt/vol)]. 10 μg of clarified lysate was transfected into v2H biosensor cells. Cells were fixed and analyzed via FRET flow cytometry 48 hours after treatment.

Chapter 4

Tau Seeding in the Healthy Human Brain

PREFACE

This chapter contains a submitted manuscript:

LaCroix, M.S., Hitt, B.D., Beaver, J.D., Estill-Terpack, S.J., Gleason, K., Tamminga, C.A., Evers, B.M., White, C.L., Diamond, M.I. Tau Seeding without Tauopathy. *submitted*.

Author contributions for the citation above:

Author Contributions: M.S.L., B.D.H., and M.I.D. designed research; M.S.L, B.D.H., J.D.B, and S.J.E. performed research; K.G., C.A.T., B.M.E., and C.L.W. contributed new reagents; M.S.L., B.D.H., and M.I.D. analyzed data; M.S.L. and M.I.D. wrote the text.

ABSTRACT

Neurodegenerative tauopathies such as Alzheimer's disease (AD) are caused by brain accumulation of tau assemblies. Evidence suggests tau functions as a prion, and cells and animals efficiently propagate unique tau assemblies. This suggests a dedicated cellular replication machinery, with normal physiologic function for tau seeds. Consequently, we hypothesized that healthy control brains would have seeding activity. We recently developed a novel monoclonal antibody (MD3.1) specific for tau seeds. We used this antibody to immunopurify tau from the parietal and cerebellar cortices of 19 healthy subjects ranging 19-65 years. We detected seeding in the parietal cortex, but not in the cerebellum, or in wild-type or human tau knockin mice, suggesting that cellular/genetic context dictates development of seed-competent tau. Seeding did not correlate with subject age or brain tau levels. Dot blot analyses revealed no AT8 immunoreactivity above background levels in parietal and cerebellar extracts and <1/100 of that present in AD. Based on binding to a panel of antibodies, the conformational characteristics of control seeds differed from AD, suggesting a unique underlying assembly, or structural ensemble. Tau's ability to adopt self-replicating conformations under non-pathogenic conditions may reflect normal function that goes awry in disease states.

INTRODUCTION

Accumulation of intracellular assemblies of the microtubule-associated protein tau (MAPT) underlies myriad neurodegenerative diseases termed tauopathies (Lee and Trojanowski, 1999). Alzheimer's disease (AD), the most common tauopathy, now afflicts ~50 million people worldwide, and is estimated to harm ~150 million by 2050 (Guerchet *et al.*, 2020). Most tauopathies are sporadic, while some are caused by dominantly inherited mutations in the MAPT gene (Lee and Trojanowski, 1999). The origin of sporadic tauopathies has remained elusive, but growing experimental evidence suggests that tau functions as a prion in pathological states. Initial work from our group and others suggested that tau stably propagates unique fibrillar structures *in vitro* (Frost *et al.*, 2009b). In living systems, exogenous tau assemblies are spontaneously taken up by cultured cells, and serve as templates for intracellular aggregation (Frost *et al.*, 2009a), and similarly tau inoculated into transgenic mouse brain induces intracellular pathology (Clavaguera *et al.*, 2009). Diverse neuropathologies also form in a tauopathy mouse model upon brain inoculation with tau fibrils prepared from human tauopathies (Clavaguera *et al.*, 2013). We have further observed that tau forms a variety of unique structures, or strains, that propagate indefinitely and transmit readily among cells, and, after inoculation into a mouse model, produce unique, transmissible patterns of neuropathology (Sanders *et al.*, 2014). We also observed unique strain composition patterns in five different tauopathies, including variation within specific neuropathological diagnoses (Sanders *et al.*, 2014). In a large survey of 18 strains propagated in cells, we determined that each gave rise to a unique pattern of neuropathology following inoculation into a mouse model (Kaufman *et al.*, 2016). This work has been confirmed and

extended by cryo-electron microscopy (cryo-EM) of tau fibril structures extracted from different tauopathies, which has revealed unique core structural features that correlate with different neuropathological diagnoses (Falcon *et al.*, 2018; Falcon *et al.*, 2019; Fitzpatrick *et al.*, 2017; Zhang *et al.*, 2020a). Recent work reports fibril diversity within a single neuropathological diagnosis in multiple tauopathies (Shi *et al.*, 2021), consistent with our prior isolation of distinct strains from individual brains (Sanders *et al.*, 2014). Taken together, considerable evidence supports the idea that pathological assemblies of distinct structure drive the development of unique tauopathies.

The faithful maintenance of tau strains in cells, mice, and humans, suggests the existence of an intrinsic replication machinery that participates in the amplification of unique structures. The normal function of tau is not entirely clear. Tau binds microtubule filaments (Cleveland et al., 1977; Weingarten *et al.*, 1975) through interactions across the interface of tubulin heterodimers (Kadavath et al., 2015; Kellogg et al., 2018) and has been proposed to stabilize microtubules *in vivo* (Bunker et al., 2004; Witman et al., 1976).Yet tau knockout mice are viable (Ke et al., 2012), suggesting microtubule stabilization is not an essential function, or that it is compensated for by other proteins.

An enormous literature suggests that many proteins form self-amplifying assemblies to regulate biological processes. The first examples were described in yeast (Wickner et al., 2015), and similar protein activities in mammals are now established. For example, the prion-like polymerization of MAVS and ASC proteins transduces signaling in innate immunity and

inflammation based on self-propagating assemblies (Cai et al., 2014; Hou et al., 2011). In mice, the cytoplasmic polyadenylation element-binding protein (CPEB) changes from a soluble to an aggregated state that promotes translation of sequestered synaptic mRNAs, maintaining long-term potentiation (Fioriti et al., 2015; Huang et al., 2006; Pavlopoulos et al., 2011; Rayman and Kandel, 2017; Si et al., 2003). Last, in hippocampi of mice exposed to cellular stress, TIA-1, which facilitates the assembly of stress granules, forms heritable aggregates through its amyloidogenic C-terminal prion-like domain (Rayman and Kandel, 2017). Given data that tau functions as a prion in experimental systems, we hypothesized a physiological role for tau conformers that serve as templates for their own replication, i.e. "seeds." According to this model, tau aggregation in disease might represent a normally occurring process that escapes physiologic regulation, not a *de novo* and purely pathological function. This model predicts the existence of tau seeds in healthy individuals, but until now they have eluded detection. In this study we use immunoprecipitation of brain lysate with a novel anti-tau antibody, and a highly sensitive biosensor assay (Hitt *et al.*, 2021) to address this question.

MATERIALS AND METHODS

Biosensor cell line v2H

Highly sensitive second-generation tau biosensor cells termed v2H (Hitt *et al.*, 2021) were used for seeding assays. These cells are based on expression of tau repeat domain fragment (246-378) containing the disease-associated P301S mutation (tau-RD) fused to mCerulean3 or mClover3. The v2H line was selected for high expression with low background signal and high sensitivity. Seeding experiments used previously established protocols (Holmes *et al.*, 2014).

Cell culture

v2H biosensors were grown in Dulbecco's Modified Eagle's medium (Gibco) supplemented with 10% fetal bovine serum (HyClone), and 1% glutamax (Gibco). For terminal experiments, 1% penicillin/streptomycin (Gibco) was included. Cells were tested free of mycoplasma (VenorGem, Sigma) and cultured at 37°C with 5% CO_2 in a humidified incubator. To avoid false-positive signal from v2H biosensors, cells were passaged prior to ~80% confluency.

Human brain samples

Human brain tissue was obtained from 19 control subjects (6 females, 13 males, age range 19-65 years, Table 1) without any known tauopathy or psychiatric diagnoses, with Institutional Review Board (IRB) approval at University of Texas Southwestern Medical Center. Informed written consent for donation of tissue was obtained from next of kin prior

to collection. Brains were sectioned and flash frozen in liquid nitrogen for long-term storage at -80°C. Pulverized frozen tissue from the cortex of the parietal lobe and cerebellum was used to prepare total soluble protein lysates for further experiments.

Human sample preparation

Fresh frozen pulverized tissue was suspended in tris-buffered saline (TBS) containing cOmplete mini protease inhibitor tablet (Roche) at a concentration of 10% w/vol. Samples were then dounce homogenized, followed by pulsing probe sonication at 75 watts for 10 min (Q700, QSonica) on ice in a hood. The sonication probe was washed with a sequence of ethanol, bleach, and distilled water to prevent cross-contamination. Lysates were then centrifuged at 23,000 x g for 30 min and the supernatant was retained as the total soluble protein lysate. Protein concentration was measured with the BCA assay (Pierce). Fractions were aliquoted and stored at -80°C prior to immunoprecipitation and seeding experiments.

Immunohistochemical Analysis

50 µm fixed and frozen sections were cut on CM3050 S Cryostat (Leica). Biotinylated AT8 primary antibody (Thermo Scientific) was used for DAB staining. Images of AT8-stained slices were collected via Olympus Nanozoomer 2.0-HT (Hamamatsu).

Mouse lines

Tau KO mice (n=10, 5 females, 5 males, average age 12.3 months) containing a GFP-encoding cDNA integrated into exon 1 of the MAPT gene were negative controls (Tucker et

al., 2001). Tau KO mice were obtained from Jackson Laboratory and maintained on a C57BL/6J background. Wild-type mice (n=9, 5 females, 4 males, average age 12.9 months) of BL6/C3H background were used as a source of murine tau. We used mice on BL6 background with the human MAPT gene knocked in at the mouse tau locus that express all six isoforms of human tau (n=10, 5 females, 5 males, average age 16.2 months) as a source of murine-expressed human tau (gift from Pfizer), and verified by genomic sequencing in the Diamond lab. All mice involved in this study were housed under a 12 hour light/dark cycle, and were provided food and water *ad libitum*. All experiments involving animals were approved by the University of Texas Southwestern Medical Center Institutional Animal Care and Use Committee (IACUC).

Mouse sample collection and preparation

Mice were anesthetized with isoflurane and perfused with chilled phosphate buffered saline (PBS) + 0.03% heparin. The forebrain and cerebellum were separated and weighed prior to flash freezing in liquid nitrogen and storage at -80°C. As described previously for human tissues, fresh frozen forebrain was suspended in TBS containing cOmplete mini protease inhibitor tablet (Roche) at a concentration of 10% w/vol. Samples were then dounce homogenized, followed by pulsing probe sonication at 75 watts for 10 min on ice in a hood (Q700, QSonica). The sonication probe was washed with a sequence of ethanol, bleach, and distilled water to prevent cross-contamination of seeding activity. Lysates were then centrifuged at 23,000 x g for 30 min and the supernatant was retained as the total soluble

protein lysate. Protein concentration was measured with the BCA assay (Pierce). Fractions were aliquoted and stored at -80°C prior to immunoprecipitation and seeding experiments.

Immunoprecipitation from protein lysate or tau monomer

Immunoprecipitations were performed using 50 µL of magnetic Protein A Dynabead slurry (Thermofisher), washed twice with immunoprecipitation (IP) wash buffer (0.05% Triton-X100 in PBS), followed by a 1 hour room temperature incubation with 20 µg of anti-tau antibody. Beads were washed three times in IP wash buffer, 1000 µg of total protein lysate or 500 ng of recombinant tau monomer was added to the Protein A/anti-tau antibody complexes on the beads and rotated overnight at 4 °C. After overnight incubation, supernatant was removed as the tau-depleted fraction and the beads were washed three times in IP wash buffer and then moved to clean tubes for elution. IP wash buffer was removed and beads were then incubated in 65 µL of IgG Elution Buffer (Pierce) for 7 min to elute tau. The elution buffer was collected in a separate microcentrifuge tube and a second elution step in 35 µL of IP elution buffer was performed for 5 min and pooled with the initial elution. The elution was then neutralized with 10 µL of Tris-HCl pH 8.4 to finalize the tau-enriched IP pellet.

Enzyme-linked immunosorbent assay for total tau

A total tau “sandwich” ELISA was performed as described previously (Acker et al., 2013). Anti-tau antibody reagents were kindly provided by the late Dr. Peter Davies (Albert Einstein College of Medicine). 96-well round-bottom plates (Corning) were coated for 48 hours at

4°C with DA-31 (aa 150-190) diluted in sodium bicarbonate buffer (6 µg/mL). Plates were rinsed with PBS three times, blocked for 2 hours at room temperature with Starting Block (Pierce), and rinsed with PBS five additional times. Total protein was diluted 1:1000 in SuperBlock solution (Pierce; 20% SuperBlock in TBS) and 50 µL sample was added per well. Tau-enriched IP pellets were diluted 1:100 in SuperBlock solution and 50 µL sample was added per well. DA-9 (raised against aa 102-150) was conjugated to HRP using the Lightning-Link HRP Conjugation Kit (Innova Biosciences), diluted 1:50 in superblock solution, and 50 µL was added per well (15 µg/mL). Sample and detection antibody complexes were incubated overnight at 4°C. Plates were then washed with PBS nine times with a 15 second incubation between each wash, and 75 µL 1-Step Ultra TMB Substrate Solution (Pierce) was added. Plates were developed for 30 min and the reaction was quenched with 2 M sulfuric acid. Absorbance was measured at 450 nm using an Epoch plate reader (BioTek). Each plate contained a standard curve, and all samples were run in duplicate. Tau concentration was calculated using MyAssays four parameter logistic curve fitting tool.

Dot blot assays

Soluble protein lysates were prepared as described previously. Lysates were diluted to a final total soluble protein concentration of 1 mg/ml in TBS containing cOmplete mini protease inhibitor tablet (Roche). For AD, serial dilutions were subsequently prepared. 2 µl/sample was spotted onto nitrocellulose membrane (ThermoFisher Scientific) and then blocked in StartingBlock (TBS) blocking buffer (ThermoFisher Scientific) for 30 min at room

temperature. After blocking, the blot was incubated overnight at 4°C with AT8 primary antibody (Invitrogen) diluted 1:1000 in blocking buffer. The membrane was washed in TBS-T five times for 5 min followed by 1 hour RT incubation with peroxidase-conjugated anti-mouse secondary antibody (Jackson ImmunoResearch) diluted 1:4000 in blocking buffer. The membrane was then washed an additional five times in TBS-T. The membrane was revealed with ECL Prime western blot detection kit (Cytiva) and imaged with a Syngene digital imager.

Transduction of biosensor cell lines, flow cytometry and seeding analyses

The seeding assay was conducted as previously described (Holmes *et al.*, 2014) with the following changes: v2H cells were plated 20 hours before seed transduction at a density of 16,000 cells/well in a 96-well plate in a media volume of 180 µL per well. Mouse and human total protein lysates were thawed on ice, while tau-depleted IP supernatants and tau-enriched IP pellets were isolated just before seeding. For total protein lysates and tau-depleted supernatants 10 µg of protein was used per well. For tau-enriched pellets, 10 µL of elution was used per well. Samples were incubated for 30 min with 0.5 µL Lipofectamine 2000 (Invitrogen) and OptiMEM such that the total treatment volume was 20 µL. For each experiment, cells treated with OptiMEM alone and Lipofectamine 2000 in OptiMEM were used as negative controls. The v2H line, which expresses high levels of tau RD, can show false-positive FRET signal when treated with Lipofectamine 2000, which is mitigated by passaging prior to ~80% confluency. Recombinant tau fibrils at 1 pM and 100 fM (monomer equivalent) were used for positive controls. Cells were incubated for an additional 48 hours

after treatment prior to harvesting. Cells were harvested with 0.25% trypsin and fixed in 4% PFA for 10 min, then resuspended in flow cytometry buffer (HBSS plus 1% FBS and 1 mM EDTA). The LSRFortessa SORB (BD Biosciences) was used to perform FRET flow cytometry. Single cells double-positive for mCerulean and mClover were identified and the % FRET positive cells within this population was quantified following a gating strategy previously described (Holmes *et al.*, 2014). For each experiment 10,000 cells were analyzed in triplicate. Flow data analysis was performed using FlowJo v10 software (Treestar).

Nuclease Treatment

50 µL of MD3.1immunopurification pellets were incubated with a mixture of RNase A (3.2 mg/mL, Thermo) and RNase T1 (316 U/µL, Thermo), DNase I (633 U/µL, NEB), or an equivalent volume of Millipore H_2O as a control. Mixtures were agitated at 750 RPM in a Thermomixer (Eppendorf) set to 37°C for 24 hr and then transduced into v2H biosensors.

Statistical analyses

Coded samples were obtained by M.S.L. from the lab of C.A.T. M.S.L. remained blinded prior to all seeding analyses. Flow cytometry gating and analysis of seeding activity was completed prior to decoding and interpreting the results. All statistical analysis was performed using GraphPad Prism v9.2.0 for Mac OS and Excel v16.52 (Microsoft).

RESULTS

Tau Seeding in Parietal Cortex

In preliminary work we screened available antibodies for those that would most efficiently precipitate seeding activity from control brain, and identified MD3.1, an antibody raised against a peptide of R1/R3 of the tau repeat domain (aa263-311 Δ275-305) with a "trans" proline residue consisting of N-Boc-trans-4-fluoro-L-proline substituted at P270. MD3.1 binds tau seeds with high efficiency (B. Hitt, *in preparation*). We then used MD3.1 to test brain lysates from 19 control subjects of diverse ages (19-65 y.o.) (Table 4.1). We prepared soluble protein lysates from fresh frozen tissue of the cortex of the parietal lobe, and immunoprecipitated the total soluble protein lysate using MD3.1 antibody. We then used Lipofectamine 2000 to deliver total protein lysate (T), tau-depleted IP supernatants (S), and tau-enriched IP pellets (P) into v2H tau biosensors (Hitt *et al.*, 2021). Non-treated and Lipofectamine-treated cells were used as negative controls; recombinant heparin-derived 2N4R tau fibrils (1pM monomer equivalent) were used as a positive control. All tau-enriched IP pellets exhibited seeding activity levels beyond that of Lipofectamine-treated controls, with 16/19 tau-enriched IP pellets reaching statistical significance ($p < 0.05$) compared to Lipofectamine-treated controls when tested by ANOVA (Figure 4.1). MD3.1 did not induce a transition from inert to seed competent tau when tested with recombinant tau monomer (Figure 4.2). We concluded that human cortical tissue contains tau seeding activity, in the absence of known tauopathy.

AT8 Signal is Absent in Brain Lysates and

One explanation for our results was that we had missed underlying tauopathy in the cases we studied, despite their selection as healthy controls. Because it was impossible to carry out histopathology on the precise brain regions studied by the seeding assay, we analyzed homogenates for phospho-tau using AT8. This mouse monoclonal antibody recognizes p-Ser202 and p-Thr205, and is an accepted standard for diagnosis of tauopathy (Biernat et al., 1992). We used a dot blot analysis to be sure that any larger assemblies would be fully detected, spotting 2 μg of brain lysate on nitrocellulose membrane for detection with AT8. We used an AD brain lysate in serial dilutions for reference (Figure 4.3). We observed signal in AD lysate at approximately 100x that observed in all parietal and cerebellar samples studied. We observed no difference in signal between parietal samples, which contained seeding activity, and cerebellar samples that did not. We concluded that there was no evidence of tauopathy within the brain tissues we analyzed.

Immunohistochemistry Reveals no AT8 Signal in Brain Sections

Despite the inability to obtain immunohistochemical analysis on the exact tissue that was used for seeding assays, neighboring fixed and frozen tissue sections were analyzed for AT8 signal via immunohistochemistry. 40-50 μm sections were obtained from the top ten seeding brains in the original seeding assay and stained with biotinylated AT8. We used sections from fixed AD brain and PS19 mouse brain for positive controls. We included wild-type human tau expressing mice that do not develop tau pathology and tau knockout mice for negative staining controls. We observed no AT8 immunohistochemical signal in any control

brain analyzed, despite statistically significant seeding in each (Figure 4.4). Further evidence of a lack of tauopathy in our control cohort.

Tau seeding is absent in the cerebellum

A past study found that tau seeding is largely absent from the cerebellum except at late Braak stages (Furman et al., 2017). Consequently, we tested for seeding activity in the cerebellum samples. We prepared total soluble protein lysates and performed immunoprecipitation with the MD3.1 antibody. We did not detect significant seeding in any sample (Figure 4.5).

Seeding is independent of total tau levels and subject age

To test the correlation of tau levels and seeding activity, we used an ELISA developed by the Davies laboratory (Acker *et al.*, 2013). Cerebellar protein lysates contained roughly half the tau of cortical lysates, although the ranges overlapped (Figure 4.6A). Tau concentration in the cerebellar tau-enriched pellets was ~60% of the cortical pellets (Figure 4.6B). These findings were consistent with previous work that indicated overall tau concentration doesn't correlate directly with seeding activity (Furman *et al.*, 2017). We further tested the correlation of tau levels and seeding activity for the cortical samples. We observed no correlation of seeding with total tau levels (Figure 4.7A) or with levels of tau following immunoprecipitation (Figure 4.7B). Age is the primary risk factor for the most common tauopathy, Alzheimer's disease, and thus we tested for its correlation with control seeding activity. We observed no correlation between seeding and age (Figure 4.7C**).** We concluded

that the seeding activity we observed most likely did not represent an incipient age-dependent tauopathy.

Tau seeding is absent in wild-type and hTau mice

The low or absent tau seeding in the cerebellum suggested that its development might be cell-type dependent. Human tau expressed in a knockin mouse provided the perfect opportunity to extend this inquiry. These mice (a gift from Pfizer) express all six isoforms of human tau under the mouse promoter. We first confirmed that these animals express human tau by using western blot with HJ8.5, a monoclonal antibody specific for human tau (Yanamandra et al., 2013). We prepared total protein lysates from the brains of adult human tau knock-in mice (hTau), BL6/C3H wild-type (WT), and tau knockout mice. We detected tau in knockin mouse brain with HJ8.5, which did not detect mouse tau in WT mice (Figure 4.9A). By contrast, a polyclonal anti-tau antibody (A0024, DAKO) that detects mouse and human tau revealed tau protein in hTau and WT mice (Figure 4.9B). We used immunoprecipitation with MD3.1 to test for seeding in the mouse brains, with human samples as a positive control. We detected no significant seeding activity in any mouse derived samples, including the tau-enriched IP pellet (Figure 4.8). It remained possible that the epitope that MD3.1 detects is not present in sufficient amounts in hTau mice and we might simply be missing seed competent tau that is present. We performed immunoprecipitation on pooled brain lysate from hTau mice followed by seeding with a variety of tau antibodies with epitopes that span the length of the tau protein to test this. We found no evidence of seeding activity in any immunoprecipitation pellet tested (Figure 4.10).

We concluded that tau expression in a cortical neuron is not sufficient to induce a seed-competent form, and other factors must be required.

Control seeding exhibits distinct epitope accessibility vs. AD

Tau assemblies in different tauopathies exhibit conformational variation that can be resolved using cryo-electron microscopy. However, in the absence of insoluble tau it is impossible to determine the structure of the tau seeds we detected. Although the subjects we studied had no evidence of AD, we further tested the conformation of the seeds using a panel of antibodies raised against distinct epitopes across the protein (Figure 4.11A). Based on dilution, AD brain contained ~1,000 x more seeding activity vs. the control (Figure 4.11B). MD3.1 most efficiently immunoprecipitated tau seeds from control brain, while antibodies against R1 and more N-terminal residues more efficiently immunoprecipitated AD seeds vs. antibodies directed against R3/R4 and more C-terminal residues (Figure 4.11C). MD5.1, directed against residues of R3/R4, most efficiently precipitated AD seeds (Figure 4.11D). Notably, compared to AD, MD6.2, directed against R4R', inefficiently bound control seeds. Given the differential efficiencies in seed capture for the antibody panel, we concluded that control seeds likely represented a distinct strain, or ensemble of strains vs. AD.

Tau Seeds Derived from Control Brain are Sensitive to RNase Treatment

One cellular factor that may be involved in the formation of tau seeds is tau-RNA interactions. RNA is known to stimulate the aggregation of tau (Kampers et al., 1996) and RNA has been observed in association with tau tangles in human brain (Ginsberg et al.,

1997; Ginsberg et al., 1998). In addition, our group has shown that both DNA and RNA can induce seed competency in recombinant tau monomer and that AD seeds are stabilized by RNA interactions (Zwierzchowski-Zarate, *Biorxiv 2022*). To test if seeds isolated form control brain are similarly stabilized by RNA, we performed RNase and DNase treatment (Figure 4.12). We observed a reduction of seeding activity upon incubation with RNase, but not DNase. We concluded that RNA, but not DNA, may be stabilizing tau seeds in healthy brain.

DISCUSSION

In this study we have used a conformation-specific antibody and an ultra-sensitive tau biosensor cell line to detect tau seeding in the parietal cortex in 19 control individuals with no known neurodegenerative or psychiatric diseases. Notably, we detected insignificant seeding within the cerebellums of these subjects, and none in WT mice or knockin mice expressing the full human tau gene. We detected no AT8 immunoreactivity in the control brain samples. Control brain seeding activity did not correlate with tau levels or subject age. Tau seeding was present in control brain at levels <1/1000 of AD brain, and had different reactivity with a panel of anti-tau antibodies, suggesting that it was composed of tau conformers distinct from AD.

Fidelity of Tau Seed Detection

We have previously determined that P301S tau biosensors are specific for tau vs. other common amyloid proteins such as a-synuclein, and huntingtin (Holmes *et al.*, 2014). Multiple controls indicate that the seeding we detected is not a result of our experimental manipulations. The MD3.1 antibody used to isolate tau seeds does not induce a transition from inert to seed competence in recombinant tau monomers. Additionally, we failed to detect strong tau seeding activity in human cerebellum or hTau knockin mice after tau immunopurification. If the experimental methods were causing seed conversion, we would expect to find seeding activity in any immunopurified sample containing FL human tau. These results suggest that tau in healthy brain adopts seed-competent conformations, and this activity is region-specific.

Tau Assemblies in Normal Brain Function

The presence of tau seeds in healthy brain would be expected if replication of unique assembly structures is linked to a normal function of tau. The precedent for functional prions exists as a mechanism of signaling in the immune system (Cai *et al.*, 2014; Hou *et al.*, 2011) and at synapses (Rayman and Kandel, 2017). If amyloid formation is a critical aspect of tau's normal biology, we would expect tau seeds to be present across all ages. Indeed, we found clear, statistically significant seeding in 16/19 samples. The absence of statistically significant seeding for 3 cases might relate to particular sub-regions of cortex that were sampled. In contrast to individuals with tauopathy, age did not predict seeding. For example, the youngest individual with significant seeding was 19 y.o., far too young to exhibit a sporadic tauopathy. Given the general paucity of healthy pediatric brain tissue we could not determine how early in human life tau seeds appear. It remains to be determined what is the functional role of tau seeds in healthy brain. Our current work demonstrates that RNA-tau interactions may be actively stabilizing tau seed ensembles in the healthy brain. which may suggest a critical interaction between tau and RNA molecules with a yet to be determined biological function. In addition, recent work from our lab suggests it might relate to RNA regulation (Zwierzchowski-Zarate, *Biorxiv 2022*). Indeed, multiple prior studies have indicated that RNA can induce tau seeding (Kampers *et al.*, 1996), and that seeds are associated with neurofibrillary tangles (Ginsberg *et al.*, 1997).

Regional and Species Specificity of Tau Assembly Formation

We observed a regional and species specificity for tau seeding. We detected seeding in the parietal cortex while observing minimal amounts in the cerebellum, and none in hTau knockin mouse brain. The absence of significant seeding in the cerebellum or an hTau mouse could reflect that tau forms no functional assemblies in these conditions, or conversely that the strains formed were not efficiently precipitated by MD3.1. This will require further study, and mechanisms controlling the formation and dissolution of tau seeds in the healthy brain will be critical to understand. If this is dynamic, then it seems likely that human genetic factors, and even the state of brain function might regulate seed abundance. Tau ligands or post-translational modifications might also regulate seed abundance. Pathogenic tau strains may thus represent perturbation of tau's normal function, in which strains form that are inefficiently cleared, or that set-in motion metabolic or genetic changes that lead to feed-forward loops of amplification.

Control Brain Harbors Unique Tau Strains Compared to AD

One explanation for our findings is that control brain seeding simply represents the earliest form of AD. We feel this is unlikely for two reasons. First, we observed no age-dependence of control brain seeding, which would have been expected if it simply represented incipient AD. Indeed, we observed relatively strong seeding in a 19 y.o. subject. Additionally, using antibodies that target epitopes across tau, we observed different immunoprecipitation efficiencies for control seeds vs. AD. As it is not possible to use cryo-EM to study soluble control seeds, further elucidation of this question must await new analytical methods. Certainly, it is possible that post-translation modifications or associated cofactors led to

differential immunoprecipitation, with the underlying seed conformation being unchanged. However, the simplest interpretation of our findings is that control seeds differ in epitope exposure because of their assembly structure, i.e. strain identity.

In summary, we have detected tau seeds in healthy brain in an age-independent, region-specific manner. The presence of tau seeds in healthy individuals suggests that the ability of tau to form self-replicating assemblies may play a functional role, rather than being purely pathologic. We predict that cofactors regulate the transition from inert to seed competent tau, and we hope to identify them in future work. In particular, more research must elucidate whether tau seeds have a functional role in healthy brain, and the critical factors or events that lead to dysregulated tau assembly formation. This could be especially important in light of therapies to clear tau assemblies, or inhibit their formation, which might have unintended consequences for normal brain function.

Case	Sex	Age	Race	Diagnoses	PMI (hrs)	Cause of Death
A	M	20	C	Control	21.2	Accident - chest compression from blunt force injuries
B	M	47	C	Control	24	Natural - cardiovascular disease and diabetes
C	M	34	C	Control	23.4	Natural - cardiovascular disease and diabetes
D	M	52	C	Control	24	Accident - Electrocution
E	F	45	C	Control	22.5	Natural - cardiovascular disease
F	M	29	C	Control	27.4	Natural - polycystic kidney disease
G	F	50	C	Control	23.3	Natural - adrenocortical deficiency
H	F	62	C	Control	19.4	Natural - result of chronic alcoholism
I	M	48	C	Control	14.7	Natural - Mitral valve regurgitation
J	M	54	C	Control	19.3	Natural - cardiovascular disease
K	M	19	C	Control	20	Homicide - gunshot wound
L	M	36	C	Control	23	Undetermined
M	M	34	C	Control	24	Accident - drowned due to diabetic episode
N	F	49	Pac Is	Control	15.3	Natural - cardiovascular disease
O	F	65	C	Control	11	Natural - cardiovascular disease
P	M	65	C	Control	14	Natural - respiratory arrest
Q	M	63	C	Control	14	Natural - myocardial infarction
R	F	55	C	Control	25	Natural - intra-cerebral hemorrhage
S	M	32	C	Control	21.5	Natural- pulmonary embolism

Table 4.1. Demographic Data from the cases studied. The 19 tauopathy negative control cases studied span six decades of life ranging in age from 19 to 65. Abbreviations: **F/M** – female/male; **age** – age in years; **C** – Caucasian; **Pac Is** – Pacific Islander; **CTRL** – control, **PMI** - post-mortem interval in hours.

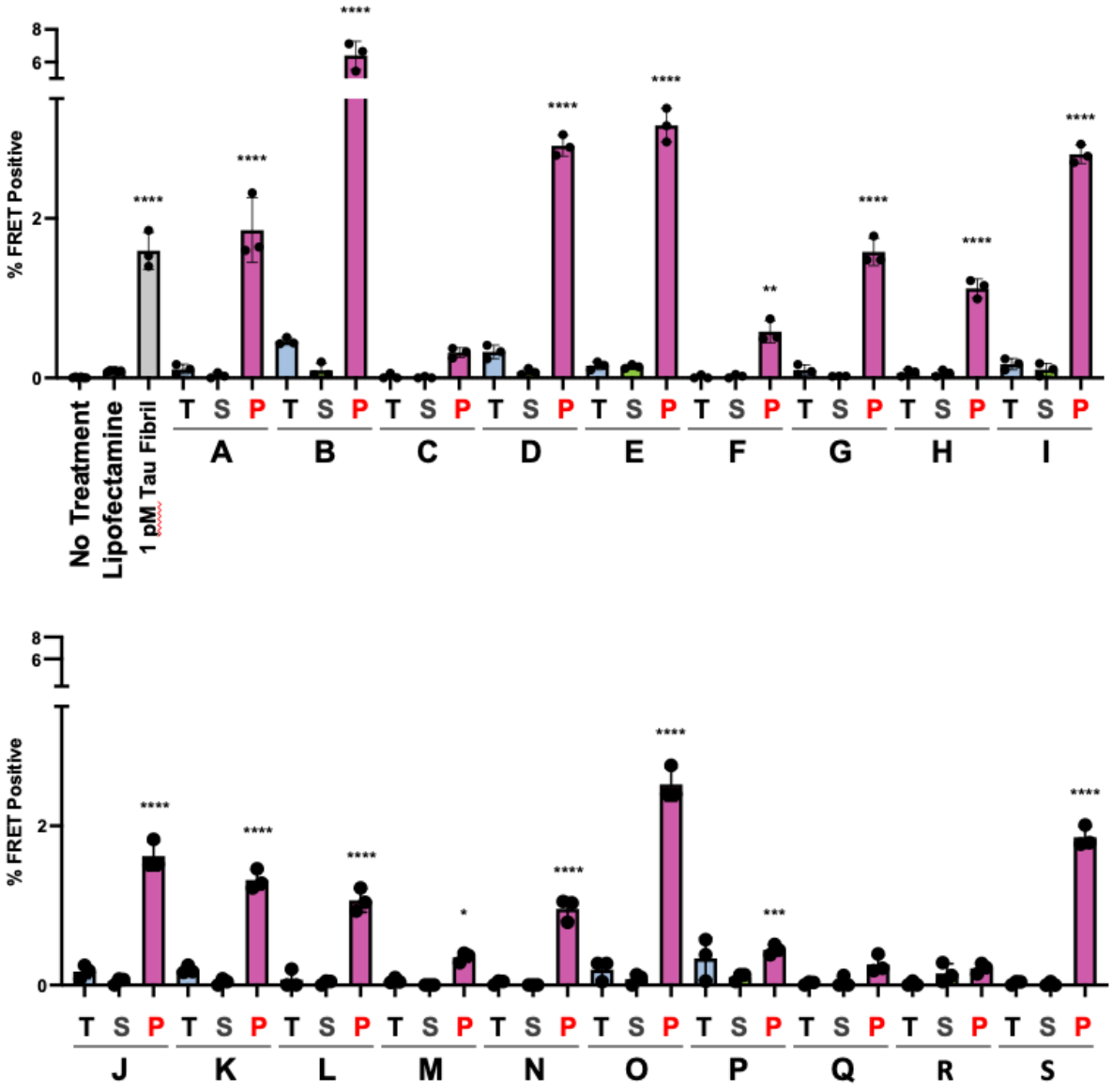

Figure 4.1. Tau seeding is present in the parietal lobe of 19 control subjects. Parietal Cortex fresh frozen samples from 19 individuals (A-S) without any known neurological diagnoses were used to create total (**T**) clarified lysate [10% (wt/vol)] followed by immunoprecipitation with the MD3.1 antibody to generate a tau depleted supernatant (**S**) and tau enriched pellet (**P**). Tau seeding was reliably detected in 16 of 19 cortical IP pellets. Columns represent the mean FRET positivity from three technical replicates (dots). Statistical significance was

determined by performing one-way ANOVA followed by Dunnett's multiple comparisons testing of all samples compared against Lipofectamine treated negative controls, *p < 0.05, **p < 0.01, ***p < 0.001, ****p < 0.0001. Errors bars = S.D. biosensors. (**C**) No seeding activity detected in PEFF tissue from nodding syndrome Case 2 using v2H biosensors. (**D**) Seeding activity on v2H biosensors from PEFF tissue from the temporal cortex of an AD case used as a positive control. Statistical significance was determined by performing one-way ANOVA followed by Dunnett's multiple comparisons testing of all samples compared against Lipofectamine treated negative controls, *p < 0.05, **p < 0.01, ***p < 0.001, ****p < 0.0001. Errors bars = S.D.

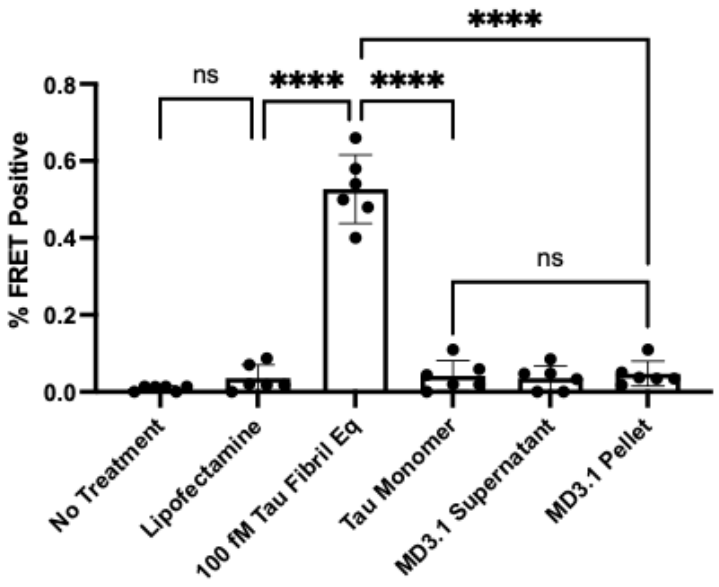

Figure 4.2. MD3.1 antibody does not induce seed conversion of recombinant tau monomer under experimental immunoprecipitation conditions. No seeding activity was detected in the pellet after immunoprecipitation of 500ng recombinant 2N4R tau with MD3.1. Statistical significance was determined by performing one-way ANOVA followed by Tukey's multiple comparisons test, *$p < 0.05$, **$p < 0.01$, ***$p < 0.001$, ****$p < 0.0001$. Errors bars show SD.

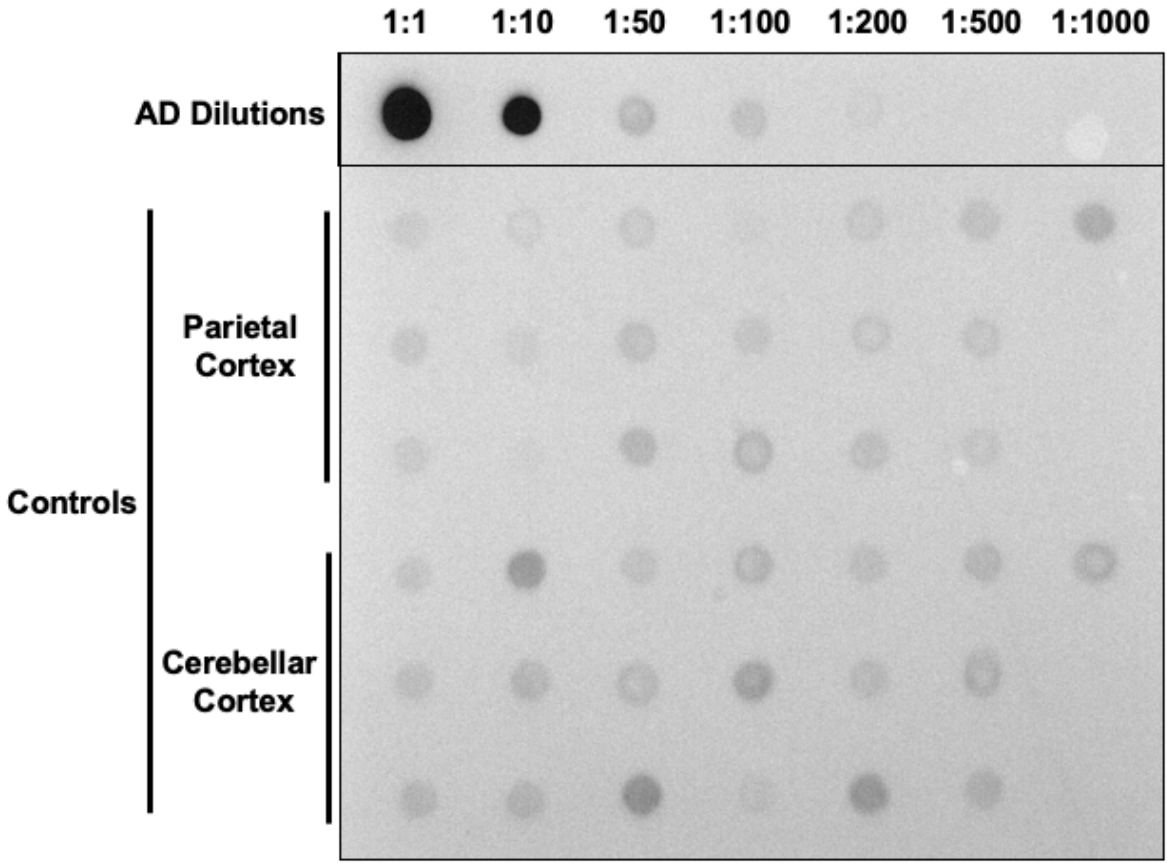

Figure 4.3. Soluble lysates from control brain contain markedly less pathologically phosphorylated tau relative to AD brain. AT8 detection of a dot blot of dilutions of soluble AD brain lysate, and control parietal cortex and cerebellar cortex lysates.

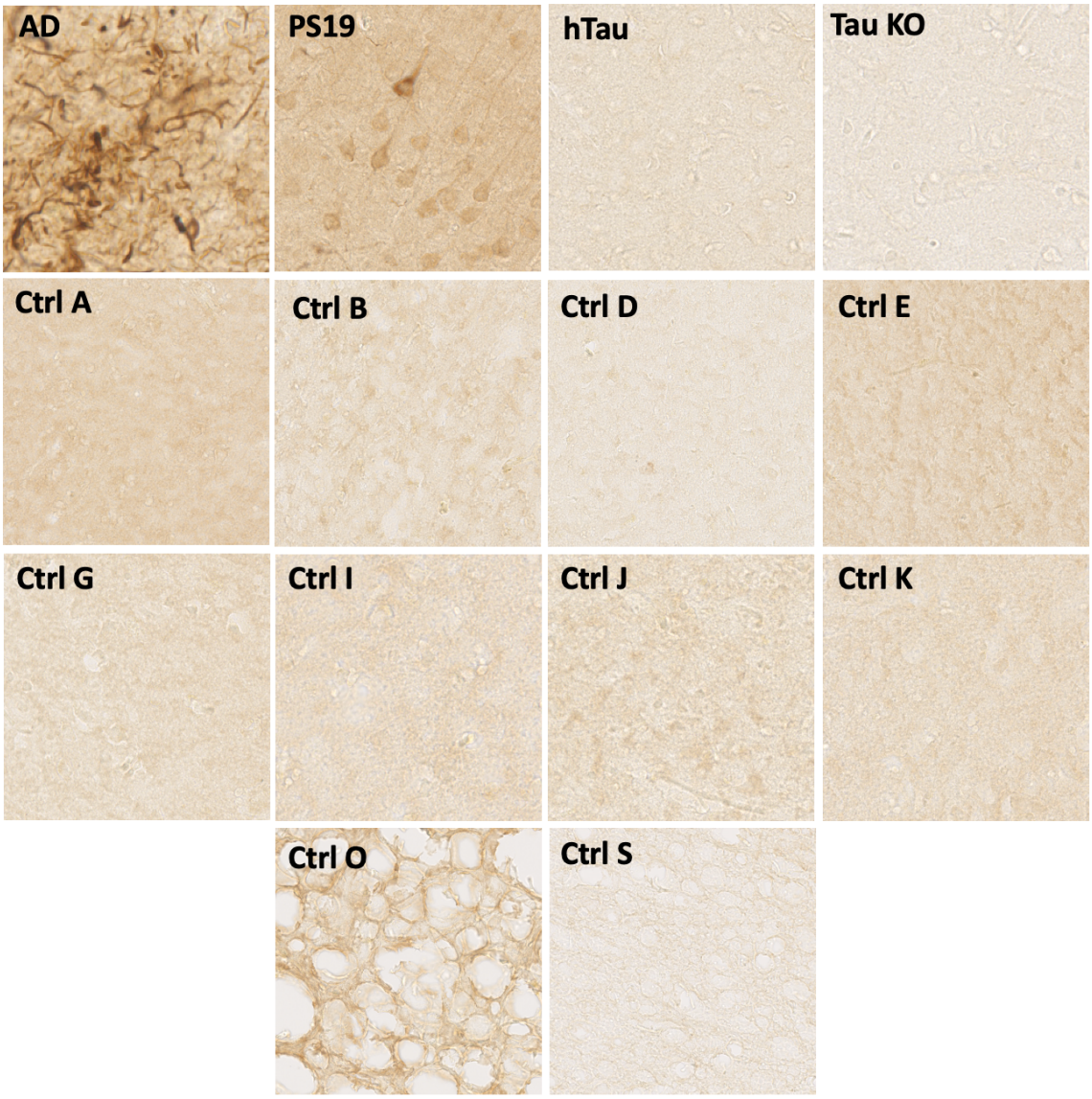

Figure 4.4. Control brain is negative for histopathological tau staining. AT8 staining of the top ten seeding control brains shows no remarkable pathology. AD and PS19 mouse brains were used as positive staining controls while hTau, and Tau KO mouse brains were used as negative controls.

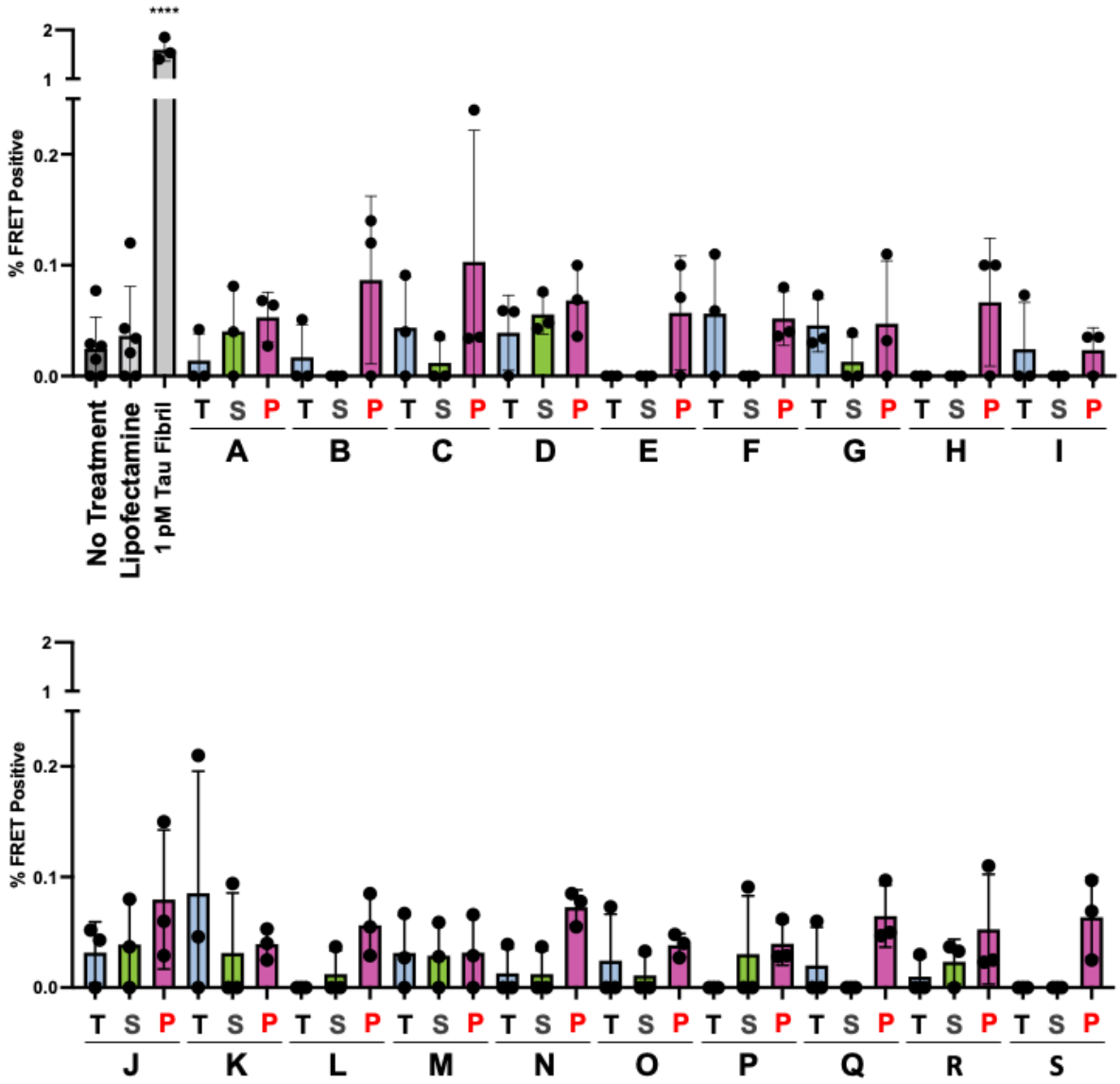

Figure 4.5. No reliable tau seeding activity is detected in the cerebellum of 19 control subjects. Fresh frozen cerebellum samples from 19 subjects without any known neurological diagnoses were used to create total (**T**) clarified lysate [10% (wt/vol)] followed by immunoprecipitation with the MD3.1 antibody to generate a tau depleted supernatant (**S**) and tau enriched pellet (**P**). No reliable tau seeding was detected across all cerebellum samples. Columns indicate the mean FRET positivity from three technical replicates (dots). Statistical

significance was determined by performing one-way ANOVA followed by Dunnett's multiple comparisons testing of all samples compared against Lipofectamine treated negative controls, *$p < 0.05$, **$p < 0.01$, ***$p < 0.001$, ****$p < 0.0001$. Errors bars = S.D.

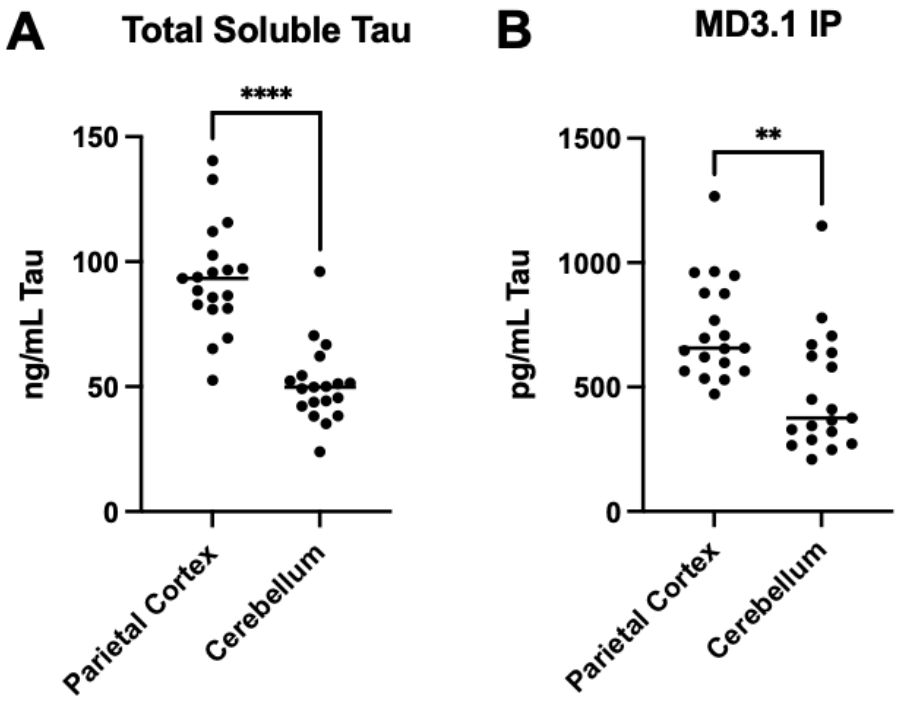

Figure 4.6. ELISA quantification of tau in brain samples. (**A**) Quantification of soluble tau in total clarified lysates from the parietal cortex and cerebellum. (**B**) Quantification of tau in the pellet following immunoprecipitation using the MD3.1 antibody. Statistical significance was determined by performing Student's t-test, **$p < 0.01$, ****$p < 0.0001$.

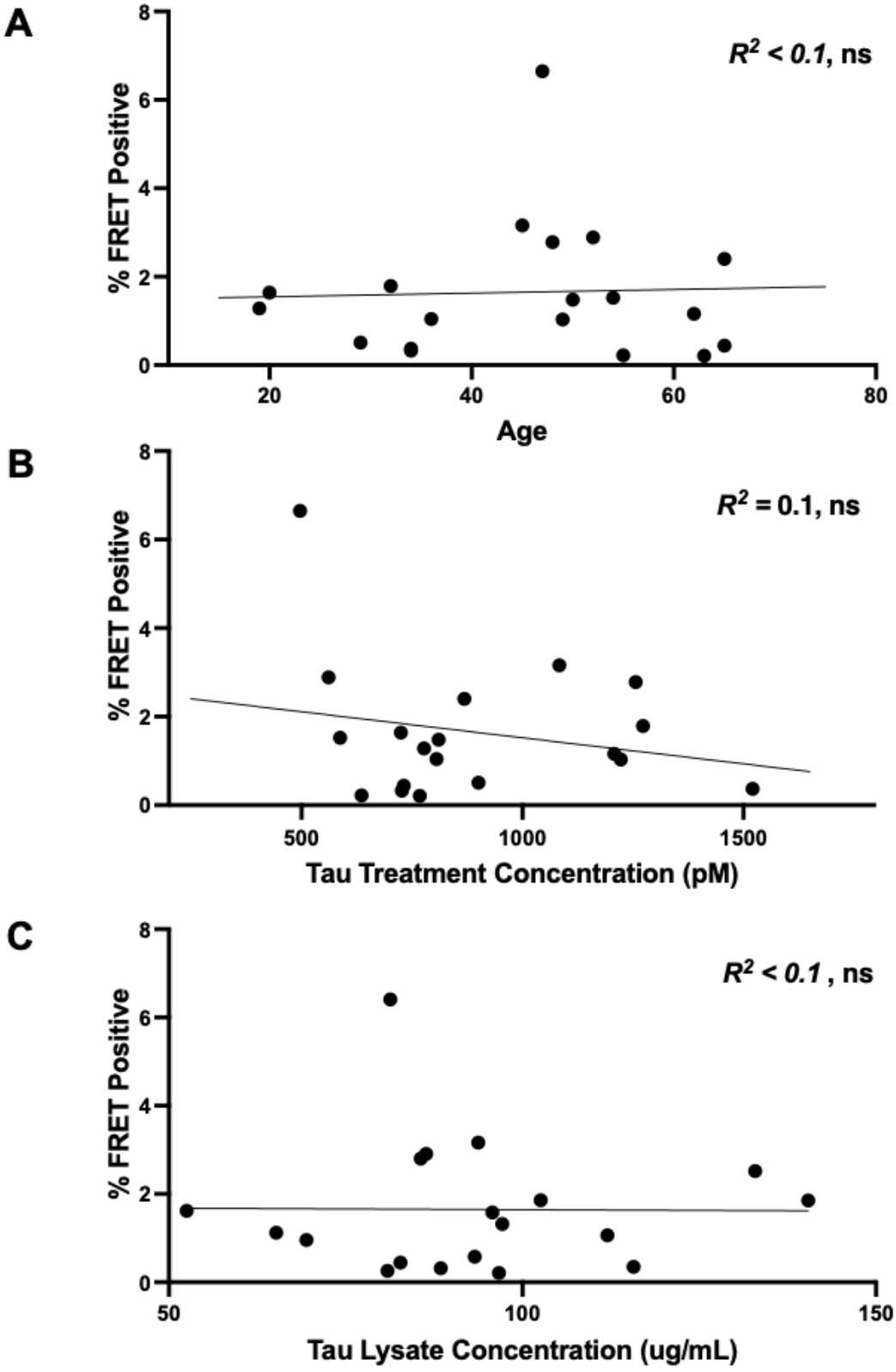
A
$R^2 < 0.1$, ns
% FRET Positive
Age
B
$R^2 = 0.1$, ns
% FRET Positive
Tau Treatment Concentration (pM)
C
$R^2 < 0.1$, ns
% FRET Positive
Tau Lysate Concentration (ug/mL)

Figure 4.7. Relationships between tau seeding, age, and tau concentration in seeding samples. (**A**) Age did not correlate with seeding in immunoprecipitation pellets. (**B**) The final tau treatment concentration from immunoprecipitation pellets did not correlate with seeding in immunoprecipitation pellets. (**C**) Initial tau concentration in total soluble protein fractions did not correlate with seeding in immunoprecipitation pellets. Data were analyzed using Pearson correlation, ns = not significant.

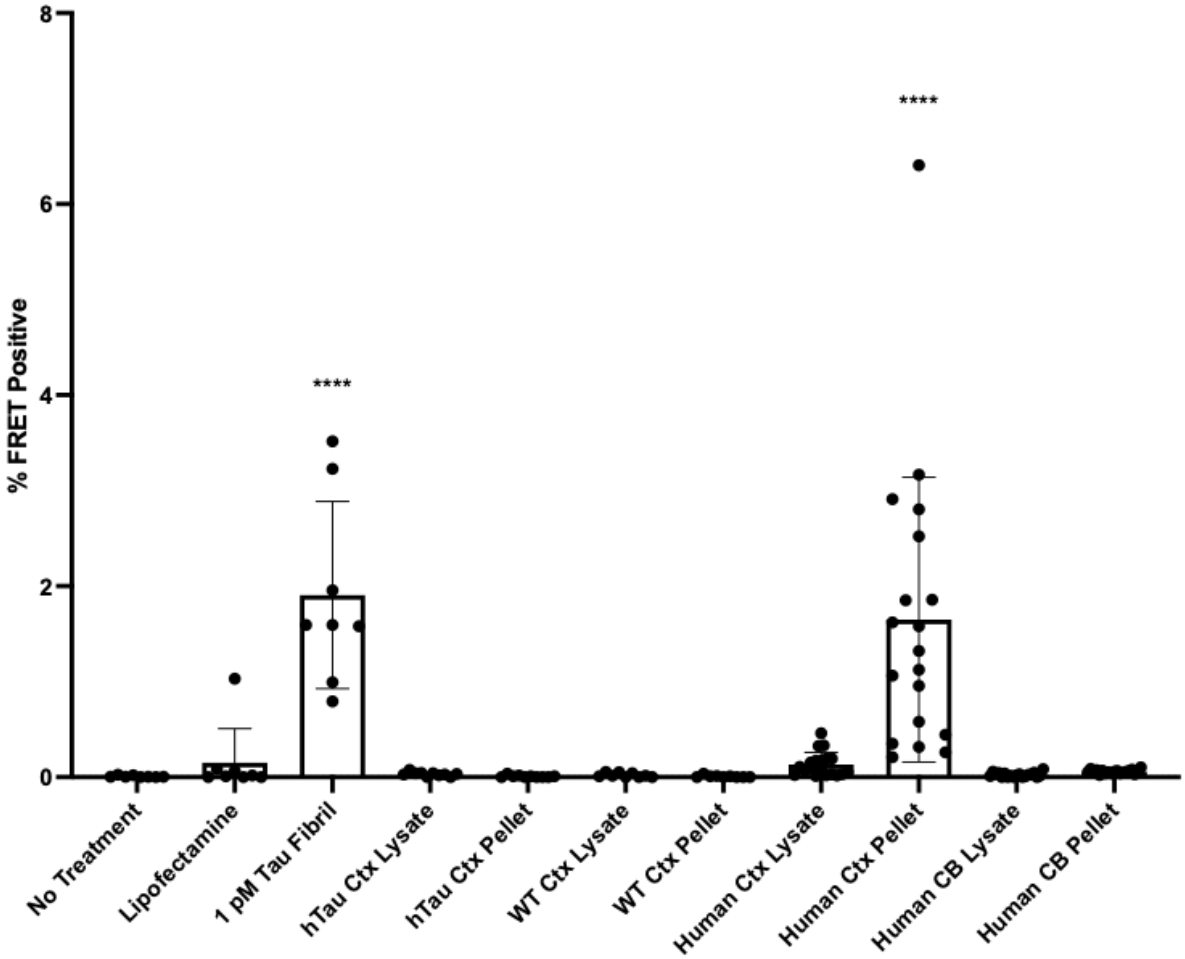

Figure 4.8. Human and mouse tau expressed in mouse cortex does not form detectable seeds. Of the groups tested, only human tau enriched via immunoprecipitation from human cortex, and not human cerebellum, formed seeds that were detectable at a statistically significant level. Tau immunoprecipitated from the cortex of mice expressing human tau (**hTau**, n=10, F=5, M=5) and wild type mouse tau (**WT**, n=9, M=4, F=5) did not show significant seeding activity. Statistical significance was determined by performing one-way ANOVA followed by Dunnett's multiple comparisons testing of all samples compared against Lipofectamine treated negative controls, ****$p < 0.0001$. Errors bars = S.D. Abbreviations: **Ctx –** cortex, **CB** – cerebellum.

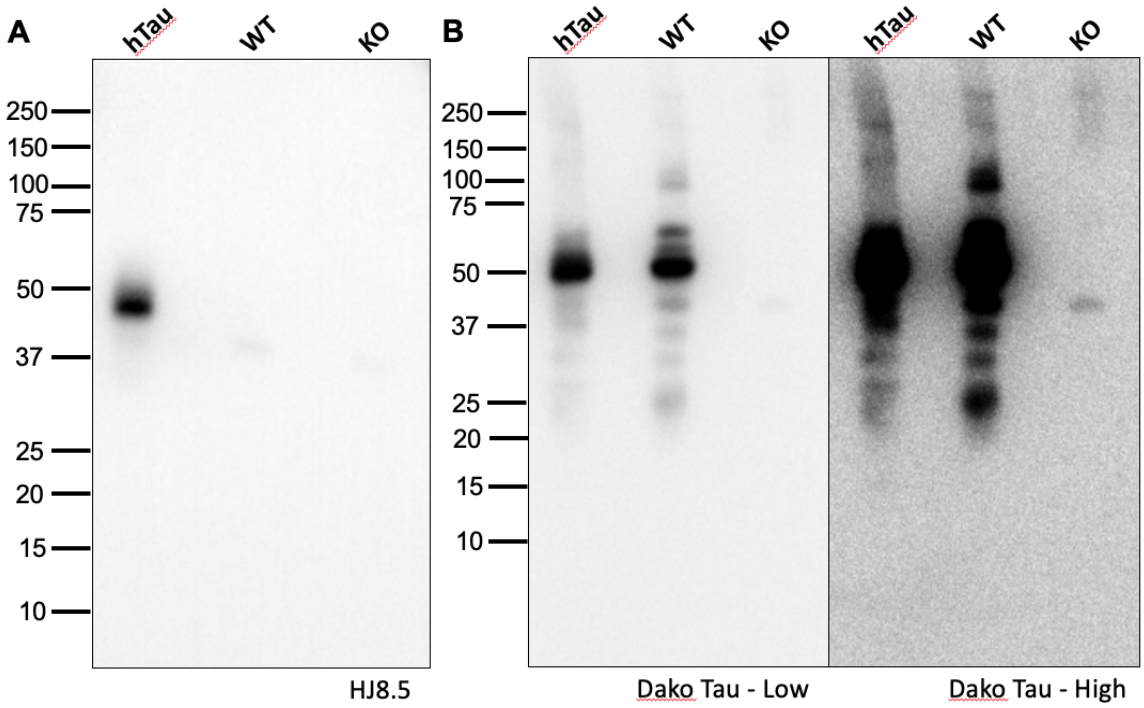

Figure 4.9. Western blots showing human tau expression in hTau mice gifted from Pfizer. (A) HJ8.5, a human tau specific antibody recognizing n-terminal residues 25-30, shows human tau expression in Pfizer human tau mice. No human tau is detected in WT mice, or tau knockout mice used as a negative control. (B) Low exposure of Dako polyclonal tau antibody reveals tau expression in hTau and WT mice, human and mouse respectively. High exposure reveals non-specific banding in knock-out mice.

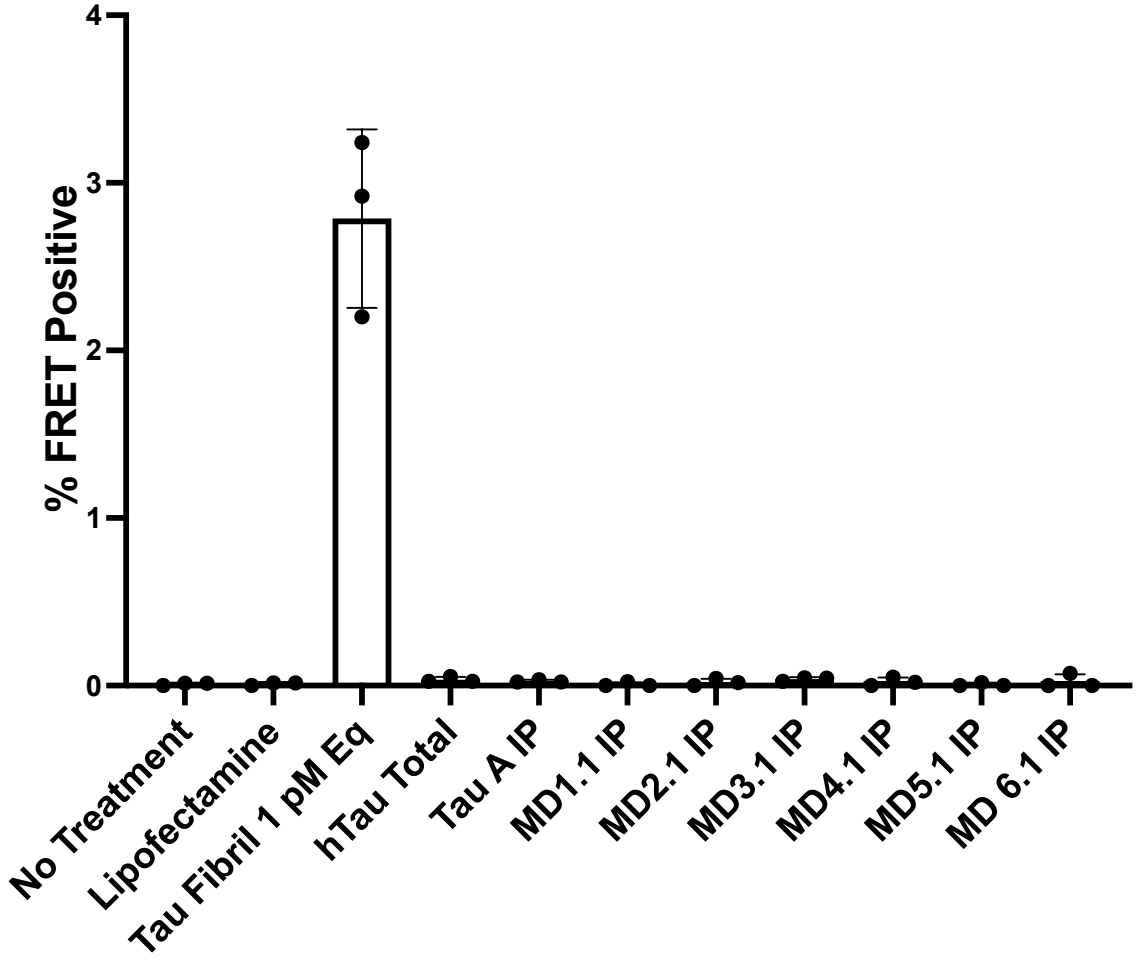

Figure 4.10. hTau mice have no detectable tau seeding activity in immunopurified samples across several different tau antibodies. Clarified lysate from hTau mouse cortices was pooled to generate enough starting material. 1000 µg of total combined lysate was used for input into each immnoupurification. 10 µL of IP pellet was transduced into v2H biosensors. Cells were fixed and harvest for FRET flow cytometry analysis 48 hours after treatment.

A

Antibody	Epitope
MD1.1	22-34
MD4.1	145-160
AT8	p202/p205
TauA	244-266
MD2.1	263-281 (R1R2)
MD2.2	263-281 (R1R2)
MD3.1	263-311 Δ275-305 (R1R3)
MD3.2	263-311 Δ275-305 (R1R3)
MD5.1	326-343 (R3R4)
MD6.1	358-375 (R4R')
MD6.2	358-375 (R4R')

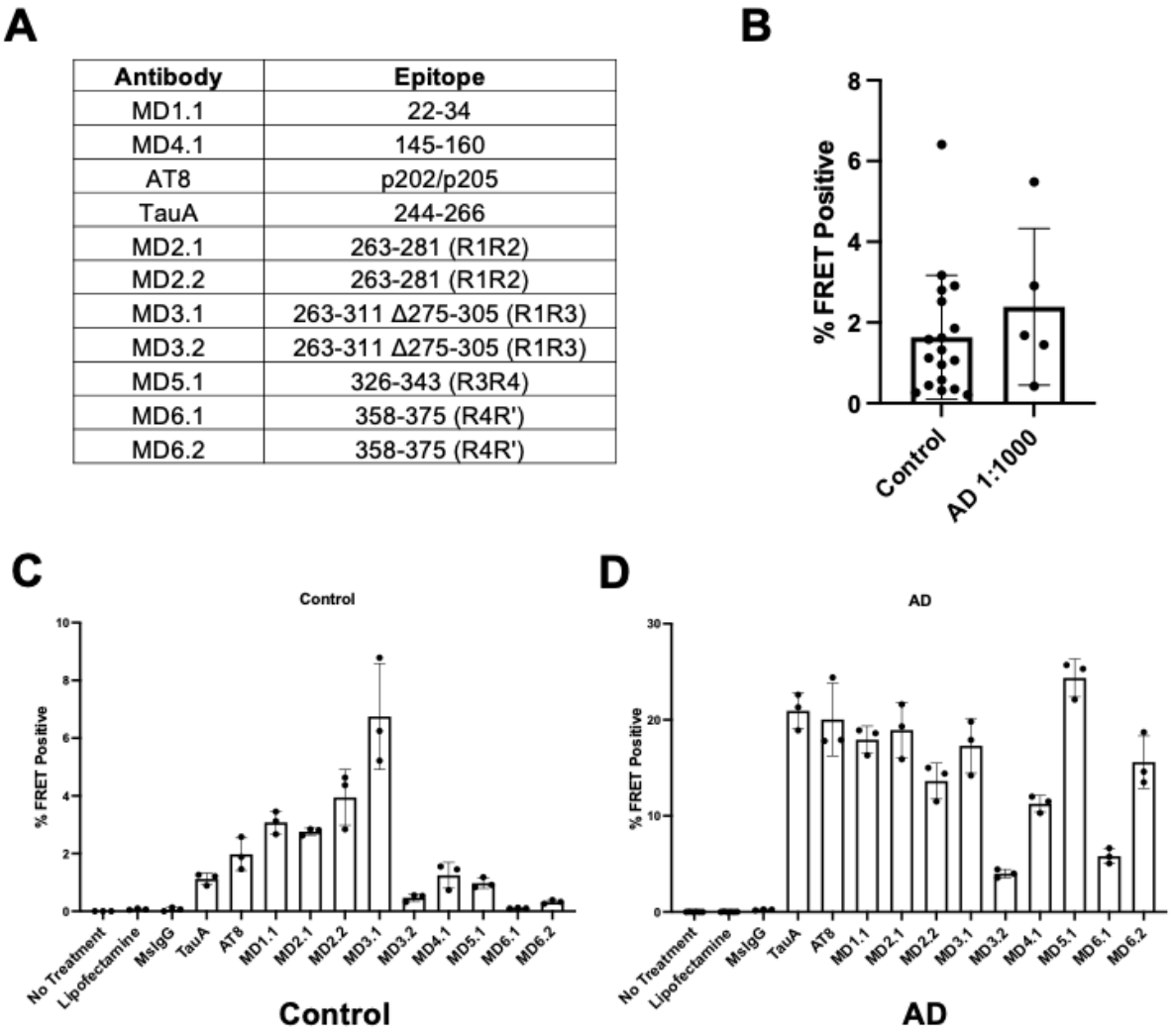

Figure 4.11. Differential seed capture efficiency from control and AD brain**.** A custom antibody panel reveals unique epitope exposure of tau seeds in control brain versus AD. (**A**) Epitopes of antibodies used. (**B**) MD3.1 immunoprecipitation pellets from AD brain have roughly 1000x seeding activity vs. MD3.1 pellets from control brain. MD3.1 pellets from AD were diluted 1000-fold prior to seeding on v2H biosensors while control pellets were used undiluted. No significant difference between undiluted control pellets and 1000-fold diluted AD pellets was found (p=0.3692), student's t-test, error bars = S.D. (**C**) MD3.1 was most

efficient at isolating tau seeds from control brain. (**D**) Multiple antibodies efficiently isolated seeds from AD brain.

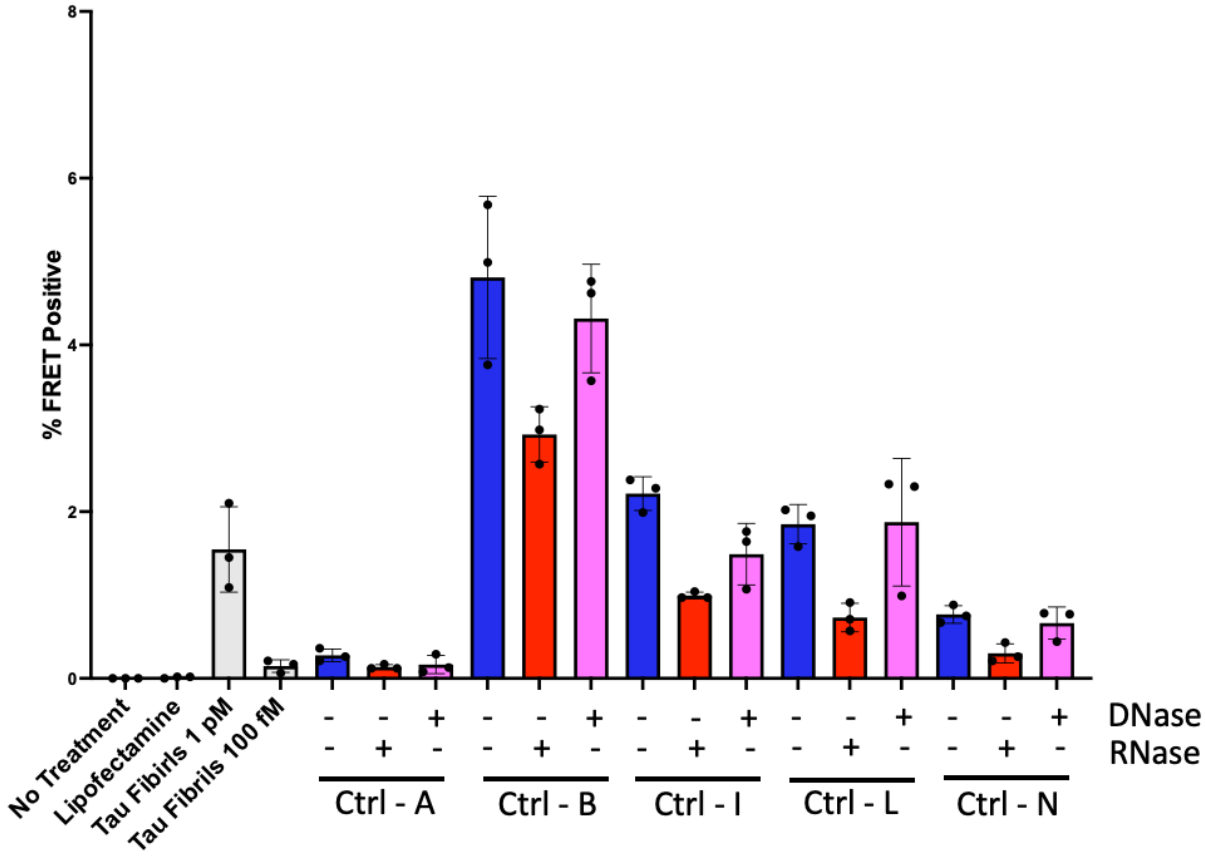

Figure 4.12. RNase destabilizes tau seeds isolated from control brain. RNase treatment, but not DNase, reduces seeding activity in MD3.1 IP pellets derived from five control cases spanning the range of seeding activity in our cohort.

Chapter 5

Conclusions and Future Directions

Summary of Results and Implications

An abundance of evidence in the literature now validates tau as a prion protein. In living systems, it adopts seed competent conformations with the remarkable ability to self-assemble and propagate from cell to cell and along neural networks, such as in the brain. Further, the precise identity or conformation of the assembly, or strain, in fact, predicts which and when certain areas of the brain will be affected and the pattern of deposition. Advances in cryo-EM have given us structural determinations of tau fibrils from a variety of tauopathies that validate this perspective. It is highly plausible that the spread of amyloids throughout the brain drive neurodegeneration in a vast majority of neurodegenerative diseases. At present, the purpose of tau's ability to undergo the transformation from an inert molecule to a self-assembling prion, as well as the inciting factors governing this transformation, remain a mystery. Understanding the initial events leading to tau seed-competency may provide us with critical therapeutic targets for the treatment and/or prevention of tauopathies, as well as provide insight into the mechanisms underlying neurodegenerative diseases generally. Additionally, the extent to which this process occurs in healthy individuals, and the potential role it plays in other CNS disorders that exhibit clear neurodegeneration is unknown. In the past decade, several diseases have reported to exhibit tau accumulation histologically, but the role of tau prion-behavior has not been examined.

During my thesis, I have contributed to furthering our understanding of the scope of tau seeding in healthy individuals, as well as in diseases not formally considered as tauopathies. Of most importance, my work revealed that tau can and does form functional prions outside

the context of disease (Chapter 4). Using next-generation tau biosensors, we uncovered tau seeding in a cohort of healthy individuals that was brain region specific, as well as species specific. Tau seeds were present in the parietal cortex, while absent in the cerebellum. We were unable to recover tau seeds from mice expressing wild-type human tau. Further, tau seeding in the healthy human brain was unrelated to age, suggesting that the presence of seed-competent tau species in our cohort was not the result of incipient tauopathy, but rather the result of normal biological processes. Corroborating our findings, seeds were detected in tau immunohistochemically negative samples in the ultrasensitive cell-free seed amplification assay called real-time quaking induced conversion (RT-QuIC) by the Caughey group (Metrick et al., 2020).

It appears likely that the prion-properties of tau have a functional role that is yet to be determined. Abundant literature supports the idea of functional prions (Cai *et al.*, 2014; Fioriti *et al.*, 2015; Hou *et al.*, 2011; Huang *et al.*, 2006; Pavlopoulos *et al.*, 2011; Rayman and Kandel, 2017; Si *et al.*, 2003; Wickner *et al.*, 2015). If tau prions exist in healthy human brain, it seems likely that there are processes that govern their formation and destruction. The striking accumulation of insoluble tau amyloids in neurodegenerative disease may be a reflection of these control mechanisms malfunctioning whether that be due to age, inflammation, genetics, or other factors such as the conformation of the tau seed itself. My work suggests tau-RNA interactions may be one factor contributing to the presence of tau amyloids in the healthy brain.

Several diseases have been reported to contain tau aggregates histologically but had not yet been analyzed for the presence of tau seeds. I was able to uncover seeding activity within temporal lobe biopsies of temporal lobe epilepsy patients, as well as in in the brain of multiple sclerosis patients at levels that exceed what we found in the healthy brain (Chapters 2 & 3). During my work, it became clear that the type of tissue (fresh frozen vs. fixed) alters the seeding activity that exists in a given sample. We were unable to detect any tau seeding activity in fixed brain tissue from Nodding Syndrome or multiple sclerosis, nor did we detect tau seeding activity in muscle tissue from sporadic inclusion body myositis (Chapters 2 & 3). The discrepancy of finding tau seeds in MS fresh frozen tissue but not fixed tissue highlights the decrease in seeding activity after fixation. For that reason, we were unable to conclude definitively if tau seeds are present in Nodding Syndrome brain or muscle tissue of sporadic inclusion body myositis.

Overall, my work suggests that tau seeding may play a significant role in the pathophysiology of multiple sclerosis and temporal lobe epilepsy patients, and does not preclude a role for tau in Nodding Syndrome or sporadic inclusion body mysotis. Uncovering tau seeding activity in inflammatory diseases like MS that are not typically considered tauopathies suggests that tau may be a critical mediator of neurodegeneration broadly, not merely in prototypical tau-related diseases, and is influenced by inflammation in the CNS.

Future Directions

To this day, we have no treatments for the prevention of tauopathies. My thesis work suggests that tau seeding is much more ubiquitous phenomenon than what we previously understood. Delineating the precise mechanisms by which tau seeds are formed, and their presence is regulated, may allow for the development of therapeutic strategies for the effective treatment and prevention of tau-related disorders. Future work will be required to understand the functional role of tau prions in normal biology.

Additionally, my work suggests that tau prions may accumulate to a significant extent in inflammatory CNS conditions such as multiple sclerosis, which may drive neurodegeneration in these diseases. If so, treatment strategies targeted at reducing tau amyloids may be an effective path for treating the neurodegenerative aspects of CNS disorders incited by inflammation. Future work investigating mechanistic ties between inflammation in the CNS and tau prion accumulation will be vital in this regard.

APPENDIX A

REFERENCES

Acker, C.M., Forest, S.K., Zinkowski, R., Davies, P., and d'Abramo, C. (2013). Sensitive quantitative assays for tau and phospho-tau in transgenic mouse models. Neurobiol Aging *34*, 338-350. 10.1016/j.neurobiolaging.2012.05.010.

Akiyama, H., Barger, S., Barnum, S., Bradt, B., Bauer, J., Cole, G.M., Cooper, N.R., Eikelenboom, P., Emmerling, M., Fiebich, B.L., et al. (2000). Inflammation and Alzheimer's disease. Neurobiol Aging *21*, 383-421. 10.1016/s0197-4580(00)00124-x.

Anderson, J.M., Hampton, D.W., Patani, R., Pryce, G., Crowther, R.A., Reynolds, R., Franklin, R.J., Giovannoni, G., Compston, D.A., Baker, D., et al. (2008). Abnormally phosphorylated tau is associated with neuronal and axonal loss in experimental autoimmune encephalomyelitis and multiple sclerosis. Brain *131*, 1736-1748. 10.1093/brain/awn119.

Anderson, J.M., Patani, R., Reynolds, R., Nicholas, R., Compston, A., Spillantini, M.G., and Chandran, S. (2009). Evidence for abnormal tau phosphorylation in early aggressive multiple sclerosis. Acta Neuropathol *117*, 583-589. 10.1007/s00401-009-0515-2.

Anderson, J.M., Patani, R., Reynolds, R., Nicholas, R., Compston, A., Spillantini, M.G., and Chandran, S. (2010). Abnormal tau phosphorylation in primary progressive multiple sclerosis. Acta Neuropathol *119*, 591-600. 10.1007/s00401-010-0671-4.

Arriagada, P.V., Growdon, J.H., Hedley-Whyte, E.T., and Hyman, B.T. (1992). Neurofibrillary tangles but not senile plaques parallel duration and severity of Alzheimer's disease. Neurology *42*, 631-639. 10.1212/wnl.42.3.631.

Askanas, V., Engel, W.K., and Nogalska, A. (2015). Sporadic inclusion-body myositis: A degenerative muscle disease associated with aging, impaired muscle protein homeostasis and abnormal mitophagy. Biochim Biophys Acta *1852*, 633-643. 10.1016/j.bbadis.2014.09.005.

Ballatore, C., Lee, V.M., and Trojanowski, J.Q. (2007). Tau-mediated neurodegeneration in Alzheimer's disease and related disorders. Nat Rev Neurosci *8*, 663-672. 10.1038/nrn2194.

Bar-Or, A., and Li, R. (2021). Cellular immunology of relapsing multiple sclerosis: interactions, checks, and balances. Lancet Neurol *20*, 470-483. 10.1016/S1474-4422(21)00063-6.

Biernat, J., Mandelkow, E.M., Schroter, C., Lichtenberg-Kraag, B., Steiner, B., Berling, B., Meyer, H., Mercken, M., Vandermeeren, A., Goedert, M., and Mandelkow, E.

(1992). The switch of tau protein to an Alzheimer-like state includes the phosphorylation of two serine-proline motifs upstream of the microtubule binding region. EMBO J *11*, 1593-1597.

Binder, L.I., Frankfurter, A., and Rebhun, L.I. (1985). The distribution of tau in the mammalian central nervous system. J Cell Biol *101*, 1371-1378. 10.1083/jcb.101.4.1371.

Bunker, J.M., Wilson, L., Jordan, M.A., and Feinstein, S.C. (2004). Modulation of microtubule dynamics by tau in living cells: implications for development and neurodegeneration. Mol Biol Cell *15*, 2720-2728. 10.1091/mbc.e04-01-0062.

Cai, X., Chen, J., Xu, H., Liu, S., Jiang, Q.X., Halfmann, R., and Chen, Z.J. (2014). Prion-like polymerization underlies signal transduction in antiviral immune defense and inflammasome activation. Cell *156*, 1207-1222. 10.1016/j.cell.2014.01.063.

Chen, D., Drombosky, K.W., Hou, Z., Sari, L., Kashmer, O.M., Ryder, B.D., Perez, V.A., Woodard, D.R., Lin, M.M., Diamond, M.I., and Joachimiak, L.A. (2019). Tau local structure shields an amyloid-forming motif and controls aggregation propensity. Nat Commun *10*, 2493. 10.1038/s41467-019-10355-1.

Clavaguera, F., Akatsu, H., Fraser, G., Crowther, R.A., Frank, S., Hench, J., Probst, A., Winkler, D.T., Reichwald, J., Staufenbiel, M., et al. (2013). Brain homogenates from human tauopathies induce tau inclusions in mouse brain. Proc Natl Acad Sci U S A *110*, 9535-9540. 10.1073/pnas.1301175110.

Clavaguera, F., Bolmont, T., Crowther, R.A., Abramowski, D., Frank, S., Probst, A., Fraser, G., Stalder, A.K., Beibel, M., Staufenbiel, M., et al. (2009). Transmission and spreading of tauopathy in transgenic mouse brain. Nat Cell Biol *11*, 909-913. 10.1038/ncb1901.

Cleveland, D.W., Hwo, S.Y., and Kirschner, M.W. (1977). Purification of tau, a microtubule-associated protein that induces assembly of microtubules from purified tubulin. J Mol Biol *116*, 207-225. 10.1016/0022-2836(77)90213-3.

Compston, A., and Coles, A. (2008). Multiple sclerosis. Lancet *372*, 1502-1517. 10.1016/S0140-6736(08)61620-7.

Couchie, D., Mavilia, C., Georgieff, I.S., Liem, R.K., Shelanski, M.L., and Nunez, J. (1992). Primary structure of high molecular weight tau present in the peripheral nervous system. Proc Natl Acad Sci U S A *89*, 4378-4381. 10.1073/pnas.89.10.4378.

Dawson, H.N., Ferreira, A., Eyster, M.V., Ghoshal, N., Binder, L.I., and Vitek, M.P. (2001). Inhibition of neuronal maturation in primary hippocampal neurons from tau deficient mice. J Cell Sci *114*, 1179-1187. 10.1242/jcs.114.6.1179.

de Camargo, L.V., de Carvalho, M.S., Shinjo, S.K., de Oliveira, A.S.B., and Zanoteli, E. (2018). Clinical, Histological, and Immunohistochemical Findings in Inclusion Body Myositis. Biomed Res Int *2018*, 5069042. 10.1155/2018/5069042.

DeVos, S.L., Goncharoff, D.K., Chen, G., Kebodeaux, C.S., Yamada, K., Stewart, F.R., Schuler, D.R., Maloney, S.E., Wozniak, D.F., Rigo, F., et al. (2013). Antisense reduction of tau in adult mice protects against seizures. J Neurosci *33*, 12887-12897. 10.1523/JNEUROSCI.2107-13.2013.

Dyment, D.A., Smith, A.C., Humphreys, P., Schwartzentruber, J., Beaulieu, C.L., Consortium, F.C., Bulman, D.E., Majewski, J., Woulfe, J., Michaud, J., and Boycott, K.M. (2015). Homozygous nonsense mutation in SYNJ1 associated with intractable epilepsy and tau pathology. Neurobiol Aging *36*, 1222 e1221-1225. 10.1016/j.neurobiolaging.2014.09.005.

Falcon, B., Zhang, W., Murzin, A.G., Murshudov, G., Garringer, H.J., Vidal, R., Crowther, R.A., Ghetti, B., Scheres, S.H.W., and Goedert, M. (2018). Structures of filaments from Pick's disease reveal a novel tau protein fold. Nature *561*, 137-140. 10.1038/s41586-018-0454-y.

Falcon, B., Zivanov, J., Zhang, W., Murzin, A.G., Garringer, H.J., Vidal, R., Crowther, R.A., Newell, K.L., Ghetti, B., Goedert, M., and Scheres, S.H.W. (2019). Novel tau filament fold in chronic traumatic encephalopathy encloses hydrophobic molecules. Nature *568*, 420-423. 10.1038/s41586-019-1026-5.

Fioriti, L., Myers, C., Huang, Y.Y., Li, X., Stephan, J.S., Trifilieff, P., Colnaghi, L., Kosmidis, S., Drisaldi, B., Pavlopoulos, E., and Kandel, E.R. (2015). The Persistence of Hippocampal-Based Memory Requires Protein Synthesis Mediated by the Prion-like Protein CPEB3. Neuron *86*, 1433-1448. 10.1016/j.neuron.2015.05.021.

Fitzpatrick, A.W.P., Falcon, B., He, S., Murzin, A.G., Murshudov, G., Garringer, H.J., Crowther, R.A., Ghetti, B., Goedert, M., and Scheres, S.H.W. (2017). Cryo-EM structures of tau filaments from Alzheimer's disease. Nature *547*, 185-190. 10.1038/nature23002.

Frost, B., Jacks, R.L., and Diamond, M.I. (2009a). Propagation of tau misfolding from the outside to the inside of a cell. J Biol Chem *284*, 12845-12852. 10.1074/jbc.M808759200.

Frost, B., Ollesch, J., Wille, H., and Diamond, M.I. (2009b). Conformational diversity of wild-type Tau fibrils specified by templated conformation change. J Biol Chem *284*, 3546-3551. 10.1074/jbc.M805627200.

Furman, J.L., Vaquer-Alicea, J., White, C.L., 3rd, Cairns, N.J., Nelson, P.T., and Diamond, M.I. (2017). Widespread tau seeding activity at early Braak stages. Acta Neuropathol *133*, 91-100. 10.1007/s00401-016-1644-z.

Garbern, J.Y., Neumann, M., Trojanowski, J.Q., Lee, V.M., Feldman, G., Norris, J.W., Friez, M.J., Schwartz, C.E., Stevenson, R., and Sima, A.A. (2010). A mutation affecting the sodium/proton exchanger, SLC9A6, causes mental retardation with tau deposition. Brain *133*, 1391-1402. 10.1093/brain/awq071.

Garcia-Cabrero, A.M., Guerrero-Lopez, R., Giraldez, B.G., Llorens-Martin, M., Avila, J., Serratosa, J.M., and Sanchez, M.P. (2013). Hyperexcitability and epileptic seizures in a model of frontotemporal dementia. Neurobiol Dis *58*, 200-208. 10.1016/j.nbd.2013.06.005.

Ginsberg, S.D., Crino, P.B., Lee, V.M., Eberwine, J.H., and Trojanowski, J.Q. (1997). Sequestration of RNA in Alzheimer's disease neurofibrillary tangles and senile plaques. Ann Neurol *41*, 200-209. 10.1002/ana.410410211.

Ginsberg, S.D., Galvin, J.E., Chiu, T.S., Lee, V.M., Masliah, E., and Trojanowski, J.Q. (1998). RNA sequestration to pathological lesions of neurodegenerative diseases. Acta Neuropathol *96*, 487-494. 10.1007/s004010050923.

Glass, C.K., Saijo, K., Winner, B., Marchetto, M.C., and Gage, F.H. (2010). Mechanisms underlying inflammation in neurodegeneration. Cell *140*, 918-934. 10.1016/j.cell.2010.02.016.

Goedert, M., and Jakes, R. (2005). Mutations causing neurodegenerative tauopathies. Biochim Biophys Acta *1739*, 240-250. 10.1016/j.bbadis.2004.08.007.

Goedert, M., Spillantini, M.G., Jakes, R., Rutherford, D., and Crowther, R.A. (1989). Multiple isoforms of human microtubule-associated protein tau: sequences and localization in neurofibrillary tangles of Alzheimer's disease. Neuron *3*, 519-526. 10.1016/0896-6273(89)90210-9.

Guerchet, M., Prince, M., and Prina, M. (2020). Numbers of people with dementia around the world. Alzheimer’s Disease International.

Guzman-Martinez, L., Maccioni, R.B., Andrade, V., Navarrete, L.P., Pastor, M.G., and Ramos-Escobar, N. (2019). Neuroinflammation as a Common Feature of

Neurodegenerative Disorders. Front Pharmacol *10*, 1008. 10.3389/fphar.2019.01008.

Hermann, B., and Seidenberg, M. (2007). Epilepsy and cognition. Epilepsy Curr *7*, 1-6. 10.1111/j.1535-7511.2007.00151.x.

Hitt, B.D., Vaquer-Alicea, J., Manon, V.A., Beaver, J.D., Kashmer, O.M., Garcia, J.N., and Diamond, M.I. (2021). Ultrasensitive tau biosensor cells detect no seeding in Alzheimer's disease CSF. Acta Neuropathol Commun *9*, 99. 10.1186/s40478-021-01185-8.

Hof, P.R., Charpiot, A., Delacourte, A., Buee, L., Purohit, D., Perl, D.P., and Bouras, C. (1992). Distribution of neurofibrillary tangles and senile plaques in the cerebral cortex in postencephalitic parkinsonism. Neurosci Lett *139*, 10-14. 10.1016/0304-3940(92)90846-y.

Holmes, B.B., Furman, J.L., Mahan, T.E., Yamasaki, T.R., Mirbaha, H., Eades, W.C., Belaygorod, L., Cairns, N.J., Holtzman, D.M., and Diamond, M.I. (2014). Proteopathic tau seeding predicts tauopathy in vivo. Proc Natl Acad Sci U S A *111*, E4376-4385. 10.1073/pnas.1411649111.

Hotterbeekx, A., Lammens, M., Idro, R., Akun, P.R., Lukande, R., Akena, G., Nath, A., Taylor, J., Olwa, F., Kumar-Singh, S., and Colebunders, R. (2019). Neuroinflammation and Not Tauopathy Is a Predominant Pathological Signature of Nodding Syndrome. J Neuropathol Exp Neurol *78*, 1049-1058. 10.1093/jnen/nlz090.

Hotterbeekx, A., Onzivua, S., Menon, S., and Colebunders, R. (2018). Histological examination of post-mortem brains of children with nodding syndrome. Ann Transl Med *6*, 134. 10.21037/atm.2018.02.04.

Hou, F., Sun, L., Zheng, H., Skaug, B., Jiang, Q.X., and Chen, Z.J. (2011). MAVS forms functional prion-like aggregates to activate and propagate antiviral innate immune response. Cell *146*, 448-461. 10.1016/j.cell.2011.06.041.

Huang, Y.S., Kan, M.C., Lin, C.L., and Richter, J.D. (2006). CPEB3 and CPEB4 in neurons: analysis of RNA-binding specificity and translational control of AMPA receptor GluR2 mRNA. EMBO J *25*, 4865-4876. 10.1038/sj.emboj.7601322.

Hutton, M., Lendon, C.L., Rizzu, P., Baker, M., Froelich, S., Houlden, H., Pickering-Brown, S., Chakraverty, S., Isaacs, A., Grover, A., et al. (1998). Association of missense and 5'-splice-site mutations in tau with the inherited dementia FTDP-17. Nature *393*, 702-705. 10.1038/31508.

Johnson, T.P., Tyagi, R., Lee, P.R., Lee, M.H., Johnson, K.R., Kowalak, J., Elkahloun, A., Medynets, M., Hategan, A., Kubofcik, J., et al. (2017). Nodding syndrome may be an autoimmune reaction to the parasitic worm Onchocerca volvulus. Sci Transl Med *9*. 10.1126/scitranslmed.aaf6953.

Jokeit, H., and Ebner, A. (1999). Long term effects of refractory temporal lobe epilepsy on cognitive abilities: a cross sectional study. J Neurol Neurosurg Psychiatry *67*, 44-50. 10.1136/jnnp.67.1.44.

Kadavath, H., Hofele, R.V., Biernat, J., Kumar, S., Tepper, K., Urlaub, H., Mandelkow, E., and Zweckstetter, M. (2015). Tau stabilizes microtubules by binding at the interface between tubulin heterodimers. Proc Natl Acad Sci U S A *112*, 7501-7506. 10.1073/pnas.1504081112.

Kampers, T., Friedhoff, P., Biernat, J., Mandelkow, E.M., and Mandelkow, E. (1996). RNA stimulates aggregation of microtubule-associated protein tau into Alzheimer-like paired helical filaments. FEBS Lett *399*, 344-349. 10.1016/s0014-5793(96)01386-5.

Kaufman, S.K., Sanders, D.W., Thomas, T.L., Ruchinskas, A.J., Vaquer-Alicea, J., Sharma, A.M., Miller, T.M., and Diamond, M.I. (2016). Tau Prion Strains Dictate Patterns of Cell Pathology, Progression Rate, and Regional Vulnerability In Vivo. Neuron *92*, 796-812. 10.1016/j.neuron.2016.09.055.

Ke, Y.D., Suchowerska, A.K., van der Hoven, J., De Silva, D.M., Wu, C.W., van Eersel, J., Ittner, A., and Ittner, L.M. (2012). Lessons from tau-deficient mice. Int J Alzheimers Dis *2012*, 873270. 10.1155/2012/873270.

Kellogg, E.H., Hejab, N.M.A., Poepsel, S., Downing, K.H., DiMaio, F., and Nogales, E. (2018). Near-atomic model of microtubule-tau interactions. Science *360*, 1242-1246. 10.1126/science.aat1780.

Kempf, M., Clement, A., Faissner, A., Lee, G., and Brandt, R. (1996). Tau binds to the distal axon early in development of polarity in a microtubule- and microfilament-dependent manner. J Neurosci *16*, 5583-5592.

King, M.E., Kan, H.M., Baas, P.W., Erisir, A., Glabe, C.G., and Bloom, G.S. (2006). Tau-dependent microtubule disassembly initiated by prefibrillar beta-amyloid. J Cell Biol *175*, 541-546. 10.1083/jcb.200605187.

Kitazawa, M., Trinh, D.N., and LaFerla, F.M. (2008). Inflammation induces tau pathology in inclusion body myositis model via glycogen synthase kinase-3beta. Ann Neurol *64*, 15-24. 10.1002/ana.21325.

Kitazawa, M., Yamasaki, T.R., and LaFerla, F.M. (2004). Microglia as a potential bridge between the amyloid beta-peptide and tau. Ann N Y Acad Sci *1035*, 85-103. 10.1196/annals.1332.006.

Lassmann, H., van Horssen, J., and Mahad, D. (2012). Progressive multiple sclerosis: pathology and pathogenesis. Nat Rev Neurol *8*, 647-656. 10.1038/nrneurol.2012.168.

Laurent, C., Buee, L., and Blum, D. (2018). Tau and neuroinflammation: What impact for Alzheimer's Disease and Tauopathies? Biomed J *41*, 21-33. 10.1016/j.bj.2018.01.003.

Lee, V.M., and Trojanowski, J.Q. (1999). Neurodegenerative tauopathies: human disease and transgenic mouse models. Neuron *24*, 507-510. 10.1016/s0896-6273(00)81106-x.

Mandelkow, E.M., and Mandelkow, E. (2012). Biochemistry and cell biology of tau protein in neurofibrillary degeneration. Cold Spring Harb Perspect Med *2*, a006247. 10.1101/cshperspect.a006247.

Maurage, C.A., Bussiere, T., Sergeant, N., Ghesteem, A., Figarella-Branger, D., Ruchoux, M.M., Pellissier, J.F., and Delacourte, A. (2004). Tau aggregates are abnormally phosphorylated in inclusion body myositis and have an immunoelectrophoretic profile distinct from other tauopathies. Neuropathol Appl Neurobiol *30*, 624-634. 10.1111/j.1365-2990.2004.00577.x.

McKee, A.C., Stein, T.D., Kiernan, P.T., and Alvarez, V.E. (2015). The neuropathology of chronic traumatic encephalopathy. Brain Pathol *25*, 350-364. 10.1111/bpa.12248.

McQuaid, S., Allen, I.V., McMahon, J., and Kirk, J. (1994). Association of measles virus with neurofibrillary tangles in subacute sclerosing panencephalitis: a combined in situ hybridization and immunocytochemical investigation. Neuropathol Appl Neurobiol *20*, 103-110. 10.1111/j.1365-2990.1994.tb01168.x.

Metrick, M.A., 2nd, Ferreira, N.D.C., Saijo, E., Kraus, A., Newell, K., Zanusso, G., Vendruscolo, M., Ghetti, B., and Caughey, B. (2020). A single ultrasensitive assay for detection and discrimination of tau aggregates of Alzheimer and Pick diseases. Acta Neuropathol Commun *8*, 22. 10.1186/s40478-020-0887-z.

Milo, R., Korczyn, A.D., Manouchehri, N., and Stuve, O. (2020). The temporal and causal relationship between inflammation and neurodegeneration in multiple sclerosis. Mult Scler *26*, 876-886. 10.1177/1352458519886943.

Mirbaha, H., Chen, D., Morazova, O.A., Ruff, K.M., Sharma, A.M., Liu, X., Goodarzi, M., Pappu, R.V., Colby, D.W., Mirzaei, H., et al. (2018). Inert and seed-competent tau monomers suggest structural origins of aggregation. Elife *7*. 10.7554/eLife.36584.

Morris, M., Knudsen, G.M., Maeda, S., Trinidad, J.C., Ioanoviciu, A., Burlingame, A.L., and Mucke, L. (2015). Tau post-translational modifications in wild-type and human amyloid precursor protein transgenic mice. Nat Neurosci *18*, 1183-1189. 10.1038/nn.4067.

Mukrasch, M.D., Bibow, S., Korukottu, J., Jeganathan, S., Biernat, J., Griesinger, C., Mandelkow, E., and Zweckstetter, M. (2009). Structural polymorphism of 441-residue tau at single residue resolution. PLoS Biol *7*, e34. 10.1371/journal.pbio.1000034.

Neve, R.L., Harris, P., Kosik, K.S., Kurnit, D.M., and Donlon, T.A. (1986). Identification of cDNA clones for the human microtubule-associated protein tau and chromosomal localization of the genes for tau and microtubule-associated protein 2. Brain Res *387*, 271-280. 10.1016/0169-328x(86)90033-1.

Oyegbile, T.O., Bhattacharya, A., Seidenberg, M., and Hermann, B.P. (2006). Quantitative MRI biomarkers of cognitive morbidity in temporal lobe epilepsy. Epilepsia *47*, 143-152. 10.1111/j.1528-1167.2006.00380.x.

Palmio, J., Suhonen, J., Keranen, T., Hulkkonen, J., Peltola, J., and Pirttila, T. (2009). Cerebrospinal fluid tau as a marker of neuronal damage after epileptic seizure. Seizure *18*, 474-477. 10.1016/j.seizure.2009.04.006.

Pavlopoulos, E., Trifilieff, P., Chevaleyre, V., Fioriti, L., Zairis, S., Pagano, A., Malleret, G., and Kandel, E.R. (2011). Neuralized1 activates CPEB3: a function for nonproteolytic ubiquitin in synaptic plasticity and memory storage. Cell *147*, 1369-1383. 10.1016/j.cell.2011.09.056.

Pollanen, M.S., Onzivua, S., McKeever, P.M., Robertson, J., Mackenzie, I.R., Kovacs, G.G., Olwa, F., Kitara, D.L., and Fong, A. (2022). The spectrum of disease and tau pathology of nodding syndrome in Uganda. Brain. 10.1093/brain/awac137.

Pollanen, M.S., Onzivua, S., Robertson, J., McKeever, P.M., Olawa, F., Kitara, D.L., and Fong, A. (2018). Nodding syndrome in Uganda is a tauopathy. Acta Neuropathol *136*, 691-697. 10.1007/s00401-018-1909-9.

Poorkaj, P., Bird, T.D., Wijsman, E., Nemens, E., Garruto, R.M., Anderson, L., Andreadis, A., Wiederholt, W.C., Raskind, M., and Schellenberg, G.D. (1998).

Tau is a candidate gene for chromosome 17 frontotemporal dementia. Ann Neurol *43*, 815-825. 10.1002/ana.410430617.

Rayman, J.B., and Kandel, E.R. (2017). Functional Prions in the Brain. Cold Spring Harb Perspect Biol *9*. 10.1101/cshperspect.a023671.

Roberson, E.D., Scearce-Levie, K., Palop, J.J., Yan, F., Cheng, I.H., Wu, T., Gerstein, H., Yu, G.Q., and Mucke, L. (2007). Reducing endogenous tau ameliorates amyloid beta-induced deficits in an Alzheimer's disease mouse model. Science *316*, 750-754. 10.1126/science.1141736.

Sanders, D.W., Kaufman, S.K., DeVos, S.L., Sharma, A.M., Mirbaha, H., Li, A., Barker, S.J., Foley, A.C., Thorpe, J.R., Serpell, L.C., et al. (2014). Distinct tau prion strains propagate in cells and mice and define different tauopathies. Neuron *82*, 1271-1288. 10.1016/j.neuron.2014.04.047.

Sarnat, H., Flores-Sarnat, L., Crino, P., Hader, W., and Bello-Espinosa, L. (2012). Hemimegalencephaly: foetal tauopathy with mTOR hyperactivation and neuronal lipidosis. Folia Neuropathol *50*, 330-345. 10.5114/fn.2012.32363.

Schweers, O., Schonbrunn-Hanebeck, E., Marx, A., and Mandelkow, E. (1994). Structural studies of tau protein and Alzheimer paired helical filaments show no evidence for beta-structure. J Biol Chem *269*, 24290-24297.

Sen, A., Thom, M., Martinian, L., Harding, B., Cross, J.H., Nikolic, M., and Sisodiya, S.M. (2007). Pathological tau tangles localize to focal cortical dysplasia in older patients. Epilepsia *48*, 1447-1454. 10.1111/j.1528-1167.2007.01107.x.

Shi, Y., Zhang, W., Yang, Y., Murzin, A.G., Falcon, B., Kotecha, A., van Beers, M., Tarutani, A., Kametani, F., Garringer, H.J., et al. (2021). Structure-based classification of tauopathies. Nature *598*, 359-363. 10.1038/s41586-021-03911-7.

Si, K., Lindquist, S., and Kandel, E.R. (2003). A neuronal isoform of the aplysia CPEB has prion-like properties. Cell *115*, 879-891. 10.1016/s0092-8674(03)01020-1.

Spillantini, M.G., Murrell, J.R., Goedert, M., Farlow, M.R., Klug, A., and Ghetti, B. (1998). Mutation in the tau gene in familial multiple system tauopathy with presenile dementia. Proc Natl Acad Sci U S A *95*, 7737-7741. 10.1073/pnas.95.13.7737.

Steffen, B.J., Breier, G., Butcher, E.C., Schulz, M., and Engelhardt, B. (1996). ICAM-1, VCAM-1, and MAdCAM-1 are expressed on choroid plexus epithelium but not endothelium and mediate binding of lymphocytes in vitro. Am J Pathol *148*, 1819-1838.

Tai, C., Chang, C.W., Yu, G.Q., Lopez, I., Yu, X., Wang, X., Guo, W., and Mucke, L. (2020). Tau Reduction Prevents Key Features of Autism in Mouse Models. Neuron *106*, 421-437 e411. 10.1016/j.neuron.2020.01.038.

Tai, X.Y., Koepp, M., Duncan, J.S., Fox, N., Thompson, P., Baxendale, S., Liu, J.Y., Reeves, C., Michalak, Z., and Thom, M. (2016). Hyperphosphorylated tau in patients with refractory epilepsy correlates with cognitive decline: a study of temporal lobe resections. Brain *139*, 2441-2455. 10.1093/brain/aww187.

Terada, T., Yokokura, M., Obi, T., Bunai, T., Yoshikawa, E., Ando, I., Shimada, H., Suhara, T., Higuchi, M., and Ouchi, Y. (2019). In vivo direct relation of tau pathology with neuroinflammation in early Alzheimer's disease. J Neurol *266*, 2186-2196. 10.1007/s00415-019-09400-2.

Thom, M., Liu, J.Y., Thompson, P., Phadke, R., Narkiewicz, M., Martinian, L., Marsdon, D., Koepp, M., Caboclo, L., Catarino, C.B., and Sisodiya, S.M. (2011). Neurofibrillary tangle pathology and Braak staging in chronic epilepsy in relation to traumatic brain injury and hippocampal sclerosis: a post-mortem study. Brain *134*, 2969-2981. 10.1093/brain/awr209.

Trapp, B.D., and Nave, K.A. (2008). Multiple sclerosis: an immune or neurodegenerative disorder? Annu Rev Neurosci *31*, 247-269. 10.1146/annurev.neuro.30.051606.094313.

Tucker, K.L., Meyer, M., and Barde, Y.A. (2001). Neurotrophins are required for nerve growth during development. Nat Neurosci *4*, 29-37. 10.1038/82868.

Vaquer-Alicea, J., Diamond, M.I., and Joachimiak, L.A. (2021). Tau strains shape disease. Acta Neuropathol *142*, 57-71. 10.1007/s00401-021-02301-7.

Weingarten, M.D., Lockwood, A.H., Hwo, S.Y., and Kirschner, M.W. (1975). A protein factor essential for microtubule assembly. Proc Natl Acad Sci U S A *72*, 1858-1862. 10.1073/pnas.72.5.1858.

Wickner, R.B., Shewmaker, F.P., Bateman, D.A., Edskes, H.K., Gorkovskiy, A., Dayani, Y., and Bezsonov, E.E. (2015). Yeast prions: structure, biology, and prion-handling systems. Microbiol Mol Biol Rev *79*, 1-17. 10.1128/MMBR.00041-14.

Williams, D.R. (2006). Tauopathies: classification and clinical update on neurodegenerative diseases associated with microtubule-associated protein tau. Intern Med J *36*, 652-660. 10.1111/j.1445-5994.2006.01153.x.

Witman, G.B., Cleveland, D.W., Weingarten, M.D., and Kirschner, M.W. (1976). Tubulin requires tau for growth onto microtubule initiating sites. Proc Natl Acad Sci U S A *73*, 4070-4074. 10.1073/pnas.73.11.4070.

Yanamandra, K., Kfoury, N., Jiang, H., Mahan, T.E., Ma, S., Maloney, S.E., Wozniak, D.F., Diamond, M.I., and Holtzman, D.M. (2013). Anti-tau antibodies that block tau aggregate seeding in vitro markedly decrease pathology and improve cognition in vivo. Neuron *80*, 402-414. 10.1016/j.neuron.2013.07.046.

Zhang, W., Tarutani, A., Newell, K.L., Murzin, A.G., Matsubara, T., Falcon, B., Vidal, R., Garringer, H.J., Shi, Y., Ikeuchi, T., et al. (2020a). Novel tau filament fold in corticobasal degeneration. Nature *580*, 283-287. 10.1038/s41586-020-2043-0.

Zhang, Y., Li, K., Pu, C., Dang, H., Liu, J., and Shi, Q. (2020b). A novel application of tau PET in the diagnosis of sporadic inclusion body myositis: A case report. Medicine (Baltimore) *99*, e21524. 10.1097/MD.0000000000021524.